Final report

Wave attenuation over marshlands

Determination of marshland influences on New Orleans' flood protection

M. Vosse
November 17th 2008

Thesis committee:
Prof.dr. S.J.M.H. Hulscher
Dr.ir. C.M. Dohmen - Janssen
Dr.ir. M. van Ledden
Ir. A.J. Lansen

ROYAL HASKONING

University of Twente
Enschede - The Netherlands

Summary

After hurricane Katrina, a lot of attention has been raised for coastal protection near New Orleans. The protection structures of New Orleans had to be restored and at some locations new structures are planned. To design these coastal enhancement plans, it is important to know the forces acting on the system. Especially the effects of the large area of marshes in front of the New Orleans coast are still uncertain. The predictions of surge heights are expected to be pretty well. For wave heights in relation to the marsh vegetation there are more doubts. The fact that very limited data is available of waves in the area and that wave models do not incorporate vegetation, results in large uncertainties in the predictions.

Therefore the objective of this study is:
Determination of marshland influences on wave attenuation in the surroundings of New Orleans.

To fulfill the objective, the following main research questions are answered:

1. How do friction formulations in SWAN perform when applied to vegetated areas?
2. What improvements can be realized with detailed friction formulations for vegetation?
3. What is the effect of marshlands on the wave propagation towards New Orleans and its surroundings?

After reproducing multiple data sets in SWAN (short-wave model), it is concluded that the present model can reproduce the data when the Collins friction coefficient is altered. Constant friction values per vegetation type are nevertheless not able to explain different wave attenuation patterns in different hydraulic situations.

The use of a detailed friction formulation of Mendez makes it possible to explain different friction coefficients in different hydraulic situations. The formula uses vegetation characteristics and adapted relations between friction and hydraulic conditions to determine the friction due to vegetation. Analysis shows that the predictions of the formula are accurate for kelp vegetation. For stiffer vegetation the method still shows too much inaccuracy. To make the formulation valid for multiple types of vegetation, a factor is added that takes into account the stiffness of the vegetation. Especially the differences in bending effects of stiffer plants should be compensated. With the added factor, stiff vegetation is described in a better way.

To determine the effects of the marshes in front of New Orleans on nearshore wave propagation, a SWAN grid of the area is used. To calculate the friction of the vegetation in the area, an iteration process is applied. The iterative process is necessary because calculated friction coefficients result in changed wave characteristics, which are part of the input for the friction calculations. A Matlab script is developed that calculates the friction coefficients and operates the iteration process of the SWAN model. The formulations developed in this study converge to the correct values for the testcases and also in the grid of New Orleans the friction coefficients converge.

With the created friction files, wave characteristics near New Orleans are calculated for the situation of hurricane Katrina. The calculations result in little effects due to the marsh vegetation when wave period, orbital motion and depth are large. Because just at the south of St. Bernard the hydraulic conditions are moderate enough, the marsh vegetation has a significant effect over there.

To get an impression of the importance of marshland protection, different scenarios are created that give predictions for the year 2050. This results in the conclusion that wave heights near the planned MRGO storm surge barrier can increase up to 20cm if no marsh restoration measures are applied. The wave heightening is mainly caused by the, to marsh restoration related, change in bottom height. South of St. Bernard, wave heights are predicted to increase up to 40cm. For a big part, these effects are directly related to the friction of the marsh vegetation.

From the results of this study it is recommended to use vegetation characteristics to obtain friction of vegetation. It is also recommended to use different hydraulic relations than for non-vegetated areas. Furthermore it is recommended to perform more experiments on wave attenuation over stiff vegetation. This is needed to validate the relations developed in this study more thoroughly.
For the flood protection of New Orleans, the model predicts marsh influences to be less important than expected before. Nevertheless, significant effects of marsh restoration on flood protection are still expected. Therefore it is recommended to consider marsh restoration for improving and restoring New Orleans' coastal defences.

Preface

This report is part of my final project to complete the Master part of the study Civil Engineering and Management at the University of Twente, The Netherlands.

The subject 'Wave attenuation over vegetation' is chosen because of the combination of ecological aspects and man made technical structures. In my opinion it is very interesting to see the effects of human activities on the natural system and the impacts that changes in the natural system have in return. This interaction has often been neglected in the past, but the relevance of the complex interaction between man and its environment became clearer in the last decennia. For me, this is one of the attractive parts of the study Civil Engineering.
The focus on the marshes near New Orleans is applied because the subject is locally under a lot of attention and the precise effects are still unclear. This makes it is an interesting subject to study. Also important for the focus on New Orleans was the opportunity to go there.

For this opportunity and all of the activities organized in the US, I would like to thank Royal Haskoning and Mathijs van Ledden a lot. It was very interesting, and a lot of fun, being there. For the good times over there I would also like to thank the other Haskoning employees in New Orleans. Especially Maarten Kluyver I would like to thank for the interest and support in the project and of course for the non-project related times. Finally I would also like to thank my two fellow students in New Orleans, Marcel van de Berg and Marcel van de Waart, for the nice three months spend together over there.

Furthermore I would also like to thank Marjolein Dohmen-Janssen, Lisette Bochev-van der Burgh, Joost Lansen and Suzanne Hulscher for the support and contributions during the different stages of the project.

Finally I would like to thank my parents and friends for the support during this project and my whole study.

Mats Vosse
Enschede, November 2008

Table of contents

Main report

Appendices

1 Introduction

1.1 Context of research problem

First the context of the research problem is described in a broad view, secondly the context is focused specifically on the area near New Orleans.

Effects of wetlands on wave propagation

All around the world, coastal areas face changing conditions. It is expected that sea level will rise and intensification is predicted of extreme weather like hurricanes and other storm and rainfall events. Next to the increased natural threat, some of the natural defense systems against flooding are affected by human activities and coastal areas got more populated in the last decennia. For instance, large parts of mangrove forests disappeared in south-east Asia and economic activities and population grew rapidly near the coast of countries like Bangladesh. With increasing flooding probability and the increase in potential damage, the total risk of inundation becomes larger.

In reaction to increasing flooding risks, large wetland restorations are executed in for instance Indonesia and Vietnam (Mazda 2005, Burger 2005). After the tsunami of December 2004 even more attention was raised for the restoration of wetlands. Not much was known about wetland influence, but it was widely believed that the loss of large areas of mangrove wetlands increased the impacts of the tsunami. Current research of Dijkman (2005) and Temmerman (2008) confirms surge reduction due to mangroves, but just after kilometers of vegetation. First, surge tends to pile up because vegetation slows down the bulge of water, resulting in higher water levels. Several kilometers of wetland are needed (depending on wetland type) before the dissipation of energy compensates the surge build up. Then the water levels become lower than they would have been without vegetation.
For waves, the influence of wetlands is still less clear. Waves are nevertheless a very important part of storm effects. For instance, as a result of cyclone Sidr in 2007, waves approaching Bangladesh were up to 6 meter high. Thereby the waves caused a significant part of the tragic flooding effects that resulted in 5-10 thousand casualties (weerwetenswaardigheden.nl from KNMI). Additional knowledge about wave propagation over wetlands can provide useful insights in safety situations in coastal areas and can help in the optimization of wetland restoration programs.

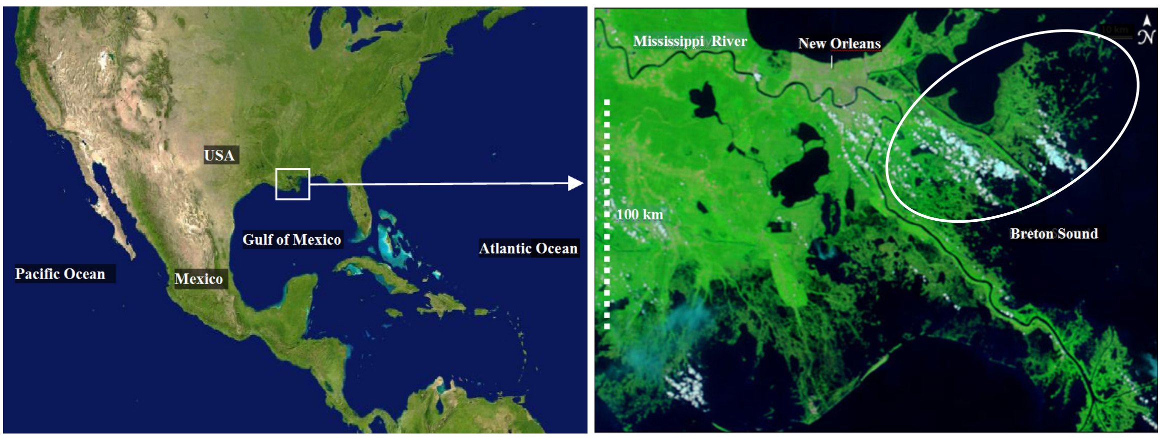

Figure 1.1.1: The location of the relevant marshes for this study (oval) and the city of New Orleans. (map24.nl, acs.org)

Marshlands near New Orleans

This project focuses particularly on the situation in the surroundings of New Orleans. The city is located in the coastal area and it is partly separated from the sea by marshlands. The marshlands which influence hurricane driven surge and waves the most are located south and southeast of the city (Figure 1.1.1). Throughout history, New Orleans flooded several times due to hurricanes approaching from the Gulf of Mexico. The most important recent inundation took place on the 29th of August 2005 as an effect of hurricane Katrina. The flooding resulted in an estimated economic damage of 125 billion dollar (usatoday.com), severe social disruption and about 1800 casualties (dhh.louisiana.gov).

After this flooding, many questions were raised on the subject of flood protection, also in relation to the wetlands of the area. It is stated in many articles that the probability of inundation increases because of wetland degradation in the city's surroundings (nwf.org, acs.org). The wetlands erode for several reasons. The main reasons are mentioned briefly.

Reduced sediment attribution to marshlands
Approximately 67 percent less sediment is transported by the Mississippi since 1950 because of reduced erosion from agricultural land and creation of upstream reservoirs. Due to man-made levees most of the remaining transported sediments flow into the Gulf of Mexico nowadays. Therefore marsh erosion is hardly compensated by accretion of river sediment anymore (USACE 2004 from Kesel 1988).
Channels through marshlands
In the study area, 10 major navigation channels and many smaller ones are present. The channels cause an increased salt intrusion in freshwater ecosystems and thereby damage the vegetation. Damaged vegetation results in less stable marshes that erode more easily (USACE 2004 from Flynn 1995). Furthermore the large channels allow waves to reach further into the marsh area. The waves cause additional erosion and even more salt intrusion into the fresh water ecosystem (USACE 2004).
Relative sea level rise
Relative sea level rise also causes increased wave and salt intrusion. The relative sea level rises both due to a world wide sea level rise and due to subsidence of the marsh area. The amount of sea level rise is not agreed upon by everyone, but a mean sea level rise is measured in many places. Subsidence occurs because sediments consolidate, groundwater is extracted and it is likely that oil and gas extractions also stimulate subsidence (USACE 2004).
Erosion of barrier islands
Another cause of marsh degradation is the degradation of barrier islands in front of the coast (Figure 1 in Appendix 4.1A). Stone (2003/2005) reports that barrier islands are important for marsh erosion. The islands separate the Gulf of Mexico from the shallow estuarine environment and thereby influence salinity levels and the propagation of waves and surge. The islands erode and get breached by hydraulic forces. This degradation of the islands is mainly expected to be a natural process, particulary due to storm events. The increased wave propagation resulting from the erosion of barrier islands causes higher energy levels onto the coast and therefore degradation of the wetlands. The additional saltwater intrusion due to higher surge and waves also stimulates the degradation process.
Storm events
Tropical storm events can directly and indirectly contribute to coastal land losses. Wave energy will erode land and its vegetation. The eroded sediments will partly be redistributed over the coast, but especially near the shoreline net erosion will occur. Storm events also cause salt intrusion far into the fresh water marshes, resulting in marsh degradation. The relevance of erosion due to storm events is indicated by the average number of hurricanes that affected the coastline of Louisiana since 1871, which is approximately 0.8 per year (USACE 2004).

The scale of the erosion since 1839 is presented in Figure 1.1.2. In total, over fifty percent of the once present marshland area has been eroded (Dijkman 2005).

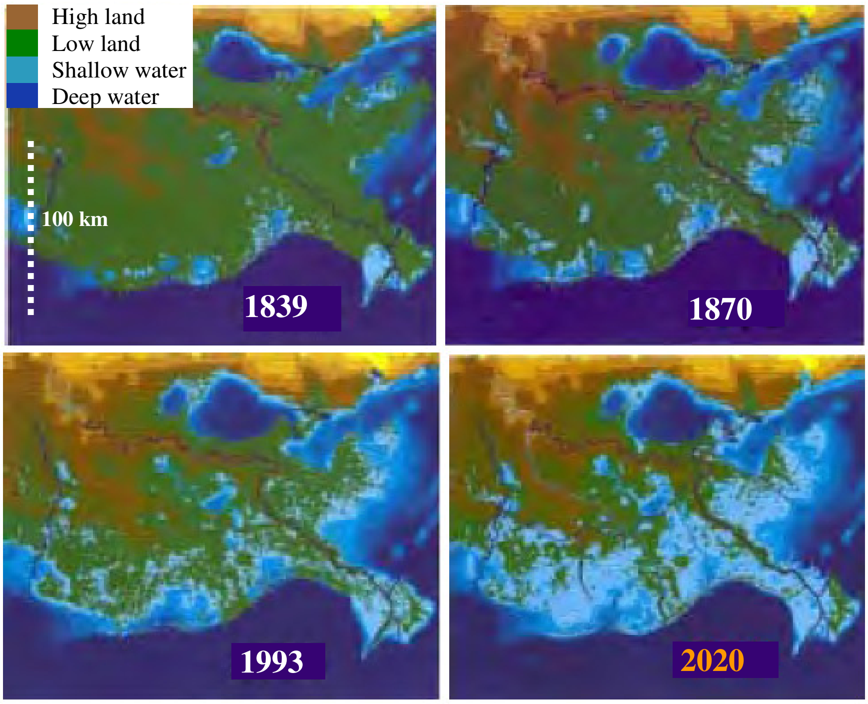

Figure 1.1.2: Deterioration of marshlands in time. (Dijkman 2005)

The deterioration of marshland influences multiple functions in the area. The ecology is damaged, tourism gets affected, fishery revenues go down and freshwater supplies (for drinking water, irrigation) are reduced. Next to these effects, also the flood protection level of New Orleans changes. However, as mentioned before, the effects of the marshlands on waves are not clear yet.
Smith (2007) predicted wave heights that decrease several meters during their propagation over New Orleans' marshlands. It is nevertheless mentioned that these results are uncertain. Elwany (1995) claims vegetation has no measurable effects in front of the Californian coast, while it is also stated that a wave height reduction of approximately 40% occurs over an 80m wide salt marsh (Moller 1999 from Brampton 1992). All together, multiple papers claim that influences of salt marshes on wave height can be significant, but also that present models do not predict the influence adequately. It is also stated that good measurements are lacking most of the time (Bender 2007, Westerink 2007, Kobayashi 1993).
Next to the wave heights, it is also important to focus on the wave periods. Both parameters determine the wave force on the flood protection structures (Van Rijn 1990).

Despite the uncertainties in wetland effects on flood protection, the US government has plans for large restoration programs. The programs cost billions of dollars and are therefore very controversial and subject of a lively debate. Especially the Coast 2050 restoration project (coast2050.gov) is mentioned frequently, which has execution costs of about 14 billion dollar. This is a huge amount of money compared to the current investments in the wetlands of 50 million dollars a year (sfgate.org), but still it got unanimous approval from all 20 Louisiana coastal parishes and various other organizations (lacoast.gov). The proposed investments are supported because of nature recovery, fishing revenues and the protection of freshwater supplies, but the projects are also expected to contribute to the flood protection.

For such large projects it is important that the marshlands' attribution to coastal defense is known. Knowledge on the subject enables the decision makers to make a better trade off between restorations and for instance levee heightening. Also for other projects in the area, like building plans, oil/gas extractions or the development of the planned MRGO storm surge barrier, more understanding of the effects of vegetation on wave propagation is desired.

1.2 Friction due to vegetation

To understand the basic problems in describing the wave-vegetation interaction, the effects that vegetation has on waves are discussed in this paragraph. There are multiple aspects of the interaction between waves and vegetation that differ from the influence of a gravel or sand bottom on waves. Aspects that cause deviations from non-vegetated bottom roughness are vegetation density, height, structure and the changes in different seasons. Also important for a better description of the vegetation friction are the water depth in relation to the vegetation height, the fact that vegetation bends due to wave forces, that wave energy can reflect back from vegetation stems, and whether vegetation is submerged or emerged (Westerink 2007).
Below it is shown why all these different aspects have to be taken into account in determining the friction caused by vegetation.

Density

The report of Meijer (2005, from Nepf 1999) shows that drag coefficients of vegetation increase in a non-linear and non-exponential way with increasing density. The different lines in Figure 1.2.1 show that the patterns in which vegetation is placed cause relevant variations. The dotted lines, with different n-values, represent the various patterns (for instance placement in straight lines or staggered). The dependency of the friction on density shows that the attribution of a specific friction value per vegetation type is probably not valid. The density of vegetation at a specific location of interest can be different from the density at other locations, resulting in a location dependent friction value.

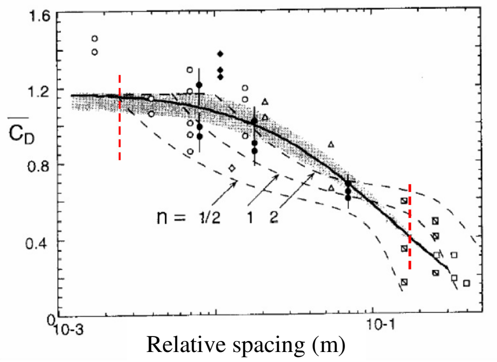

Figure 1.2.1: Influence of vegetation density on the drag coefficient. The n-values represent different vegetation patterns. (Meyer 2005 from Nepf 1999)

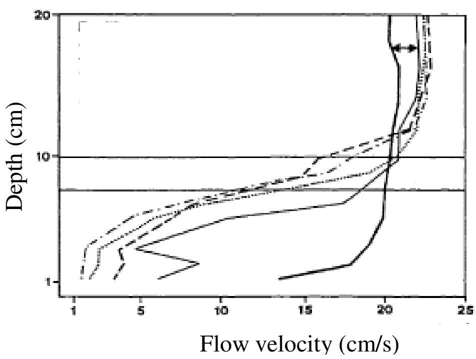

Figure 1.2.2: Velocity profiles over depth. Thickest line is without vegetation, other lines are with vegetation. (Tschirky 2000 from Gambi 1990)

Vegetation height / relative water depth

The height of vegetation causes a different resistance pattern over the water depth and therefore also a different flow pattern and a different influence on waves. Figure 1.2.2 shows the effect of bottom roughness compared to vegetation effects, measured in flume experiments. It is concluded that vegetation height influences the flow pattern and different vegetation heights therefore cause different flow patterns. Velocities within the vegetation field are reduced while flow velocities above the vegetation increase compared to the non-vegetated situation. Therefore it is relevant to determine the vegetation height.

As becomes clear from Figure 1.2.2, the flow through the vegetation encounters a different friction than the water above the vegetation. Therefore, the total friction in the water column will change differently with depth for vegetated areas than for non-vegetated areas. For this reason, the vegetation height in relation to the overall water depth should be taken into account too.

Vegetation structure

Different plant species have a different structure. For instance, the amount of leaves and branches per plant and their distribution over the height are different per species. Figure 1.2.3 shows a distribution of the amount of structures per stem over height. So in this case, the vegetation is denser near the bottom than at the top. The presence of more structures leads to a higher resistance at certain heights.

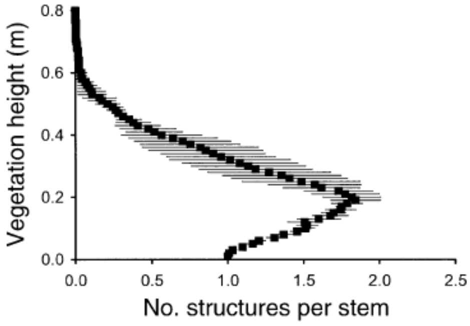

Figure 1.2.3: The average number of structures per stem over the height of a specific plant species. (Bouma 2005)

Seasonal changes

As is clear from falling leaves in autumn, vegetation properties can change significantly over the year. It ranges from total disappearance each year to constantly green vegetation. For this reason it can be relevant in which season storm events occur.

Bending of vegetation

The stiffness of vegetation causes different bending patterns of vegetation due to wave forces. This results in different friction values. Figure 1.2.4 shows that stiffer vegetation results in increased wave dissipation, which can be explained by the fact that stiffer vegetation will less easily follow the flow patterns below waves. The inertia of mass will also reduce the bending of vegetation due to water motion and therefore this will also increases the friction on waves.
The flow patterns that occur as a result of propagating waves are shown in Figure 1.2.5. Waves result in an orbital motion that has its maximum velocity at the top of the water column. Near the bottom, orbital flow velocities are reduced and the flow pattern is flattened (more oval than circular) in shallow water.

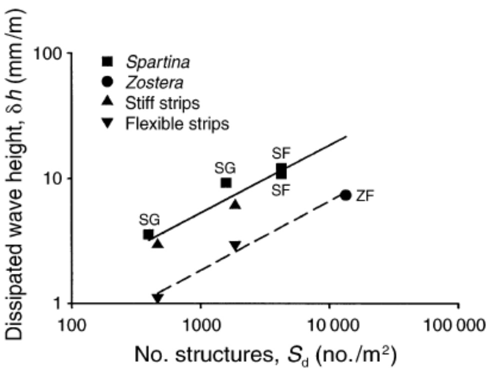

Figure 1.2.4: Different friction effects for different vegetation stiffness. (Bouma 2005)

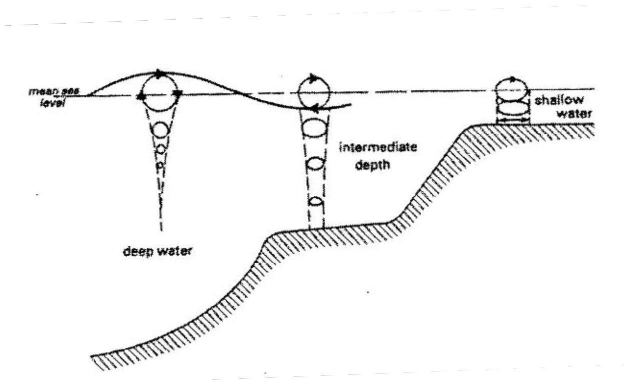

Figure 1.2.5: Orbital motion in the water column as a result of waves. (Van Rijn 1990)

Wave energy reflection of vegetation

Just like waves can reflect from levees, wave energy can also reflect from the edges of vegetation. The amount of reflection will depend on the height of the vegetation edge, the stiffness of the vegetation and the density of the vegetation field.

Submerged or emerged vegetation

As mentioned above, the water depth in relation to vegetation height has impact on the wave dissipation. This relation between inundation depth and dissipation has an abrupt transition when the situation changes from emerged towards submerged vegetation. According to Westerink (2007), submerged vegetation can result in 60% less energy dissipation than emerged vegetation. One of the possible reasons for this difference is that emerged structures can induce breaking of waves. This principle is for instance applied in wave breaking structures that protect multiple coastal areas.

1.3 Modeling friction due to vegetation

To determine the impact of vegetation on waves that approach New Orleans, it is necessary to use a model for the calculations. The area is about 50x100km large and has a complex bathymetry with lakes and canals. Because the area of interest is in shallow waters and wind waves are analyzed, a short wave model should be used. These models are designed to compute wave propagation in coastal areas on a 2-dimensional horizontal grid. The present wave models do not specifically incorporate the effects of vegetation. It is therefore investigated in this study how vegetation can be represented in such a model properly. Therefore, the appropriate model for this project is selected in this paragraph, the friction formulations in this model are discussed and previous model representations of vegetation are presented.

Short wave model choice for this project

The short wave models that are applied most often in the study area are STWAVE and SWAN. These models have both been run and tested with the bathymetry of the area and are therefore the best options for this project. A description of both models is presented below. The model selection for this project is also presented below.

SWAN

SWAN (Simulating WAves Nearshore version 40.51) is developed at the Delft University of Technology. In principle it is a stand alone program, however it can also be integrated in other software. It is for instance integrated in the well known Delft3D software. The basic idea of SWAN is that a wave spectrum is implemented at the borders. Subsequently, the attributed bathymetry, bottom friction, water levels and wind fields are used to calculate different aspects of wave propagation (netcoast.nl, wldelft.nl).

The SWAN calculations are based on the action balance. The advantage is that a wave action approach can handle additional currents correctly, while an energy spectrum approach cannot. The following aspects are taken into account for calculating the propagating waves; the wave propagation in time and space, shoaling, refraction due to currents and depth, frequency shifting due to currents and non stationary depth, wave generation by wind, nonlinear wave-wave interactions, whitecapping, bottom friction, depth induced breaking, wave induced setup, propagation from laboratory up to global scales, diffraction, transmission through and reflection from obstacles. Two limitations are that a mild bottom slope is assumed and that currents are supposed to be depth uniform (fema.gov I, netcoast.nl, tudelft.nl).

An indication that SWAN is a general accepted model is given by the fact it is used in about 50 countries and 700 institutes are registered users (tudelft.nl). The current version of SWAN is supported by the Dutch government (Rijkswaterstaat). Previous releases of SWAN have also been supported by the US government (Office of Naval Research) but in the new release this is not the case (netcoast.nl).

STWAVE

The STWAVE (STeady state spectral WAVE) model is developed by the USACE (US Army Corps of Engineers) Waterways Experiment Station (WES). Because the USACE is the major institute responsible for water management in Louisiana, it is a commonly used model for projects near New Orleans. To run the model, input is needed on the wave spectrum, the wind field, water levels and bathymetry (fema.gov I).

STWAVE is also based on the wave action balance and almost the same aspects are taken into account as in SWAN. It computes wave refraction, shoaling induced by depth and current interaction, wave breaking based on water depth and steepness, wind induced wave growth and wave whitecapping influence on the wave spectrum (usace.mil I).
The assumptions in the model are a mild bottom slope, spatially homogeneous offshore wave conditions and steady-state waves, currents, and wind fields. Furthermore, a linear refraction and

shoaling is assumed and currents are supposed to be depth-uniform. Diffraction and bottom friction are not taken into account yet, but these developments are in progress (usace.mil II).

Trade off

The performance of the short wave models is probably not that different that this will exclude one of them. Smith (2007) uses both the SWAN and STWAVE model and compares the two. It is tested whether the fact that STWAVE assumes that the waves reach an equilibrium state is a problem. In this case, the steady-state assumption was assessed as adequate and the models did coincide reasonably well.

However, from the mentioned models, the SWAN model is used in this project. This choice is based on several aspects. An important aspect is that it is available to use, including the bathymetry of the project area. Next to this, there is experience with the SWAN model within Royal Haskoning and there is an example available in which vegetation is modelled to some extend. Another major advantage of the SWAN model for this project, is the presence of bottom friction in the model. This is helpful for the implementation of vegetation. So overall, SWAN has practical and technical advantages over STWAVE for this study.

Friction formulations in SWAN

Three different friction calculation methods are implemented in the SWAN model. These are the method of JONSWAP, Collins and Madsen. All of the methods are created to represent continental shelf seas with sandy bottoms (Booij 1999). The formulations for these bottom friction models can all be expressed as in Equation 1.3.1. The different characteristics of the methods are presented below. A trade-off on the best method to be applied in this study is also presented. The parameters applied in the equations of this paragraph (1.3) are explained in Table 1.3.1.

Table 1.3.1: Parameters applied in Paragraph 1.3.

Parameter	Meaning of parameter	Unit
θ	wave direction normal to wave crest	degree
σ	wave frequency	s^{-1}
a_b	near-bottom excursion amplitude	m
C_b	bottom friction	m^2/s^3
C_f	Collins friction coefficient (0.015 for North Sea sand)	-
d_v	vegetation height	m
D	stem diameter	m
E	wave energy	J/m^2
E_d	dissipation of wave energy	J/m^2
f_w	friction factor	-
g	acceleration of gravity	m/s^2
h	depth	m
k	wave number	m^{-1}
K_N	bottom roughness height (0.05m for North Sea sand)	m
m_f	-0.08 (tudelft.nl from Jonsson 1976)	-
N	vegetation density	units/m^2
$u_{c,bottom}$	near bottom orbital velocity	m/s

$$E_d = -C_b \frac{\sigma^2}{g^2 \sinh^2 kh} E(\sigma, \theta)$$

Equation 1.3.1: Dissipation of wave energy.

JONSWAP method

The JONSWAP method is based on empirical measurements in the North Sea during the JOint North Sea WAve Project. From these measurements, a bottom friction was determined of $C_b = C_{JON} = 0.038 m^2 s^{-3}$ for swell conditions (tudelft.nl from Hasselmann 1973). For fully developed wave conditions in shallow waters, a bottom friction of $C_{JON} = 0.067 m^2 s^{-3}$ was extracted from the JONSWAP data. Both values are available in SWAN (tudelft.nl from Bouws 1983).

Collins method

The Collins method is based on the drag law model of Collins. The expression is based on a conventional formulation for periodic waves which is adapted to cope with wave spectra. The dissipation rate is again calculated with the presented formula for energy dissipation (Equation 1.3.1). In this method a variable bottom friction is implemented (Equation 1.3.2), including the orbital velocity near the bottom (Equation 1.3.3) (tudelft.nl from Collins 1972).

$$C_b = C_f g u_{c,bottom}$$

Equation 1.3.2: Bottom friction in the Collins method.

$$u_{c,bottom}^2 = \int_0^{-2\pi}\int_0^{\infty} \frac{\sigma^2}{g^2 \sinh^2 kh} E(\sigma,\theta) d\sigma d\theta$$

Equation 1.3.3: Orbital velocity near the bottom.

Madsen method

The Madsen method is based on the eddy viscosity. This results in a formulation where bottom friction is a function of the bottom roughness height and wave conditions. Equation 1.3.4 presents this formulation (tudelft.nl from Madsen 1988). In this relation, a non-dimensional friction factor is included that can be calculated by a formulation of Jonnson (tudelft.nl from Jonsson 1966), as presented in Equation 1.3.5. In this equation, the excursion amplitude (a_b) is implemented, that is calculated with Equation 1.3.6.

$$C_b = f_w \frac{g}{\sqrt{2}} u_{c,bottom}$$

Equation 1.3.4: Bottom friction in the Madsen method.

$$\frac{1}{4\sqrt{f_w}} + \log_{10}\left(\frac{1}{4\sqrt{f_w}}\right) = m_f + \log_{10}\left(\frac{a_b}{K_N}\right)$$

Equation 1.3.5: Formulation to determine the non-dimensional friction factor (f_w). For values of a_b/K_N smaller than 1.57 the friction factor f_w is 0.30. (tudelft.nl from Jonsson 1980)

$$a_b^2 = \int_0^{-2\pi}\int_0^{\infty} \frac{1}{\sinh^2 kh} E(\sigma,\theta) d\sigma d\theta$$

Equation 1.3.6: Determination of the near-bottom excursion amplitude

Trade off

Because the JONSWAP method cannot account for variations over the model area, it is not useful in this project. Therefore just the Madsen and the Collins method are compared briefly. The performance of both the methods is compared for a situation with and without vegetation. These measured data sets are from the experiments of Lovas (Mendez 2004), as presented in Chapter 2.

The Madsen method uses the bottom roughness height K_n. The default value for situations without vegetation is 0.05m. Collins uses a dimensionless coefficient with a default value of 0.015 for non-vegetated bottoms.
For the measurement in non-vegetated shallow water (Figure 1.3.1), the SWAN calculations with the Collins method show an average deviation of 2% and a maximum deviation of 5% with the data. With the Madsen method these deviations are respectively 6% and 10%.
For the vegetated measurement (Figure 1.3.2) the best fitting Collins coefficient (0.3) results in an average deviation of 3% and a maximum deviation of 6%. For the Madsen method the best-fit has deviations of respectively 8% and 17%. The Madsen runs with a roughness height above 0.5m (0.5/1/50/100/130) all have about the same results. This can be explained by the fact that the friction factor cannot exceed 0.3, as shown in Equation 1.3.5. Nevertheless, more friction is needed to represent the data properly.

Because the maximum friction with the Madsen method is too low, the method is less applicable here. For this reason the Collins friction formulation is used in this project. Another reason to use the Collins method is that a vegetation module for SWAN, that would possibly be used, is also programmed using the Collins coefficient (Burger 2005).

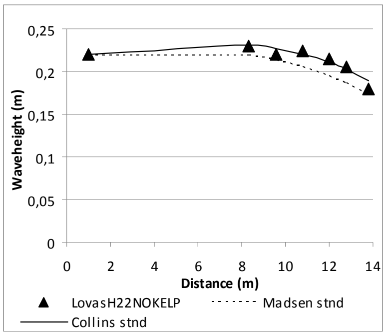

Figure 1.3.1: Lovas' data without kelp compared to a SWAN run with standard Collins friction coefficient (0.015) and standard Madsen coefficient (0.05m).

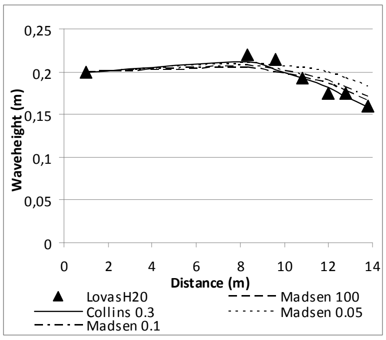

Figure 1.3.2: Lovas' data with kelp compared to a SWAN run with fitted Collins friction coefficient (0.3) and best fitting Madsen coefficient (.5-100m).

Previous vegetation representations

To get an impression on how vegetation can be represented in a detailed way, some of the previous developed theories are described in this paragraph. Some of the older methods to represent vegetation are described in Appendix 1.3A. The methods presented here are the most relevant ones for different reasons. They are improvements of the previous developed theories, they are validated with data sets and/or they are practical to use within a model like SWAN.

Mendez 1999

Mendez (1999) produced an advanced model that describs many of the physics related to vegetation below wind waves. Computations are implemented using momentum, forces on vegetation and for instance the specific gravity and stiffness of vegetation. Limitations of the model are that it assumes a flat bottom and that wave breaking is not taken into account. With a lot of the physics described in the model, it became possible to calculate many aspects of vegetation friction on waves. For instance, the friction of plants is based on relative water motion, the drag coefficient of the vegetation surface and the shape of the vegetation. Vegetation motion and its effects are calculated with the friction between water and vegetation related to the stiffness of vegetation.

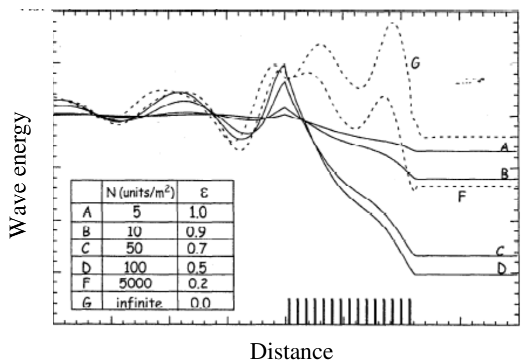

Figure 1.3.3: Reflection of wave energy due to vegetation. ε is the volume density of vegetation in water. (Mendez 1999)

Wave reflection from vegetation does strongly depend on the porosity of the vegetation edge and the height of the vegetation. Effects of emerged vegetation can also be calculated, because all of the forces are described in detail. The water level can just be lowered in the calculations resulting in the fact that all of the wave motion is within the vegetation field. Effects of the interaction between vegetation and the water surface are not taken into account specifically. The model is also developed in such a way that it is possible to calculate all of the effects for wave spectra. Figure 1.3.3 shows the results of wave propagation calculations with the model. The energy pattern in front of the vegetation edge occurs due to energy reflection from the vegetation, a steep decrease after the vegetation edge does also result from the model (lines A,B,C,D).

Mendez 2004

In 2004, Mendez created a simplified model compared to the previous described model. One of the mentioned reasons is an easier implementation in short wave models. Aspects such as reflection are neglected, just like vegetation motion. Nevertheless, it is still valid for wave spectra and also for sloping bottoms now (it is mentioned this is the first vegetation model incorporating both these effects). The model is valid for subsurface vegetation that is relatively low with most of its strength in its lower parts. As examples, the vegetation species L. Hyperborea, P.Oceanica are mentioned just like seagrass meadows and Spartina marshes.
The swaying motion, bed friction and inertia of mass due to vegetation are included in a drag coefficient C_D. It is therefore called a bulk drag coefficient. The formula is verified with kelp vegetation, but not for other plants yet. As a basis for the formulation, the energy dissipation formula of Dalrymple (Appendix 1.3A) is used. Formulas of this method are presented in Chapter 3.

De Vries

De Vries implemented vegetation in SWAN by replacing the Collins friction coefficient. The Collins method is replaced by an energy dissipation formulation of Van Rijn. The formula is presented in Equation 1.3.7. So characteristics of vegetation are taken into account and related to orbital motion. The model results showed a good agreement with measurements in the Paulinapolder salt marsh (The Netherlands). Only the wave propagation near the edge of the salt marsh did not correspond very well with the observed waves. Furthermore there is a, vegetation dependent, friction factor that still needs calibration (Burger 2005 from De Vries 2004).

$$E_d = \frac{4}{3\pi} \cdot \rho \cdot u_{c,bottom}^3 \cdot f_w \cdot D \cdot N \cdot d_v$$

Equation 1.3.7: Dissipation of wave energy in De Vries' method.

Meijer and Burger

Meijer (2005) and Burger (2005) also developed a module in SWAN to take the vegetation effects into account. Therefore, the energy dissipation formulae by Mendez (2004) are used. To cope with different resistances over depth, due to vegetation structure, the module can calculate different layers of energy dissipation for the same location. The energy dissipation in every layer is calculated with the same flow velocities and is added afterwards, without interaction. The bulk drag coefficient (C_D) is used as a calibration parameter. Because C_D varies even with constant vegetation, the module is not suitable to predict friction due to vegetation. It is not clear why the Mendez (2004) formulation for C_D is not used in these projects. Another problem that occurred was similar to the problem that occurred in the model of De Vries. Near the edge of the Paulinapolder marsh, the calculated wave heights did not correspond very well with data.

1.4 Problem analysis

Problem formulation

No detailed estimations can be made for the influence of marshlands on wave attenuation in front of the New Orleans coast. This lack of knowledge limits the ability to predict the forces on the coastal protection structures. It is therefore a limitation in the decision making process on restoring and improving New Orleans' coastal protection.

A problem in determining the effects of marshlands is that short wave models do not contain vegetation modules. One of the reasons that these models do not account for vegetation is probably that it is still unclear what the precise effects of vegetation on friction are. Adaptations in the friction computations of a short wave model, or determination of the best way to represent vegetation within the model, might be necessary to determine the marsh influences in a proper level of detail.

Objective

Determination of marshland influences on wave attenuation in the surroundings of New Orleans.

Scope

This project focuses on the coastal protection structures of New Orleans. Therefore the influence of marshland on waves at the eastside of the Mississippi is relevant.
To determine the influence of marsh restoration on coastal protection, scenarios are developed with estimated future conditions. The temporal scope for these scenarios is between 2008 and 2050. The final year is selected because wetland restoration programs are focused on this moment in time and provide estimations of land development for this year. Furthermore, it seems a reasonable period of time to see the effects of land reclamation, and it is not that far into the future that it would be considered as irrelevant for current events.

Research questions

Based on the problem formulation and the research objective for this study, the following main research questions are formulated:

1. How do friction formulations in SWAN perform when applied to vegetated areas?
2. What improvements can be realized with detailed friction formulations for vegetation?
3. What is the effect of marshlands on the wave propagation towards New Orleans and its surroundings?

1.5 Approach and outline of report

To answer the research questions, the following research approach is applied. A schematised overview of this outline is presented in Figure 1.5.1.

First, in Chapter 1, the basic principles of wave attenuation over vegetation are presented. Also the choice is made on which model to use and it is decided which bottom friction formulation from the model is used in this project. Furthermore several previous developed theories are discussed.

In Chapter 2, the SWAN model is used to test whether the Collins friction formulation can represent wave attenuation due to vegetation. Therefore, a data set is obtained that contains measurements of propagating waves over vegetation. It is tested whether an adapted value of the friction coefficient in the model can reproduce the effects of vegetation. It is also tested whether each vegetation species can be described with a single friction coefficient. Finally, it is investigated whether there are patterns that point at certain relations between vegetation or hydraulic characteristics and the friction coefficient.

The second research question is examined in Chapter 3. It is investigated whether detailed formulations on the relation between vegetation and friction can improve the model results. Results of the method are compared to a fixed friction coefficient per species. The used detailed friction formulations are based on the most suitable theory selected from Paragraph 1.3. This theory is validated with the available data set and adaptations are made where necessary. Because it is the objective to use the friction coefficient for friction calculations in the New Orleans grid, it is also determined how friction coefficients can be attributed to a large 2-dimensional grid.

Chapter 4 focuses on the impact of the marshes on propagating waves towards New Orleans. Thereto SWAN is run with the most suitable friction formulation that is found for vegetation in relation to waves. To show the predicted importance of marsh restoration, the effects of the marshes on waves in different future scenarios are evaluated.

In Chapter 5, the discussion is presented. Various subjects that are limitations, drawbacks or implications of this study are discussed briefly. Finally, the conclusions and recommendations are presented in Chapter 6.

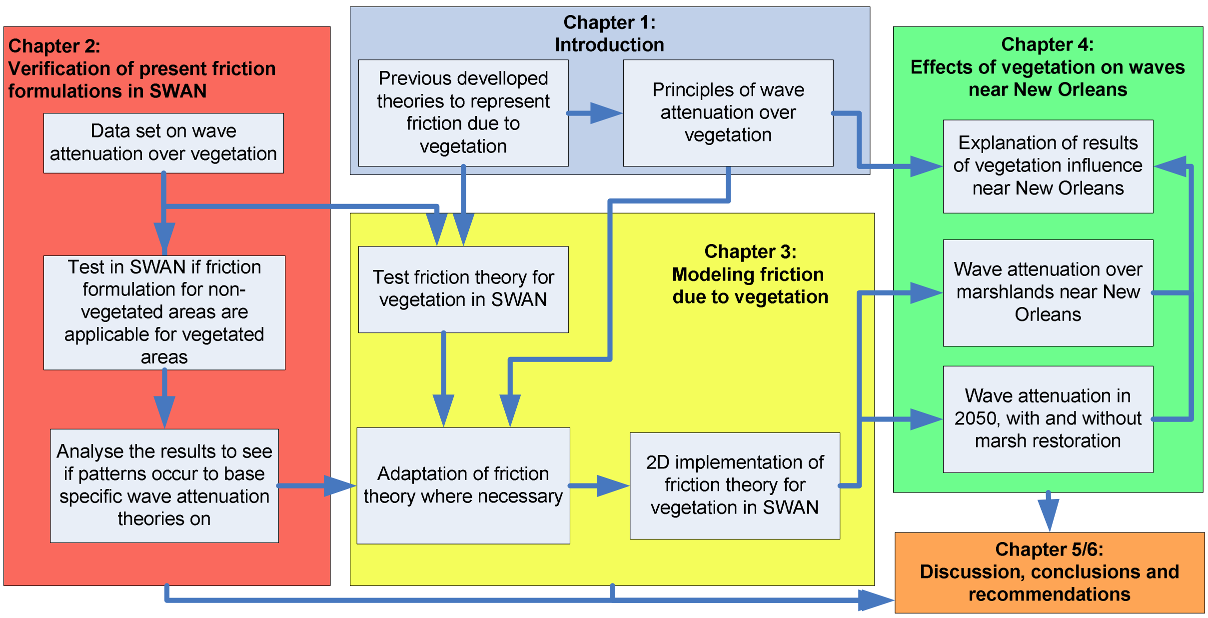

Figure 1.5.1: Schematized representation of the outline of this study

2 Verification of existing friction formulae in SWAN for vegetated situations

To prevent confusion, the terminologies used for describing the test cases are explained first.
- Case: refers to the complete set of measurements executed in a flume or at a field site.
- Measurement: refers to one set-up within a case, so a specific hydraulic and/or vegetation setting.

As mentioned in Chapter 1, this project is executed with the short wave model SWAN. The friction formulation in SWAN that is used, is the Collins formulation. In this chapter, the Collins method in the SWAN model is analyzed and conclusions are drawn on the possibilities to use the Collins coefficient to represent vegetation.

The analysis of SWAN and the Collins friction formulation are performed in the following steps:
- It is investigated whether the measurements over vegetation can be reproduced by altering the Collins friction coefficient for each measurement. The coefficients are supposed uniform over the vegetated area. This is done to determine if the wave dissipation over vegetation follows the same pattern as over other rough surfaces.
- An average friction coefficient per case is tested. For most cases this means a fixed friction coefficient per vegetation set-up, because vegetation is constant within the measurements of these cases. With such an average friction coefficient per vegetation type, no model adaptations would be needed if it fits the requirements.
- It is attempted to find patterns between different parameters (vegetation characteristics, hydraulic situations) and the friction coefficient. This is done by relating the parameters to the best fitting Collins coefficients and by analyzing the deviations that occur with a fixed friction coefficient. The influence of different parameters on the friction coefficient can help in finding the best representation of vegetation.

The description of the used testcases is presented in Paragraph 2.1, the set-up of the SWAN model is described in Paragraph 2.2. Paragraphs 2.3-2.6 show the results of the analysis.

To decide when the SWAN model predicts the different situations accurate enough, a threshold is determined. This threshold is set to 10% deviation between wave heights from the model output and the actual wave heights from the data. This value is taken because it is the same deviation that is often assumed for SWAN model output in non-vegetated situations.

2.1 Description of testcases

To check the performance of the SWAN model in a vegetation field, data sets are necessary to compare with model output. The six cases used for this purpose are described below. More details are presented in Appendix 2.1A. The main reason why these data sets are used is that they represent measurements of waves over vegetation. The quantity of data on this subject is very limited. Therefore, every case obtained from literature is used when it is described in a reasonable amount of detail.

Within the acquired data set, no data is present that is specifically focused on waves that are created by hurricanes. Nevertheless, for the basic characteristics of vegetation-wave interaction the effects are assumed to be equal. This assumption is made because waves during hurricanes, as well as other short waves, are both created by wind and are essentially the same. The main difference is that the wind speeds are much higher during hurricanes. When characteristics of the testcases are compared to the situation during hurricane Katrina, the waves seem not that different. The most important wave factors, wave height and period, are considered. The flume experiments are scaled 1:10 and therefore represent waves up to 2.3m. The wave periods range from 0.8 up to 6.4 seconds. According to current SWAN computations with hurricane Katrina, the wave heights nearshore are most of the time below 3 meter (Chapter 4). Wave periods near the coast of New Orleans are for the main part between 2 and 6 seconds. So the waves due to hurricane Katrina correspond quite well with the data set used in this chapter.

1 Dubi testcase

Mendez (2004) presents data of wave propagation from nine measurements of Dubi. The measurements are performed in a flume with a flat bottom and an 8m long uniform vegetation field. The artificial vegetation represents the species named Laminaria Hyperborea. It consists of a thin stipe of half the height which splits in a few flexible segments (see Appendix 2.1A). The measurement characteristics are presented in Table 2.1.1.

Table 2.1.1: Range of characteristics Dubi measurements

Wave height (root-mean-square)	H_{rms}	0.08-0.23m
Peak period	T_p	1.6-3.8s
Depth	h	0.4-1.0m
Vegetation height	d_v	0.2m
Vegetation density	N	1200 stems/m^2
Vegetation width	b_v	0.025m
Vegetation thickness	t_v	0.001m
Wave spectrum		JONSWAP

2 Osana testcase

Mendez (1999) and Kobayashi (1993) present eight measurements of Osana's experiments. The measurements are performed in a flume with a flat bottom and an 8m long uniform vegetation field. The vegetation consists of artificial seaweed, one flexible strip per plant. The measurement characteristics are presented in Table 2.1.2.

Table 2.1.2: Range of characteristics Osana measurements

Wave height (regular)	H	0.08-0.16m
Peak period	T_p	0.8-2.0s
Depth	H	0.45-0.52m
Vegetation height	d_v	0.25m
Vegetation density	N	1110-1490 stems/m^2
Vegetation width	b_v	0.052m
Vegetation thickness	t_v	0.0003m
Wave spectrum		regular

3 Lovas testcase

Mendez (2004) presents the data sets of wave propagation from nine of Lovas' measurements. The measurements are performed in a 20m long flume with a sloping bottom and an edge in front of the vegetation. The uniform vegetation field has a length of 7.2m. The applied artificial vegetation is the same as in the Dubi case, so it represents Laminaria Hyperborea.
Table 2.1.3 shows some other characteristics.

Table 2.1.3: Range of characteristics Lovas measurements

Wave height (root-mean-square)	H_{rms}	0.12-0.22m
Peak period	T_p	2.5-3.5s
Depth at start of flume	h	0.69-0.77m
Vegetation height	d_v	0.2m
Vegetation density	N	1200 stems/m^2
Vegetation width	b_v	0.025m
Vegetation thickness	t_v	0.001m
Wave spectrum		JONSWAP

4 Bouma testcase

For this case, nine measurements are available from Bouma's (2005) experiments. The main differences between the measurements are the vegetation species. Stiff strips are applied, flexible strips and the real vegetation species Zostera Noltii and Spartina Anglica (Appendix 2.1A for more details). The wave propagation is measured over 2m of vegetation. The other characteristics are presented in Table 2.1.4

Table 2.1.4: Range of characteristics Bouma measurements

Wave height (regular)	H	0.029-0.032m
Peak period	T_p	1s
Depth at start of flume	h	0.12m
Vegetation height	d_v	0.1m
Vegetation density	N	225-13400 stems/m^2
Vegetation width	b_v	0.003-0.005
Vegetation thickness	t_v	-/0.005
Wave spectrum		regular

5 NL testcase

Meijer (2005 from WL|Delft Hydraulics 2003) presents nine measurements of a field experiment in the Netherlands (Paulinapolder). The field site has a length of 25 meter and differs in depth. The main vegetation is Spartina Anglica which characteristics differ between the measuring locations (Appendix 2.1A). Table 2.1.5 shows the other aspects of this case.

Table 2.1.5: Range of characteristics NL field case

Waveheight (significant)	H_s	0.06-0.09m
Peak period	T_p	2.1-6.4s
Depth at start experimental site	H	1.28-2.57m
Vegetation height	d_v	0.30-0.42m
Vegetation density	N	620-1704 stems/m^2
Vegetation width	b_v	0.0023-0.0039m
Vegetation thickness	t_v	0.0023-0.0039m
Wave spectrum		-

6 England testcase

From Moller (1999), nine measurements are obtained of a field measurement in England (Stiffkey). The field site was about 420m long with about 220m of vegetation. The type of vegetation varied over the area, as visible in Appendix 2.1A. Just the average peak period and vegetation height are available. Plant thickness and width are not known and vegetation density is expressed differently (kg/m^2). Therefore the data set is hard to use. The large vegetated area and the relatively high waves are enough to keep this case interesting to analyze (Table 2.1.6).

Table 2.1.6: Range of characteristics Eng field case

Waveheight (significant)	H_s	0.31-0.67m
Peak period	T_p	3s
Depth at start experimental site	h	1.12-1.57m
Vegetation height	d_v	~0.2m
Vegetation density	N	-
Vegetation width	b_v	-
Vegetation thickness	t_v	-
Wave spectrum		-

2.2 Description of model set-up

The basic characteristics of the SWAN model are described in Chapter 1. Here the settings are described that are used to reproduce the testcases. A Matlab script used to calculate the Osana case is shown in Appendix 2.2A.

Grid and bathymetry

The model used in a later phase, representing New Orleans and its surroundings, is two dimensional. For this reason, the testcases are also modeled two dimensionally, despite the one dimensional data. To prevent boundary influences, the width of the bathymetry is set to 20km. This width is more than necessary but does not cause problems.
The bathymetry of each testcase is known, see Appendix 2.1A. It is modeled in as much detail as available from the case descriptions. So sometimes the depth is known at two locations and with more complex bathymetries depth is implemented at more locations.
The resolution for every testcase is set to about 100 calculation points over the length of each test site. The frequency range of each testcasse is set between 0.05 and 2Hz

Boundary conditions

The boundary conditions in SWAN that need to be implemented are wave height, wave spectrum and wave period. At the end of the modeled area all of the wave energy does get absorbed.

For all the testcases, the wave spectrum is set to regular waves. For the Bouma and the Osana case regular waves were applied in the measurements, therefore the regular wave heights at the start of the flumes are implemented and also the regular wave periods from the measurements are implemented. For the Dubi and Lovas case the value of H_{rms} (root mean square wave height) is applied as an estimation of the regular wave height and the peak period (T_p) is implemented. These measurements were in reality performed with a JONSWAP spectrum. At the end of this paragraph it is shown that this simplification performs very well. The spectra of the Dutch and the England case are unclear. Only the significant wave heights (H_s) are known for each case. Also the T_p is known for the Dutch case, for the England case there is only an averaged T_p available. Therefore these values are applied with the same regular spectrum as in the other cases. The effects of the spectrum choice are briefly discussed in Appendix 2.2B.

Physical settings

As described in Chapter 1, the Collins coefficient is used to describe friction. It is implemented as one value for the vegetated part of the grid. Furthermore, the cases are run without wind and its influences because the flume cases did not have any wind and the field cases did not provide information on this subject. Because of the relation between wind and whitecapping, this physical element is also turned off. Quadruplet interaction is essentially the interaction between different frequencies within a wave spectum. Because of the regular wave spectrum this is also turned off.

The remaining physical settings are applied with the default settings. These are depth-induced breaking and triad interactions.

Output

As output, especially wave height is used. This is the most interesting parameter, also because the data of wave propagation is expressed in wave height. Most of the time, just the locations of the sensors require output. Sometimes more locations are used to get a better overview of the attenuation pattern of the waves.

Results for non-vegetated cases

To test if the model set-up is correct, the model is run for a few measurements without vegetation. For this test, data is used from the same Lovas measurements as discussed in Paragraph 2.1. Only the measurements in which vegetation is not implemented in the flume are taken into account. SWAN should be able to predict such situations in detail. These measurements are reproduced in SWAN with the standard Collins friction coefficient (for non-vegetated sea beds) of 0.015. Results are satisfactory, since all of the data is reproduced within 10% deviation. This is presented in Figure 2.2.1-3.

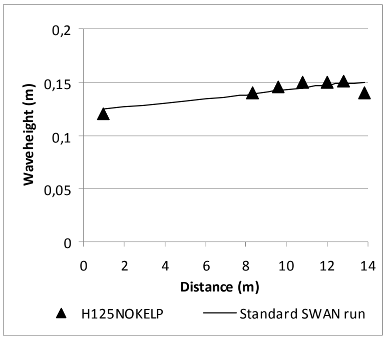

Figure 2.2.1: Lovas data without kelp compared to SWAN output. Average deviation 3%, maximum deviation 6%.

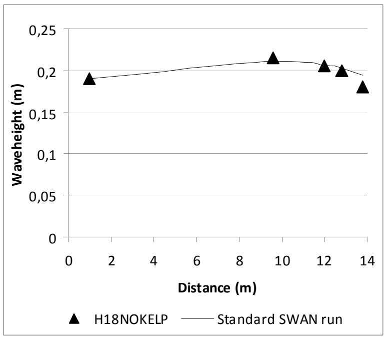

Figure 2.2.2: Lovas data without kelp compared to SWAN output. Average deviation 2%, maximum deviation 7%.

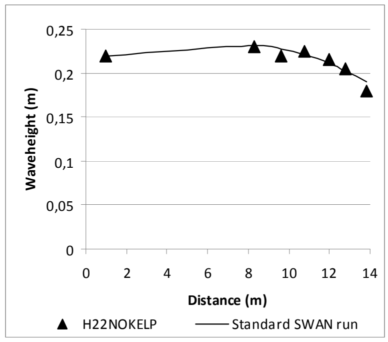

Figure 2.2.3: Lovas data without kelp compared to SWAN output. Average deviation 2%, maximum deviation 5%.

2.3 Best-fit Collins coefficient per measurement

To see if SWAN is able to reproduce situations with vegetation, a uniform best-fit Collins friction coefficient is determined for each measurement. The procedure used to obtain this best-fit value is as follows:

First, a random Collins coefficient is applied uniform over the whole vegetation field. (Figure 2.3.1) The uniform coefficient is enlarged when the wave heights from the model output exceed the wave heights from the measurements at all measuring locations. The coefficient is decreased when the wave heights from the measurements exceed the wave heights from the model output at all measuring locations.
Then the maximum deviation between data and model output is investigated (Figure 2.3.2). When the desired threshold of 10% is exceeded, or when it is clear that a better result is possible, the uniform friction coefficient is changed to minimize the differences in wave height between model output and data (Figure 2.3.3). The Collins coefficient is changed with steps of 0.05, unless smaller steps are needed to reduce the deviation below 10%.

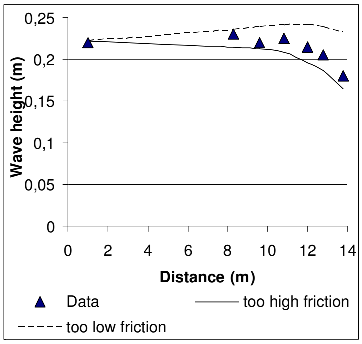

Figure 2.3.1: Step 1 in finding the best-fit friction coefficient. Visual determination whether the friction is too high or too low.

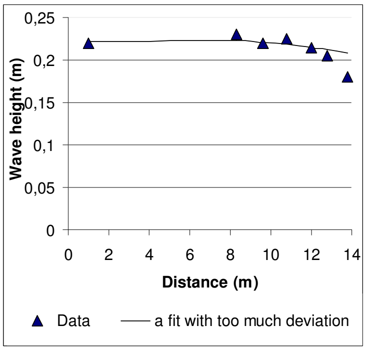

Figure 2.3.2: Step 2 in finding the best-fit friction coefficient. Model output fits through the data, but the maximum deviation is above 10%.

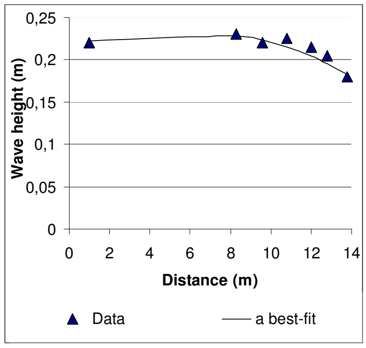

Figure 2.3.3: Step 3 in finding the best-fit friction coefficient. When the minimum deviation is reached, the best-fit is found.

Range in best-fit Collins coefficients

When a Collins coefficient is fitted per measurement, the best-fit coefficients of each case deviate a lot. For instance in the Dubi case, a Collins coefficient of 0.5 is the best-fit for the measurement with *H=0.225m h=0.6m T=2.2s* as hydraulic aspects. In the same case, the measurement with *H=0.114m h=0.6m T=1.6* requires a Collins coefficient of 2.2 for the best representation of the data. The range for every case is presented in Table 2.3.1. These ranges of best-fit coefficients for a uniform friction coefficient per measurement are quite large. This indicates that one fixed value per case is probably not applicable. In Appendix 2.3A it is shown that the best-fit for one measurement causes too much deviation in another measurement within the same case. Paragraph 2.4 reviews fixed friction coefficients per case in more detail. The deviations in wave height between model output and the data are discussed below.

Table 2.3.1: Best fit friction coefficients

Case	Mean Collins	Range Collins
Dubi	1	0.5-2.2
Osana	2.7	1.5-15
Lovas	0.5	0.3-0.65
NL	8	1.5-10
Eng	0.1	0.001-0.2

Deviation case Lovas, Bouma, Osana and Dubi

For the Lovas, Bouma and Osana case the deviations between wave heights from the model output and from the data remain below 10%. In the Dubi case, 7/8 of the measurements comply with the set limit of 10%. Only the measurement with the smallest wave height cannot be represented due to the fact that the fluctuations in the measurements exceed the twenty percent. Therefore the model output cannot predict the measurement well enough.

Deviation case The Netherlands

It is also possible to represent the measurements of the Dutch field case with a uniform Collins value over the area. The dissipation of wave height over the marshland can be reproduced within the margin of 10% deviation. So the dissipation over the vegetation is reproduced well. One of the case's measurements also includes data near the edge of the marshland. These data points are not reproduced very well with a uniform Collins coefficient in SWAN. When the data points near the edge are observed, see Figure 2.3.1, it is visible that wave heights first increase near the edge and then steeply decrease. The SWAN model does not reproduce these results properly with a uniform friction coefficient. It is likely that the steep decrease of wave heights behind the edge, and a part of the

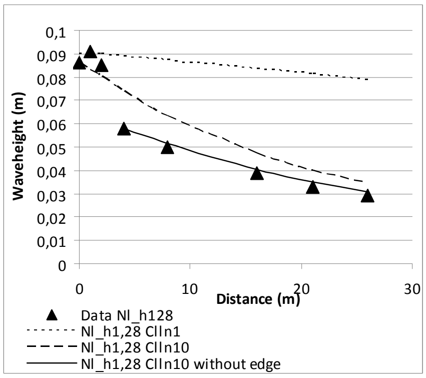

Figure 2.3.1: With a uniform friction coefficient, SWAN cannot predict the effects on the edge of the Dutch marsh.

wave heightening in front of the edge, are caused by energy reflection from the marsh border. This reflection is both from the vegetation as from the steep slope of the bottom. The edge can also contribute to wave breaking. Wave breaking due to steep edges is not calculated in SWAN because of the mild bottom slope assumption, as mentioned in Chapter 1. Reflection is just taken into account in SWAN for loose objects that are programmed. Figure 1.1.3 in Chapter 1 supports the theory of reflection because the wave reflection presented in the figure shows similar patterns as the data from the Dutch marsh. Resemblances are the increase in wave energy in front of the marsh and the steep wave energy reduction just behind the vegetation edge (lines A,B,C,D).

Deviation case England

The field case from England is badly reproduced in SWAN. It also includes the edge of the marshland, but the limited amount of measuring points (3) makes it hard to analyze the effects in detail. Also the lack of a detailed bathymetry description limits the analysis possibilities.
The problems encountered are presented in Figure 2.3.3. Even without bottom friction the model predicts too much wave dissipation in the first 200 meters. The first 200 meters contain a sandy bottom without vegetation, the last 200 meters contain marshland. It is possible that the middle measurement station measures the effect of the marsh edge. The edge of a marsh usually has a steep slope, because the vegetation roots hold on to the sand (Figure 2.3.4). This steep edge can cause wave energy reflection and wave breaking, as discussed in the previous paragraph.

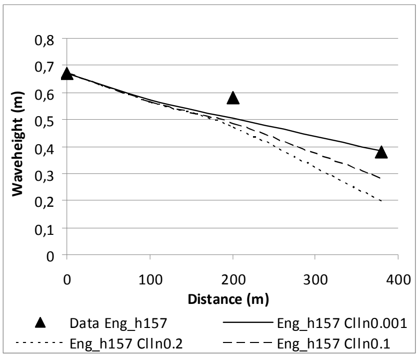

Figure 2.3.3: Measurement of the England case.

Figure 2.3.4: The edge of a salt marsh. (habitas.org.uk)

Results in general

In general, most of the measurements can be reproduced very well with a uniform friction coefficient for the vegetation. Just the one measurement near the edge of the Dutch salt marsh and the England case are represented badly. The fact that the data is generally reproduced very well, suggests that the process of energy dissipation is reasonably alike and adaptations in the Collins coefficient can be used to represent vegetation fields.

2.4 One Collins coefficient for all cases

In Paragraph 2.3 it is shown that (in most cases) the wave propagation can be reproduced by a uniform Collins coefficient per measurement. Within each case, a different best-fit Collins coefficient is found for each measurement. In this paragraph it is analyzed if it is possible to represent all of the vegetation with one, mean Collins coefficient. Therefore each measurement from every case is run with the average bets-fit Collins coefficient of 2.2

The results of these runs show that applying an average Collins coefficient for all cases is inappropriate. When all of the measurements are reproduced in SWAN with the mean Collins coefficient, deviations between de wave heights from the model output and wave heights from the data are very large. This is shown in Appendix 2.4A, this results will not be discussed here in detail.

2.5 Best-fit Collins coefficient per case

Another used method to represent vegetation is a fixed friction coefficient per vegetation type. This is a very practical way to represent vegetation and is very simple to use. In this paragraph it is investigated whether the results are satisfying when this method is applied. Therefore the mean best-fit Collins coefficients per case are used. Because vegetation is constant in the Osana, Dubi, Lovas, Dutch and English cases, this method investigates a constant friction coefficient per vegetation composition for these cases. In the Bouma case each measurement is performed with different vegetation, therefore this case is not taken into account here.

When the testcases (Osana/Dubi/Lovas/NL/England) are reproduced in SWAN with a single Collins coefficient per case, the deviations within most cases do not exceed the 10% limit much. Figure 2.5.1 shows the results when all of the Lovas measurements are reproduced in SWAN with a fixed Collins coefficient of 0.5. The results at all the measuring points of all the measurements of the Lovas case are shown in the figure. The x-axis shows the wave heights that result from the SWAN model, the y-axis shows the wave heights from the measurements. Most of the wave heights at the measuring points are reproduced by SWAN within 10% deviation. The other cases are also reproduced reasonably well by a case-averaged Collins coefficient. Just the England case is represented badly. This is as expected because even with the best-fit method per measurement, deviations are too large.
Table 2.5.1 presents the maximum deviating data points per case. When kept in mind that measurements always have a certain amount of inaccuracy, it can be stated that the results are reasonably well. On the other hand does the fact that the average best-fit Collins coefficient is taken, result in biased results.

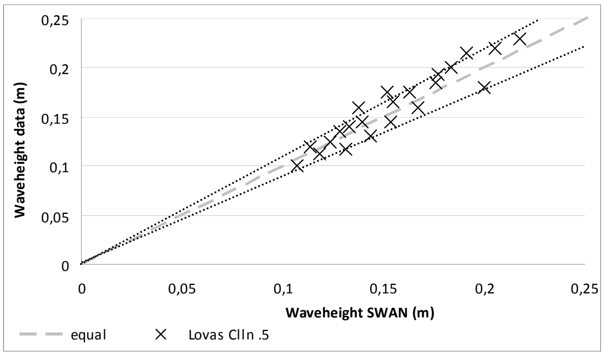

Figure 2.5.1: Model output with a case-averaged Collins coefficient versus the data of the Lovas case. The dotted lines present 10% deviation.

Table 2.5.1: Wave height deviations between data and model output with case-averaged friction coefficient.

Case	R^2	Number of data points	Max deviation (% above 10%)	Collins coefficient
Osana	0.97	24	2	2.7
Dubi	0.99	49	4(2x), 16*	1.0
Lovas	0.89	22	1, 3, 5, 6	0.5
NL	0.83	20	1(2x), 3, 4, 5, 7, 8, 10	8.0
Eng	0.87	18	1-20(10x), 21, 26, 35, 52	0.1

*(*one 4% and one 16% are from the measurement within the Dubi case that has so much fluctuation it cannot be fitted with a best-fit Collins parameter either.*

From these results it is concluded that the patterns of energy dissipation are quite similar for vegetated and non-vegetated bottoms. This is concluded because the calculations are performed with formulations that are meant for sand and gravel surfaces and do also give reasonable results when applied to vegetated bottoms. Although when a strict limit is set, none of the cases could be represented with a fixed Collins value, since there are data points exceeding the 10% deviation in every case.

The fixed Collins values also cause other errors. For instance, the Lovas and Dubi vegetation is equal, but the averaged Collins coefficient is not. Therefore the use of a fixed coefficient per vegetation type would results in too much deviation for one of the cases. Averaged Collins coefficients per vegetation type will therefore not be very accurate in practice. When hydraulic situations are changed significantly, friction due to vegetation changes in another way than in the Collins method. Therefore specific friction formulations for the influence of vegetation are needed.

2.6 Vegetation influence on friction in testcases

With the data-set applied in this chapter, it is investigated whether relations can be determined between the friction coefficient and all of the available parameters known of the cases (wave height, period, relative depth, vegetation density and vegetation height). Three different methods are used and briefly discussed below. The analyses are described in more detail in Appendix 2.6A/B/C.

- All of the best-fit Collins coefficients per measurement are compared to one specific characteristic of each measurement. So graphs are created with the friction coefficient on the y-axis and a hydraulic or vegetation characteristic on the x-axis. It is determined if the points in the graphs show a relation. Because all of the relations remain below a correlation (R^2) of 0.6, no firm conclusions are obtained. The reason for this result is probably that when the parameter on the x-axis changes, all of the other parameters do also change and therefore disturb possible relations. Despite the large scatter, the following trends did show: Higher densities result in higher Collins coefficients. Larger vegetation height results in higher Collins coefficients. Higher waves result in lower Collins coefficients. Higher periods result in lower Collins coefficients and higher depth results in lower Collins coefficients. As mentioned, the trends are too weak to base theories on.

- The friction coefficient is compared with a parameter that includes all of the hydraulic aspects. This parameter is the near bottom, maximum horizontal velocity. Because all of the hydraulic aspects are included, the impact of different vegetation characteristics can become clear when added to the parameter on the x-axis. The horizontal velocity against the friction coefficient shows a relation with a R^2 of 0.69. This suggests some kind of relation is present, but vegetation characteristics do not improve the correlation. Therefore no firm conclusions are drawn about the relation between vegetation and the friction coefficient.

- In the third method, subgroups are created for each parameter. The subgroups contain a part of the range of each parameter. For instance, the total data set is divided in a subgroup with a period below 2s, between 2 and 3s and above 3s. With these groups it is investigated if there are parameters that are the main cause for deviations from a (all case-averaged) fixed Collins coefficient. This can be seen when certain groups have a far worse correlation. Again no firm conclusions are drawn. Probably because the correlation with the coefficient is more case-dependent than dependent on one of the parameters.

Concluded from these methods is that no firm conclusions can be drawn on the impact of different vegetation characteristics on the friction coefficient. The different testcases have too much deviation in multiple parameters. Therefore the relatively small amount of data it is not suitable to determine the influence of separate characteristics.

3 Modeling of friction due to vegetation within SWAN

As concluded in Chapter 2, a more detailed friction determination is needed to calculate wave attenuation over vegetation. It is concluded that bottom friction can be used to represent vegetation but a different friction coefficient is needed for different hydraulic situations and for different vegetation characteristics. The exact adaptations that are needed are nevertheless still unclear.

To find accurate and applicable relations, theories and methods to represent vegetation (discussed in Chapter 1) are analyzed. In Paragraph 3.1 the best applicable method is selected and the implementation is described in Paragraph 3.2-3.4. In Paragraph 3.5-3.7 the implementation is verified with data sets.

3.1 Approach used to represent vegetation

First, the most suitable theory to represent vegetation is selected.

From the theories presented in Chapter 1, Mendez (1999) has the most detailed description of vegetation influence on waves. However, the implementation in SWAN is estimated to be too time consuming. The model requires complex computations with several parameters that are not present in the short-wave model. Another disadvantage of this method is that it does not take wave breaking into account and that it assumes a flat bottom. Implementation in SWAN could therefore cause additional problems.
The model of De Vries is still no prediction tool because it uses a parameter that has to be calibrated and is that unclear at the moment. The module of Meijer and Burger also needs a calibration parameter, but especially the implementation of the code in SWAN is expected to take up a lot of time.

The approach that is assessed as most feasible is related to Mendez (2004). This is the only method that can calculate drag coefficients based on only hydraulic and vegetation characteristics and can also be coupled to SWAN relatively easy. The coupling possibility to SWAN is there because it uses the same wave energy dissipation term. The relations are just applicable for flexible vegetation but with some adaptations it can be a predictive tool for more types of vegetation. To validate the model for other types of vegetation, best-fit Collins coefficients are obtained for various plant species. Next to the coefficients obtained in Chapter 2, best-fit Collins coefficients are also determined for mangrove trees. This is again done by reproducing the measurements in SWAN and finding the best fitting friction coefficient. Details of the Vietnam cases are presented in Appendix 3.1A.

Implementation

Implementation is done without changing the model code of SWAN. A separate Matlab script is written that calculates the friction input for SWAN. In the following paragraphs, the modeling of flexible vegetation, stiff vegetation and a 2-dimensional grid are discussed separately. This is done because these aspects represent different modeling tasks. The flexible vegetation is represented by the original Mendez formulation, stiff vegetation needs some additional adaptations and the 2-dimensional grid needs a more advanced Matlab script.

3.2 Implementation of friction for flexible vegetation

The formulations of Mendez can be used in its original form to represent flexible vegetation. The formulas are used in SWAN by relating the dissipation term of Mendez (Equation 3.2.2) to the dissipation term of SWAN (Equation 3.2.3). Rewriting this comparison results in a new formulation of the Collins coefficient (Equation 3.2.4). The Collins coefficient is one of the standard options for friction input in SWAN, so it can easily be implemented to run testcases.

The parameters applied in the equations of this paragraph (3.2) are explained in Table 3.2.1.

Table 3.2.1: Parameters applied in Paragraph 3.2.

Parameter	Meaning of parameter	Unit
α	relative vegetation height	-
ρ	density water	kg/m^3
σ	wave frequency	s^{-1}
a	wave amplitude	m
b_v	vegetation width	m
C_b	bottom friction	m^2/s^3
C_D	bulk drag coefficient	-
C_f	Collins friction coefficient (0.015 for North Sea sand)	-
d_v	vegetation height	m
E	wave energy	J/m^2
E_d	dissipation of wave energy	J/m^2
g	acceleration of gravity	m/s^2
h	depth	m
H_s	significant wave height	m
$H_{s,middle}$	significant wave height in middle of grid cel	m
k	wave number	m^{-1}
K	Keulegan–Carpenter number	-
L	wave length	m
N	vegetation density	$units/m^2$
T_p	peak period	s
$u_{c,bottom}$	near bottom orbital velocity	m/s
u_c	orbital velocity at half the vegetation height	m/s

Basic equations used

As a first step, the used basic equations are described. These equations (except for the relative depth) are based on a shallow water assumption and obtained from Van Rijn (1990). The formulas are presented in Equation 3.2.1. To obtain the significant wave height (H_s) from a root mean square wave height (H_{rms}), the Rayleigh distribution of waves is used. Resulting in H_s=1.48*H_{rms} (Chadwick 2004).

$$\sigma = 2\pi / T_p \qquad k = 2\pi / L \qquad L = T_p\sqrt{gh} \qquad E = 1/8\rho g H_s^2 \qquad a = 1/2 H_{s,middle} \qquad \alpha = d_v / h$$

Equation 3.2.1: The basic formulas that are used.

Energy dissipation due to vegetation

The formulation of Mendez (2004) is based on the formulation of Dalrymple. To make it a prediction tool, Mendez created a formulation for the bulk drag coefficient C_D. Both formulas are presented in Equation 3.2.2. The influence of each parameter on the Collins coefficient is presented in Appendix 3.2A. Most of the time, the results do comply with the spotted trends in Chapter 2.

$$E_{v,vegetation} = \frac{2}{3\pi}\cdot\rho\cdot C_D\cdot b_v\cdot N\cdot\left(\frac{k\cdot g}{2\sigma}\right)^3\cdot\frac{\sinh^3(k\cdot\alpha\cdot h)+3\sinh(k\cdot\alpha\cdot h)}{3k\cdot\cosh^3(k\cdot h)}\cdot H_s{}^3$$

$$C_D = \exp(-0.0138Q)/Q^{0.3} \qquad Q = K/\alpha^{0.76} \qquad K = u_c\cdot T_p / b_v \qquad u_c = \frac{\cosh(k\cdot(h+(h-0.5d_v))}{\sinh(k+h)}\sigma\cdot a$$

Equation 3.2.2: Energy dissipation due to vegetation and the bulk drag coefficient by Mendez (2004).

Energy dissipation in SWAN

To obtain the Collins coefficient, the directional component of the waves is not relevant. Because the energy dissipation due to vegetation is calculated with H_s, this is also done with the energy dissipation of SWAN. Therefore the SWAN computations can be simplified for obtaining the Collins friction coefficient, as presented in Equation 3.2.3.

$$E_{v,SWAN} = -C_b \cdot \frac{\sigma^2}{g^2 \cdot \sinh^3(k \cdot h)} \cdot E \qquad C_b = C_f \cdot g \cdot u_c \qquad u_c = \frac{1}{\sinh(k+h)} \sigma \cdot a$$

Equation 3.2.3: Simplified energy dissipation and Collins bottom friction in SWAN.

Obtaining Collins coefficient

Wave energy dissipation due to vegetation should be equal to the dissipation due to bottom friction in SWAN. This can be rewritten in a formulation for the Collins friction coefficient (C_f), as presented in Equation 3.2.4. When both dissipation formulations are combined, the Collins coefficient can be moved to the left and all of the other (known) parameters form a new expression for the Collins coefficient. The right part of the equation does not contain C_f because $E_{v,SWAN}/C_f$ removes it.

$$E_{v,SWAN} = E_{v,vegetation}$$

$$C_f = \frac{E_{v,vegetation}}{E_{v,SWAN} / C_f}$$

Equation 3.2.4: Obtaining the Collins coefficient.

3.3 Implementation of friction for stiff vegetation

Creation of a 'stiffness factor'

To create a representation that also complies with stiff vegetation, some additional steps are taken. First the data available from Vietnam (Burger 2005 from Mazda 1997) is analyzed and reproduced in SWAN. With the model, the best-fit Collins coefficients are extracted (Appendix 3.1A). All of the available best-fit coefficients (also from testcases of Chapter 2) are compared to the calculated Collins coefficient for flexible vegetation, except from the England case and the edge of the Dutch marsh. To compensate for the deviations of stiff vegetation, a 'stiffness factor' is created. The bulk drag coefficient (C_D) is multiplied with the factor because this parameter incorporates the bending effects (Mendez 2004) and should therefore be different when vegetation has a higher stiffness.

To create the stiffness factor, it is determined with which factor the C_D of Mendez has to be multiplied to get the desired C_D. The desired C_D is the one that results in the best-fit Collins friction coefficient that is found for each measurement. The desired multiplying factors are related to each hydraulic and vegetation characteristic to see if patterns occur. The clearest pattern results when the multiplying factors are related to stiffness (E), vegetation width (b_v, just the main stems for the Vietnam cases) and relative depth (α). This is shown in Figure 3.3.1., where the water density (ρ) and the gravitational acceleration (g) are implemented to

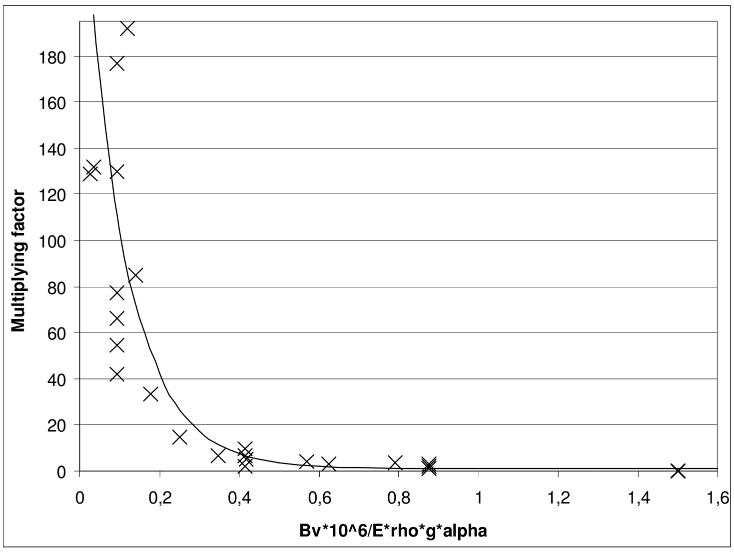

Figure 3.3.1: The multiplying factor needed for the desired Collins coefficient compared to vegetation characteristics. Resulting in a trendline with a R^2 of 0.94.

make the parameter on the x-axis non-dimensional.

There are several reasons that could explain why E, b_v and α are the most suitable parameters to create a stiffness factor. The stiffness is a logical step to implement because the whole purpose of the factor is to compensate for the effects of stiff vegetation. The most commonly used description of stiffness is the Young's Modulus (E [N/m^2]), therefore this parameter is applied. The E values per case are presented in Appendix 3.3A. Next to the stiffness, bending of vegetation is also dependent on the cross-sectional area of the stems. Because the stems of the stiff vegetation in the data sets are round, it is sufficient to capture the cross-sectional influence with the width of the vegetation. It could be that the thickness of the vegetation is more important than the width, or the other way around, but because of the cylindrical stems of the data it is not possible to draw conclusions on this subject. The presence of relative depth (vegetation height divided by depth) in the formulation can probably be explained by the influence of bending on the relative depth. Since bended vegetation is closer to the bottom and therefore has a smaller relative depth.
As mentioned, water density and the gravitational acceleration are added to keep the stiffness factor non-dimensional. This is done because the bulk drag coefficient should stay non-dimensional and the energy dissipation due to vegetation should remain comparable to the energy dissipation in SWAN.

The stiffness factor that is obtained from this method is presented in Equation 3.3.4. As mentioned, this factor has to be multiplied with the original Mendez value of C_D to get the new C_D that also fits for the data of stiff vegetation (Equation 3.3.5). The maximum value of the stiffness factor for the data of this project is 266, the minimum 1. So outside these boundaries the factor is not verified and less reliable.
The impact of the applied parameters in the stiffness factor on the value of the stiffness factor is presented in Appendix 3.3B. This shows that the deviations in vegetation width and relative depth have a contradictory impact in comparison to their impact in the Mendez formulation. Therefore, the stiffness factor reduces the variety in C_D induced by both parameters. So stiffer vegetation results in a more stable C_D because it changes less with vegetation width and relative depth. This is as expected because the bulk drag coefficient (C_D) manly varies because of bending of vegetation. Therefore vegetation that bends less (stiffer vegetation) will needs a less varying C_D. Stiffness is only implemented in the stiffness factor, it will therefore directly impact the bulk drag coefficient.
The parameters applied in the equations of this paragraph (3.3) are explained in Table 3.3.1.

Table 3.3.1: Parameters applied in Paragraph 3.2.

Parameter	Meaning of parameter	Unit
α	relative depth (vegetation height / depth)	-
ρ	density water	kg/m^3 (with kg =N/g)
b_v	vegetation width	m
C_D	bulk drag coefficient	-
E	stiffness	N/m^2
g	gravitational acceleration	m/s^2

$$Stiffness\_Factor = 260.83 \cdot e^{\left(\frac{-9.2221 \cdot 10^6 \cdot b_v \cdot \alpha \cdot \rho \cdot g}{E}\right)} + 1$$

$$[-] = \frac{[m] \cdot [-] \cdot [N \cdot g^{-1} \cdot m^{-3}] \cdot [g]}{[N \cdot m^{-2}]}$$

Equation 3.3.4: Stiffness factor and relevant units of the parameters.

$$C_D = Stiffness\_Factor \cdot \exp(-0.0138Q)) / Q^{0.3}$$

Equation 3.3.5: New bulk drag coefficient. Q is explained in Equation 3.2.2

Implementation of multiple layers to cover changing structure of trees over height

Next to the stiffness factor, it is also necessary to implement multiple vegetation layers into the calculations. This is necessary because in the Vietnam cases there are trees with different structural characteristics over height. To cope with these different layers, each layer is calculated separately and the energy dissipation is added afterwards.

In these calculations, each layer is calculated as if it makes contact with the ground. For instance, the depth for the tree top calculations could be 1 meter, while the depth for the energy dissipation calculations of the stem is 3 meter. Figure 3.3.2 visualizes the calculation in layers. Burger (2005) added the energy dissipation of the layers as if each layer was at the bottom of the total depth. With the method used here, the orbital velocities per layer change and also the relative depth per layer is different. For instance, if no water flows above the top-layer, the relative depth is 1. Considering the fact that no water flows unhindered above the vegetation, this is seen as a better estimation. Also the orbital motion of the top layer should be higher than the orbital motion for the bottom layer. Because of the different depths applied to different layers, this is now the case.
Despite the fact that these adaptations are expected to be more realistic, it is still a simplification of the actual situation. An example of these simplifications is the fact that energy dissipation of the different layers does not influence other layers.

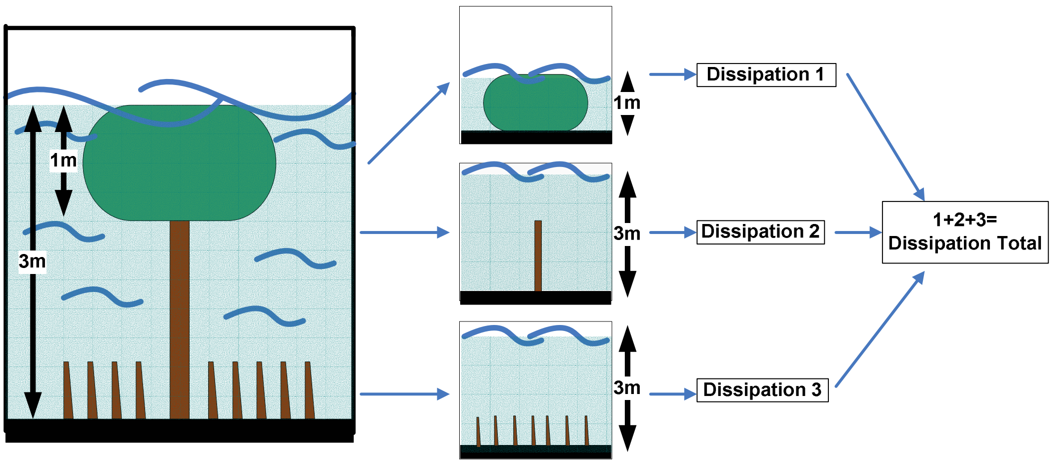

Figure 3.3.2: Calculation of energy dissipation for vegetation with different structural layers. Each layer is calculated as if it makes contact with the ground and the dissipation of each layer is added afterwards.

3.4 Implementation of friction for the 2-dimensional grid

For a large 2-dimensional grid it is necessary to calculate a Collins coefficient for every grid point. A uniform Collins coefficient, that is applicable in the small testcases, is not sufficient. Therefore a Matlab code is created that uses wave heights, period and depth from a SWAN run. Because model output is required to create friction terms, multiple iterations are necessary. This is the case because the newly calculated wave characteristics cause different friction coefficients again. The iteration process should converge to a situation where results do not change significantly anymore. The threshold for 'no change' is (arbitrarily) set to a deviation in the Collins coefficient that is below 10%. The maximum amount of iterations is, arbitrarily, set to 40.

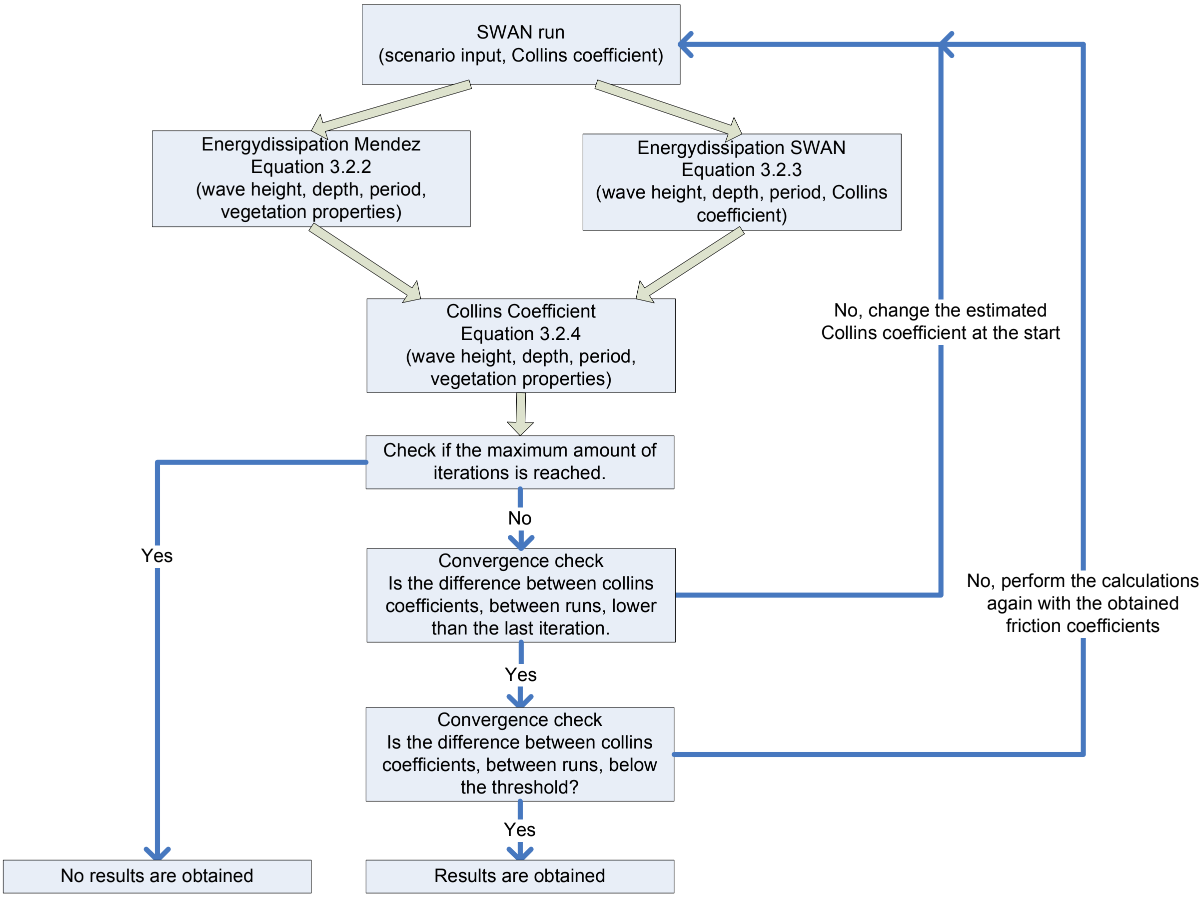

Figure 3.4.3: Schedule of the required calculations to obtain the Collins friction coefficient. The schedule shows the iteration step, the check if the maximum amount of iterations is exceeded and the check if results converge.

The process of calculating Collins friction coefficients is presented in Figure 3.4.3. So first a SWAN run with an estimated Collins coefficient is performed. With the output, the calculations presented in the previous paragraphs are executed (Equations 3.2.1-3.2.4). These calculations result in new Collins coefficients that can be used for a new SWAN run. When the Collins coefficients converge, this process should continue until the threshold or the maximum amount of iterations is reached. The Matlab script is presented in Appendix 3.4A.

3.5 Validation of the representation of flexible vegetation

For the validation test with flexible vegetation, the same testcases are used as described in Chapter 2. Because these testcases can be represented by a fixed Collins coefficient per measurement, one average coefficient is calculated for each measurement. With this single value per measurement it is verified if the Mendez formulations perform adequately when used in SWAN and applied to the testcases of this project.

The Mendez formulation is supposed to perform adequately when the results are as good as the results of a best-fit Collins coefficient per testcase (Lovas/Dubi/Osana/NL). This threshold is set because the results of the best-fit Collins coefficients were well and for a prediction model it is a good performance when it can reproduce best-fit values. The method with the case-averaged Collins coefficients is used for comparison because it resembles the best way that predictions are made nowadays. The best way that vegetation is represented is an average value per vegetation species or land type, almost similar to what is done with the case-averaged Collins coefficients.

First the results of the Dubi, Lovas and Osana case are described. As can be seen in Table 3.5.1-3.5.3, the Mendez formulation gives about the same results as the best-fit, case-averaged, Collins coefficient. The correlation averaged over the three cases (R^2) is 0.96 for the Mendez formulation and 0.95 for the best-fit Collins coefficients. The sum of the deviations that exceeds the 10% threshold (the sum of all of the deviations in the tables) is 29% for the Mendez formulation and 41% for the best-fit Collins coefficients.
The biggest advantages of the Mendez formulation is that it can predict friction values without earlier wave attenuation measurements and that it can now be explained why the friction coefficients of the Lovas and Dubi case differ. This is the case because the differences in water depth, wave height and wave period are used in the calculation of the friction coefficient. These different friction coefficients for exactly the same vegetation could not be explained with the fixed Collins coefficients per vegetation type.

Table 3.5.1: Results of the Mendez formulation compared to the results with the best-fit coefficient for the Dubi case.

Dubi case	Correlation between wave height from the data and the model output. (R^2)	Number of data points (without input point)	Exceeding of 10% wave height deviation from data, (% above 10% per exceeding data point)
Calculated Collins by Mendez	0.982	49	1, 3, 4, 12^x
Case-averaged best-fit Collins	0.985	49	4, 4, 16*
*(^{x} the 12% and (*one 4% and the 16% are from the measurement within the Dubi case that cannot be fitted with an best-fit Collins parameter either*			

Table 3.5.2: Results of the Mendez formulation compared to the results with the best-fit coefficient for the Lovas case.

Lovas case	Correlation between wave height from the data and the model output. (R^2)	Number of data points (without input point)	Exceeding of 10% wave height deviation from data, (% above 10% per exceeding data point)
Calculated Collins by Mendez	0.936	22	1
Case-averaged best-fit Collins	0.888	22	1, 3, 5, 6

Table 3.5.3: Results of the Mendez formulation compared to the results with the best-fit coefficient for the Osana case.

Osana case	Correlation between wave height from the data and the model output. (R^2)	Number of data points (without input point)	Exceeding of 10% wave height deviation from data, (% above 10% per exceeding data point)
Calculated Collins by Mendez	0.962	24	1, 3, 4
Case-averaged best-fit Collins	0.968	24	2

The Dutch salt marsh is mainly covered with Spartina Anglica. Although Spartina marshes are mentioned as flexible vegetation, the formulation does not work for this type of Spartina marsh. Spartina Anglica has relatively stiff stems and is therefore not well described with the Mendez formulation. This is presented in Table 3.5.4. The next paragraph shows the effects of adding a 'stiffness factor' to the computations.

Table 3.5.4: Results of the Mendez formulation compared to the results with the best-fit coefficient for the Dutch case.

Dutch case	Correlation between wave height from the data and the model output. (R^2)	Number of data points (without input point)	Exceeding of 10% wave height deviation from data, (% above 10% per exceeding data point)
Calculated Collins by Mendez	0.09	20	1, 2 (2x), 5, 6, 39 (2x), 43, 66, 91
Case-averaged best-fit Collins	0.83	20	1(2x), 3, 4, 5, 7, 8, 10

3.6 Validation of the representation of stiff vegetation

In this paragraph the results are presented for when the stiffness factor is added. All of the testcases (including the Vietnam cases) are run in SWAN with the newly calculated Collins coefficient. The results are presented in Figure 3.6.1/2. Table 3.6.4 shows the correlation and the deviations in wave height between model output and data for the different cases.

Table 3.6.4: Wave height deviations with the friction formulation including the stiffness factor.

Data set	Correlation R^2	Deviations > 20% (% of data points)	Mean deviation
Total	0.99	19%	10%
Flexible total	0.98	1%	5%
Stiff total	0.88	36%	20%
Original Mendez, stiff total	0.88	43%	39%
NL	0.83	10%	6%
Bouma	0.85	33%	21%
Vietnam total	0.86	67%	35%

Because the validation is performed with the same data as is used for the development of the stiffness factor, the results are biased. Because of the very small amount of data that is available on stiff vegetation, it is not possible to check the formulation with other data. The results do nevertheless show that the stiffness factor explains the effects of stiffer vegetation reasonably for the used data set. The deviations between the data and the model output show however, that the formulation is not perfect. All of the main deviations (above 1cm/30%) are caused by the Vietnam cases. Part of these deviations can probably be explained by the inaccuracy in the data sets. The method applied to calculate the different structural layers is probably also responsible for a part of the deviations. Wave height and period cannot be determined in detail and for instance the exact densities of the treetops are hard to determine. It is nevertheless the best data-set available. Better data would give more opportunities for improvement of the relation.

The fact that the Dutch marsh is reproduced well and that the predictions improved significantly is especially positive for this project. This is the case because the main part of the marsh area near New Orleans is also dominated by Spartina vegetation (Chapter 4).

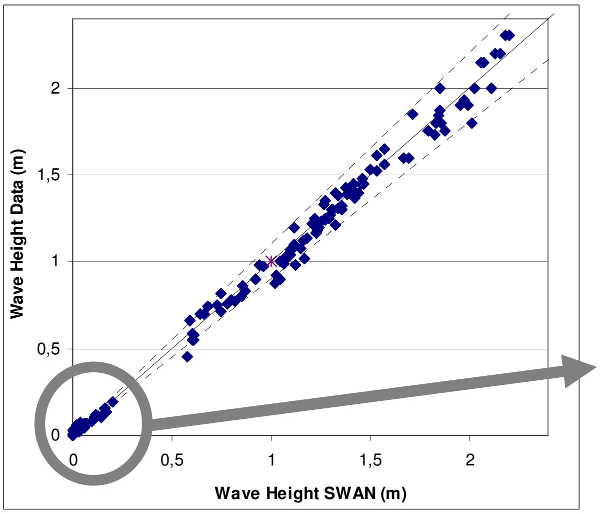

Figure 3.6.1: Model output, including the stiffness factor, compared to the data of all the cases (in real scale). The dotted lines mark a 10% deviation. R^2=0.99

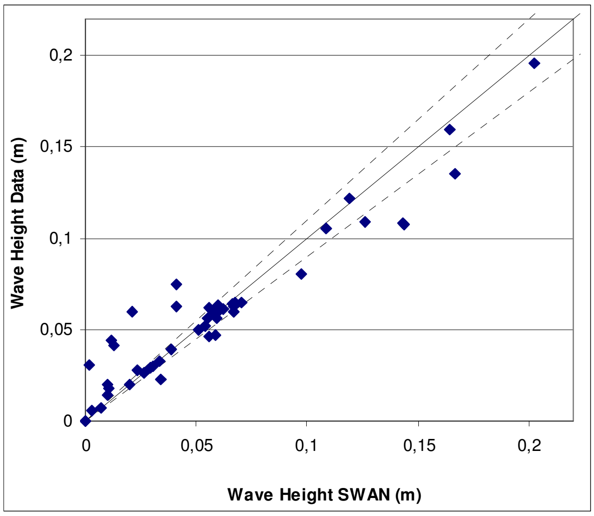

Figure 3.6.2: Model output for a selection of the data points, including the stiffness factor, compared to the data of the stiff vegetation cases. The dotted lines mark a 10% deviation. R^2=0.88

3.7 Validation of the representation in a 2-dimensional grid

In this paragraph it is tested if the created 2-dimensional Matlab script converges towards the desired outcome. Therefore, runs are performed with a starting Collins value that is too high and with a too low starting Collins coefficient.

Table 3.7.5 shows results for the Osana case. Even with an extreme Collins coefficient of 100 the results converge towards a good outcome in three iterations. From a low initial value of 0.5, the results also converge. The final outcome of the iterations has a maximum deviation from the data of 6%.

Table 3.7.5: Convergence of the Collins coefficient and wave height.

Calculated Collins with SWAN output and vegetation properties (Case Osana, Measurement H12)	Output H start	Output H end
Collins = 100 (a random initial value)	1.23	0.043
Collins = 3.4	1.23	0.69
Collins = 1.9	1.23	0.85
Collins = 1.7	1.23	0.88
Collins =1.67	1.23	0.88
	6% deviation in comparison to the data	
Collins = 0.5 (a random initial value)	1.23	1.10
Collins = 1.57	1.23	0.90
Collins = 1.64	1.23	0.89
Collins = 1.66	1.23	0.89
	6% deviation in comparison to the data	

Because the results converge in a 2-dimensional grid for this case, the results are also expected to converge in the large grid applied for the area of New Orleans. Therefore, the friction calculations developed in this study are applied for the grid near New Orleans in Chapter 4.

4 Effects of vegetation on waves near New Orleans

In this chapter, the theory of the previous chapters is applied to the surroundings of New Orleans. First a short description is presented of how the area is presented in the model. Then several scenarios are considered. The current situation is called the 0-scenario, the other scenarios represent the future situation when restoration measures are applied or when deterioration of marshlands continues. Based on the results, conclusions are drawn on the effects of the marshlands in front of New Orleans.

4.1 *Description of the SWAN set-up for New Orleans*

Grid and bathymetry

The area covered by the grid that is used in this chapter is presented in Figure 4.1.1. The size of the cells in the applied grid is 600x600m. The implemented bathymetry of the surroundings of New Orleans is based on the situation prior to the passing of hurricane Katrina (Appendix 4.1A).

Boundary conditions

Runs are performed with wind input representing hurricane Katrina. This was a severe hurricane and therefore it is seen as a representative way to determine the effects that marshes have on waves in a normative safety situation for New Orleans. The corresponding wave spectrum is also implemented into SWAN at the boundaries. Each boundary point has a wave spectrum expressed in m^2/Hz/degr. So for every point the different wave frequencies, wave directions and wave heights are taken into account.

Figure 4.1.1: The area covered by the grid of the SWAN model (map24.nl)

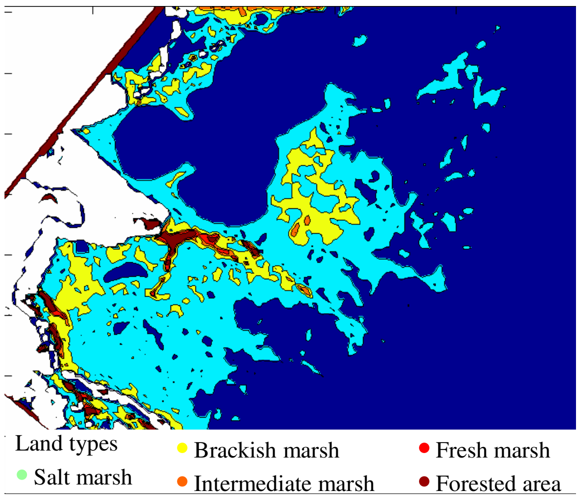

Figure 4.1.2: Different land types.

Physical settings

The physical settings applied in SWAN follow from the activation of the 'Gen3 Westh' modus. This modus activates the use of whitecapping formulations of Alves and Banner (swan.nl from Alves and Banner 1987) and the wind growth formulation of Yan (swan.nl from Yan 1987). Furthermore, the modus activates the default depth-induced wave breaking formulation and the default triad interaction and quadruplet interaction calculations.
For the friction settings, several options are used for different calculations on marshland impacts.

Collins friction file

The SWAN model is used for modeling the waves approaching the storm surge barrier that is in development. For the design of the barrier, runs are performed with Collins friction as presented in

Appendix 4.1A. This friction is lower than the general friction applied for sandy bottoms in the North Sea (C_f=0.015). To use this friction file, the friction settings are set to Collins.

Madsen friction file

Within the LACPR project (Louisiana Coastal Protection and Restoration Project, develops hurricane protection plans and analyses multiple water management issues extensively) some calculations are performed that do take vegetation into account. The friction in these calculations is expressed in roughness height (the Madsen method in SWAN) and is based on Manning values that are attributed to the vegetated areas in the ADCIRC model. ADCIRC is the most used model to calculate surge levels in the New Orleans area and in several other places in the world. These Manning values are validated with expected surge outcomes of different hurricanes (Wamsley 2008). The Manning values contributed to the different marsh types are presented in Table 4.1.1, the calculated roughness heights from these values are presented in Appendix 4.1A. The roughness heights are significantly higher for the marshes than the value of North Sea sand of 0.05m. To use this friction file, the friction settings in SWAN are set to Madsen.

Table 4.1.1: Manning friction coefficient contributed in ADCIRC and SWAN, per vegetation type (Bender 2007)

Land Cover	Manning-n ($m^{1/6}$)
Fresh marsh	0.055
Intermediate marsh	0.05
Brackish marsh	0.045
Saline marsh	0.035
Wetland forest - mixed	0.15
Upland forest - mixed	0.17
Dense pine thicket	0.18
Open water	0.02

Friction formulations developed in this project

For the method created in this project, the friction settings of Collins should be applied. The friction file that SWAN uses is calculated for each iteration, as explained in Chapter 3.

The wave characteristics are calculated with the three mentioned friction settings. The calculations with the friction formulation of this project are compared to the Collins and Madsen calculations because it are currently the best estimations for waves approaching the New Orleans coast.

Figure 4.1.2 shows land types in the area. This is based on the Manning values attributed to the area (calculated from the available roughness heights from the Madsen friction file) combined with the matching land types from Table 4.1.1. Appendix 4.1A shows data that supports this land type composition.

4.2 Current situation

The current situation is defined in this project as the 0-scenario. This is the reference situation to compare the changes in the other scenarios with.

Description of the 0-scenario

As discussed in Paragraph 4.1 the land type at each location is determined. The characteristics of the plant species that are present in different marsh types are discussed in Appendix 4.2A. The area is mainly covered with brackish marsh and salt marsh. These land types are dominated by grasses. For the small parts that are covered with trees, the different layers (as discussed in Chapter 3) are applied again. The most important characteristics applied for the different salt marshes and the forested areas are presented in Table 4.2.1.

Because many small lakes and channels are present, the density of the vegetation is reduced with 50% for this scenario. This is based on data from (LDNR/CRD, 1998) as presented in Appendix 4.4A. The minimum Collins coefficient is set to 0.006. This minimum value is applied to prevent friction below the friction of non-vegetated bottoms. The applied minimum Collins coefficient is lower than the standard value for the North Sea because roughness heights (as mentioned in Chapter 4.1) at sea are also estimated lower than the standard North Sea value.

Table 4.2.1: Vegetation characteristics per land type (from Appendix 4.2A).

Land type	Height (m)	Width (m)	Density (units/m^2)	Stiffness (MN/m^2)
Salt marsh	1.72	0.01	2000	300
Brackish marsh	1.40	0.004	2000	300
Intermediate & fresh marsh	0.85	0.01	2000	300
Forrest layer 1	1.20	0.005	300	400
Forrest layer 2	3.00	0.08	0.02	800
Forrest layer 3	1.20	0.005	300	400

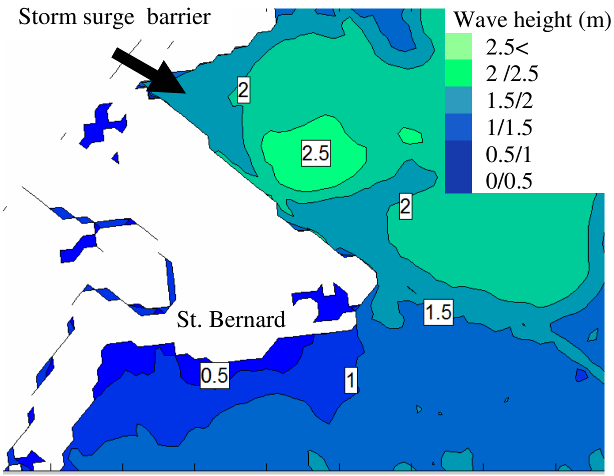

Figure 4.2.1: Significant wave height (m) with new friction calculations (0-scenario). With the location of the planned storm surge barrier and St. Bernard.

Results

For a clear comparison, only the wave heights and the changes in wave height are presented in the results. The resulting wave heights for the 0-scenario are presented in Figure 4.2.1. The changes in the Collins coefficients are small enough to state that the results have converged. In the last iteration, the maximum change of the Collins coefficient is just 1.7%. The stiffness factor stays within the range that is verified with data. The maximum value is 258, the mean value in the marshes is about 100. Appendix 4.2B shows the resulting Collins coefficients, wave periods, orbital velocities and the resulting depths.

To see the effect of the new calculation method, Figure 4.2.2 shows the deviations in wave height from a model run without friction. From this figure, it can be concluded that the marsh vegetation does just influence the waves significantly near the south of St. Bernard.

The differences with the originally applied Manning friction values (as discussed in Paragraph 4.1) are shown in Figure 4.2.3. It is clear that the marsh influence near the planned storm surge barrier is much smaller with the new calculation method than with the contribution of Manning values per marsh type. South of St. Bernard however, the marshes cause more wave dissipation than in the original calculations.

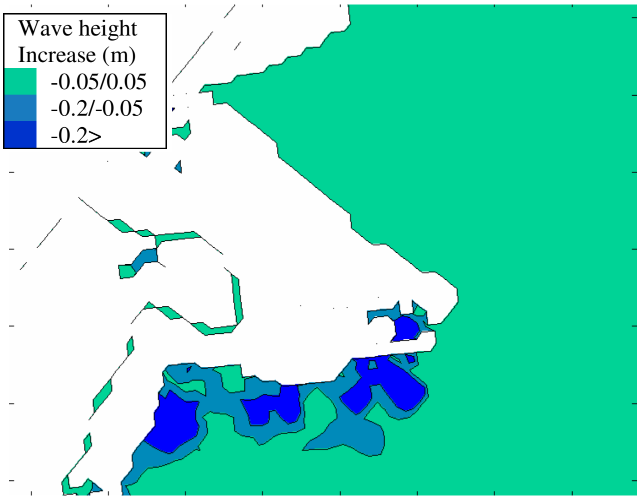

Figure 4.2.2: The new calculations compared to the wave heights without friction. Especially the wave heights south of St. Bernard decrease. In the rest of the area the marsh influence is limited.

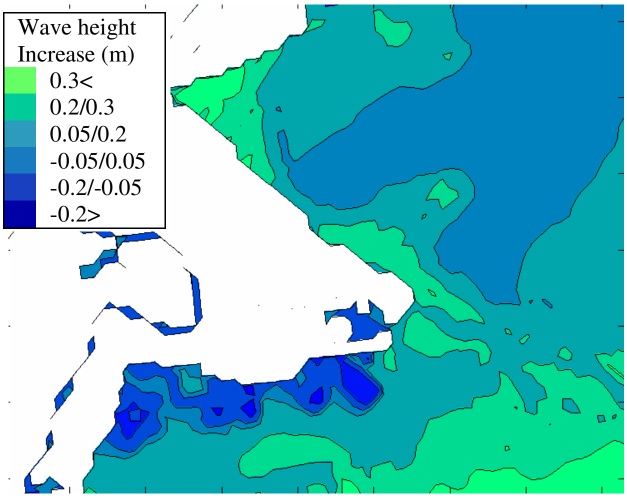

Figure 4.2.3: The new calculations compared to the original wave heights with Manning friction. Near the storm surge barrier wave heights increase about 30cm. South of St. Bernard wave heights decrease.

4.3 2050 scenario without measures

When no restoration measures will be executed in the area, it is expected that the deterioration will continue. From the several reasons for marsh degradation (Chapter 1), the increasing sea level rise will play a more important role in the upcoming decades. For the area near New Orleans the sea level rise is expected to be 50cm for 2050 (USACE 2004 from Penland 1991). As a representation for this scenario, two situations are run. In the first situation, the relative land elevation decreases with 20 cm. So for this scenario it is assumed that sediment deposition compensates the sea level rise partly. Because of this assumption, it is a moderate scenario. In the other situation, the relative sea level rise will be 50cm, so the sea level rise is not compensated at all. The vegetation density is reduced to 40%, because more erosion will take place when waves can enter the marshes more easily. Land could also erode faster because of sea level rise, but this is not taken into account here.

Results

When the relative land elevation decreases with 20cm, the wave heights increase with 5-10cm in the main part of the study area (Figure 4.3.1). The dissipation due to vegetation has decreased significantly in this model run. That can be seen in the fact that wave heights do increase much more on the places where vegetation had a reducing effect in the 0-scenario.
For the situation with a relative land elevation decrease of 50cm, the wave heights increase with 10-20cm in the main part of the study area (Figure 4.3.2). The effect of the vegetation is, as expected, reduced even more than when the relative land height decrease was 20cm.

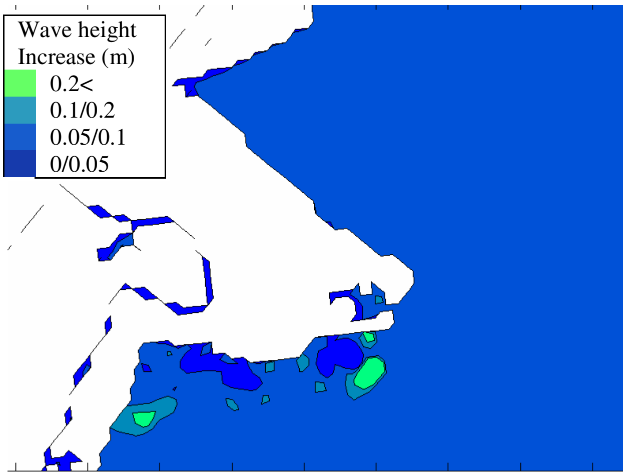

Figure 4.3.1: Relative sea level rise of 20cm. For most of the area, wave heights increase 5/10cm in comparison to the 0-scenario.

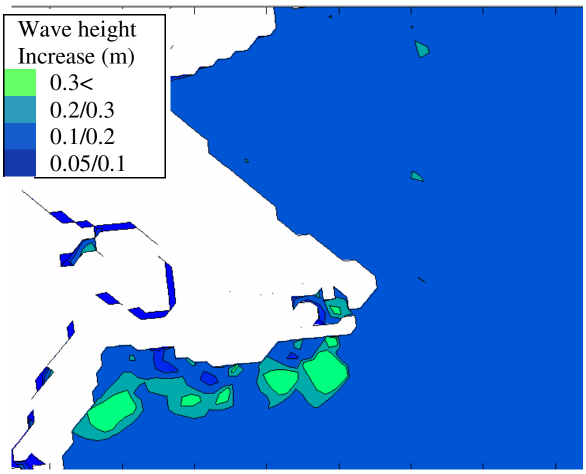

Figure 4.3.2: Relative sea level rise of 50cm. For most of the area, wave heights increase 10/20cm in comparison to the 0-scenario.

4.4 2050 scenario including restoration measures

When restoration measures are applied, it is expected that almost no land gain will occur. It will be very hard to compensate for the predicted sea level rise of 50cm. The most positive scenario that is found suggests that the marked areas in Figure 4.4.1 will get denser vegetated and get higher bottom levels (Wamsley 2008). The remaining part of the area will at best stay the same, so the sea level rise is compensated by the measures in the total area. These developments in the marshes are the result of diversions, pipelines and nourishments that are considered. The diversions will allow fresh Mississippi water to enter the marshes and to deposit the sediments it contains. The pipelines will transport sediment from other locations, and the nourishments include the planting of marsh vegetation. All together, the marked areas are modelled 10cm higher and the vegetation is expected to occupy 75% of the surface area in the restored areas. The remaining part of the grid is kept the same. A more detailed description of the restoration measures and the model implementation is presented in Appendix 4.4A.

Results

The differences with the 0-scenario are presented in Figure 4.4.2. In the largest part of the area, the waves do not change more than 2cm. In the locations where the influence of the vegetation was already significant, a decrease in wave height occurs of more than 2cm. The Biloxi marsh (Figure 4.4.1) also has a small local influence now.

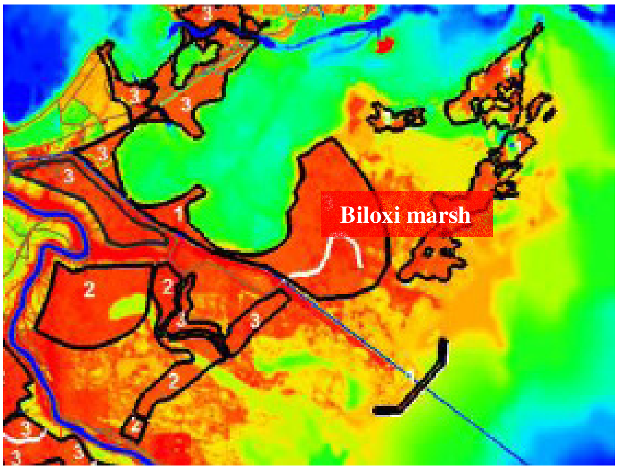

Figure 4.4.1: Areas influenced by restoration measures are outlined in black (Wamsley 2008)

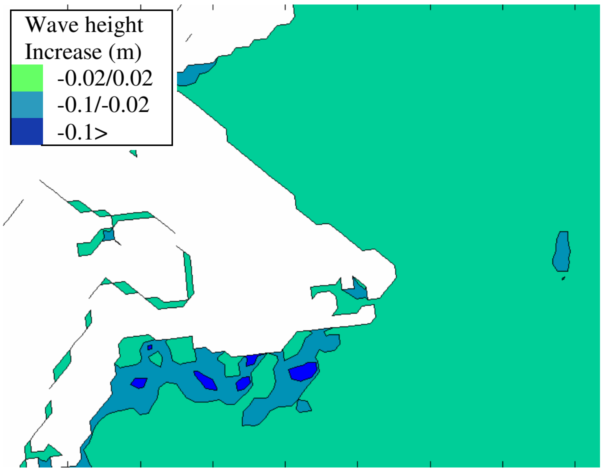

Figure 4.4.2: Restored areas get denser vegetated and bottom levels rise 10cm. The difference with the 0-scenario is -2/2cm for most of the area.

4.5 *Comparison of results*

When the results of the simulated scenarios are compared to each other, some interesting differences show. These results are mentioned briefly, the sensitivity of the model results to the Collins coefficient is analyzed and the results are explained physically.

Differences between model runs

Differences from the computations with the Manning friction file

With the method created in this project, vegetation has less influence near the upcoming storm surge barrier than with the Madsen friction file (Chapter 4.1). For the area south of St. Bernard, the vegetation has more influence in the new calculations. The calculations result in a wave height increase of about 30cm near the storm surge barrier, and a decrease of about 20cm near St. Bernard.

Differences between scenarios

The difference in wave height between the restoration and deterioration scenarios is about 20cm near the planned storm surge barrier and up to 40cm for the area south of St. Bernard. The differences in wave height near the storm surge barrier are mainly influenced by the alterations in the relative land elevation. Because restoration of marshes also needs land heightening to keep up with sea level rise, the relative land elevation and marsh restoration are strongly related. South of St. Bernard, both the land heightening and the vegetation have influence on the wave height decrease when the marshes are restored.

When the changes in wave height are expressed in percentages, they are most of the time significantly above 10%. This is the uncertainty margin that is usually applied for SWAN results. Just the wave height changes between future scenarios near the storm surge barrier are close to the 10% uncertainty of the model.

Sensitivity of the SWAN model near New Orleans to the Collins coefficient

In this paragraph it is shown what the influence of the Collins coefficient can be on the results of the SWAN model near New Orleans. Therefore the model is run with uniform Collins coefficients over the whole grid of 0.01, 0.1, 1 and 10. The wave heights are observed at two locations, as presented in Figure 4.5.1, one near the upcoming storm surge barrier and one south of St. Bernard.

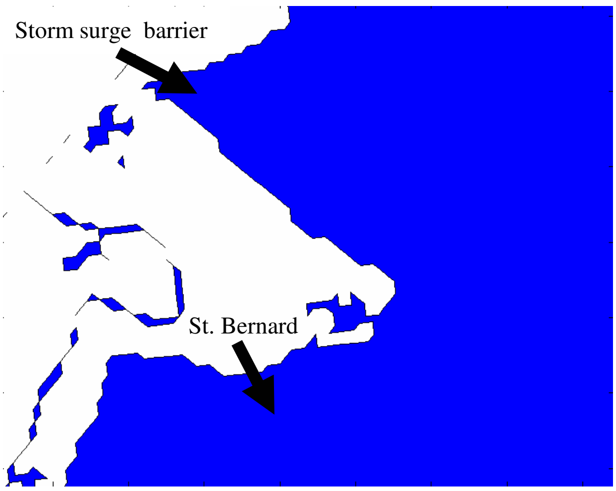

Figure 4.5.1: Locations of the two presented locations.

Table 4.5.1: Sensitivity of resulting wave heights to changes in the Collins coefficient

Collins coefficient	0.01	0.1	1	10
Wave height, storm surge barrier (m)	1.89	1.63	1.20	0.72
Wave height, St.Bernard (m)	1.46	1.23	0.92	0.74

This sensitivity analyses shows bottom friction can have a very significant influence when the Collins coefficient is applied. This is also clear from the results of the scenarios near St.Bernard. Near the upcoming storm surge barrier little effects are noticeable because the Collins coefficients are expected to be low.

Explanation of the differences

Explanation of the differences from the computations with the Manning friction file

The differences with the Madsen friction file can be explained by the fact that the new calculation method does depend to a larger extent on water levels, orbital velocities and wave periods. The low friction due to vegetation in the main part of the study area can be explained by high water levels, orbital velocities and wave periods. The values of these parameters within the study area are presented in Appendix 4.2B. The reasons for the occurrence of low friction coefficients when these parameters have high values can be found in the following theories:

- When vegetation occupies a larger part of the water column, it will have a larger impact. A bigger depth results in a smaller occupation by vegetation and therefore in lower friction coefficients.
- During acceleration and deceleration of the water, more turbulence occurs than in steady flow conditions. Small wave periods cause a more intensive acceleration and deceleration pattern and will therefore cause higher friction coefficients. Therefore, the large wave periods in the study area cause lower friction coefficients (Burger 2005 from Booij 1992). Next to the turbulence, the energy dissipation due to the bending of plants occurs more often with small periods and less often for larger periods. This results in lower friction coefficients for the study area.
- The orbital velocity causes a wake behind a vegetation stem. Because vegetation that is present in this wake will have less friction influence, higher orbital velocities reduce friction coefficients. So the high orbital velocities in the study area decrease the friction coefficients (Burger 2005).

Explanation of the differences between the scenarios

As mentioned, the differences between scenarios can partly be explained by the reduced influence of vegetation and is partly the effect of increased depth.
The reduced influence of vegetation can be explained by the principles discussed above. The wave height increase due to the increased depth (when vegetation has negligible influence) can be explained by the following aspects:

- Orbital velocities reduce with depth (Figure 1.2.5). Because the energy dissipation due to bottom friction depends on the motion of water over the bottom, reduced orbital velocities result in reduced energy dissipation. Therefore higher waves result from an increasing depth.
- Waves approaching the coast are influenced by shoaling. The reducing depths towards the coast cause a decreasing wave velocity, wave length and wave period. It also results in an increasing wave height. The increased depths in the scenarios therefore cause lower wave heights and higher wave periods, resulting in lower orbital velocities. As explained above, lower orbital velocities result in reduced energy dissipation due to bottom friction. Therefore higher waves occur in the scenarios with a higher water level.

5 Discussion

In this chapter, the limitations and possible drawbacks of the suggested methods are discussed. Furthermore the implications of the results of this study are mentioned briefly.

Validation of new formulations

The first point of discussion is the validation of the newly created formulation for representing vegetation. The available data was limited and particulary the data set of Vietnam was pretty rough on some aspects. It is likely that additional data will cause adaptations to the formula. It is for instance likely that next to the height and the width, also the thickness of vegetation and specific gravity plays a role. It is also mentioned by Westerink (2007) that vegetation being emerged or not causes deviations. Furthermore it is expected that reflection of wave energy and wave breaking on the edge of a marsh have impact on the England and Dutch case. This aspect is neglected in the final calculations, again because a limited amount of data is available.

Increased complexity of friction computations

A drawback of a friction formulation, as applied in this project, is that more data is needed and computations get more complex. Although the complex computations can be attributed to a model (as done in this project) it still takes up more computation time. The additional data that is needed on vegetation characteristics can of course be simplified to averaged values per vegetation species or land type. When averaged values get developed, modelling vegetation impacts would become as demanding as adding a specific friction coefficient as is done at the moment.

Differences with hurricane waves

Wave characteristics of the used data sets and the waves during hurricane Katrina are compared in Chapter 2. This resulted in the conclusion that the Katrina waves are close to the data set. The combination of high waves and stiff vegetation is nevertheless not present. Furthermore it is not investigated whether the spectrum of the waves near New Orleans differs significantly from the spectra of the other data sets. Just the significant wave height is applied in the friction calculations.

Effect determination near New Orleans with one hurricane

The determination of the marsh influence on waves that approach New Orleans is performed with just one hurricane. Other normative hurricanes will show different wave and surge patterns and therefore different friction effects. On the other hand will normative situations for the coastal protection of New Orleans probably result in about the same range of surge, wave period, and wave heights. Otherwise the storm would probably not be normative. When the hydraulic aspects are in the same order as with hurricane Katrina, the effects of the marsh vegetation will probably be of the same order too.

Limitations of the New Orleans grid

The used grid is based on the situation prior to hurricane Katrina. During hurricane Katrina, the bathymetry has changed a certain amount. This limits the precise values that result from the model, but does not alter the main conclusions on the effects of vegetation on waves in the area.
A standard limitation of a model grid is that values can be attributed as detailed as the level of detail of the grid, in this case 600x600m. This causes that several values are averaged and to some extend the results will deviate from reality. For instance, local deviations in land elevation and local structures (for instance houses) are not taken into account because of the grid size. Small areas with a higher bottom level. or local structures, could cause additional wave energy dissipation.
Also other restrictions of the model may limit the results. The model is for instance not equipped for steep bottom slopes.

Reduced vegetation influence during storm events

The method applied in this study results in reduced influence of vegetation during storm events compared to previous assumptions. For the calculations of the MRGO storm surge barrier in New Orleans, the results indicate that the currently used calculations with just non-vegetated bottom friction are a reasonable estimation.

Impact of marsh edges

Data sets of a Dutch and English marsh show that the edge of a marsh can have significant influence. This influence can occur due to wave energy reflection and because wave breaking can be induced. The precise effects are still unclear, but these effects could have large implications because large marslands have many small lakes and edges. If the impact is in fact significant, the presence of multiple edges per grid cel can possibly create new challenges for modelling wave propagation.

Reduction of model uncertainties

When a model of wave attenuation over vegetation is validated extensively it can reduce uncertainties in designs of coastal protection structures. Reduction of uncertainties can reduce the safety margins that have to be applied and can therefore result in less expensive and more adequate protection structures.

6 Conclusions & recommendations

6.1 Conclusions

The conclusions are referred to the research questions:

1. How do friction formulations in SWAN perform when applied to vegetated areas?
2. What improvements can be realized with detailed friction formulations for vegetation?
3. What is the effect of marshlands on the wave propagation towards New Orleans and its surroundings?

First the conclusions are drawn on the consistency of SWAN calculations with measurements in vegetated areas. When some vegetated testcases are reproduced in the model, the results are most of the time within 10% of the wave heights in the data set. To obtain these results, just the Collins friction coefficient is adjusted for each measurement. This suggests that the basic principle of energy dissipation is roughly the same and that waves propagating over vegetation can be calculated with the current (Collins) friction formulation in SWAN.
It is also evaluated whether a fixed Collins coefficient per vegetation species is applicable. When two testcases are analyzed that have exactly the same artificial vegetation, each case needs a Collins coefficient that differs significantly. Therefore it is concluded that friction due to vegetation need different relations with hydraulic aspects than friction in non-vegetated situations.

On the second research question it is concluded that detailed friction descriptions can improve the results. In the applied Mendez (2004) formulation the parameters vegetation width, vegetation height, vegetation density, water depth, wave height and wave period are used to obtain the friction coefficients. With this specific formulation for friction due to vegetation, the different friction coefficients in different hydraulic situations can be explained. The formulation only has the problem that its use is limited to flexible vegetation. To cope with this, a stiffness factor is added that should mainly compensate for the reduced bending of stiffer vegetation. This results in a description that reproduces the data of stiff vegetation in a better way.

The conclusions on the last research questions are obtained with the SWAN model that has the grid of New Orleans' surroundings implemented. As normative storm, the data of hurricane Katrina are used. The friction is calculated with the adapted Mendez formulation and is implemented in a Matlab script. This script performs multiple iterations with the SWAN model to come to the desired friction values. For the data set, the calculations result in wave heights that are close to the measurements. Therefore, the implementation of the formulae is assessed to be correct. When the computations are performed for the New Orleans grid, it results in very small influences of the marshes near the upcoming MRGO storm surge barrier. The wave attenuation is a lot smaller than when the calculations are performed with roughness heights based on Manning values per land type. The large depth, wave period and high orbital velocities during a hurricane are the reason for the low friction with the new formulation. South of St. Bernard the depth, periods and velocities are much lower, resulting in a higher friction and more wave height reduction than in the original SWAN calculations.

Despite the fact that the influence of the vegetation itself is assessed as small for most of the area, the differences between future scenarios are significant. The difference in wave height between the scenario with and without restoration measures can be up to 40cm near the south of St. Bernard and up to 20 cm near the planned storm surge barrier. Near the storm surge barrier the effects mainly occur because restoration of the marshes compensates the relative sea level rise. The relative sea level rise that is expected without restoration measures has significant influence on the waves approaching the New Orleans' coast. Near St. Bernard, lower waves due to restoration measures occur because of both the changing friction of the vegetation and the change in bottom level.

If the predictions obtained in this project are better or worse than before is unclear because there is no data of the study area. The fact that friction is now obtained from vegetation characteristics with a specific relation between vegetation and waves is considered an improvement. It is considered as such because it is shown in Chapter 2 that a fixed friction coefficient is probably not valid for different hydraulic situations. The precise values are nevertheless still uncertain because more measurements are needed for a better validation of the formula.

6.2 Recommendations

The recommendations that are made based on this project are as follows:

- It is recommended to use friction formulations that depend differently on hydraulic conditions than friction formulations for non-vegetated bottoms. It is also recommended to implement vegetation characteristics in these calculations. This is desired to be able to cope with the different influences of vegetation on friction as illustrated in Chapter 1.

- It is recommended to perform multiple measurements on wave attenuation over vegetation. The data that is available at the moment is particularly limited when stiff vegetation is considered. With a better data set, there are more possibilities to validate the model and to improve the friction formulations.

  The data that would help the most for the New Orleans situation would be the combination of Spartina vegetation and high water levels, high wave heights and high wave periods.
  For the mangrove forests in south-east Asia it would be helpful to have measurements of wave propagation over vegetation with various structures and different stiffnesses. When the different structural layers are well described, the interaction of tree-tops, stems and aerial roots can be described in a better way.

- Wave energy dissipation near the edge of a marsh also needs some additional research. The England case and the Dutch case show patterns that indicate reflection and wave breaking near the marsh edge can be significant. Wave heights in front of the edge could be a little higher and, more important, the wave heights decrease more behind the edge.

  Just one measurement was available with some detailed measurements near a marsh edge, this was not enough to test theories on this subject. Therefore it is recommended to use more measuring stations near the edge of a vegetation field when new measurements are performed.

- It is recommended to perform analyses on the uncertainties of the method developed in this project. It can be analyzed how the 'stiffness factor' would change when one of the data sets is not taken into account in the development of the factor. It is also interesting to see how such changes in this factor would influence predicted wave heights near New Orleans.

- For the decision if marshes near New Orleans should be protected or not, there are too many factors into play to give a proper recommendation. That is a political trade off that should consider multiple valuable aspects. It can nevertheless be recommended to consider the effects on wave heights for the situation that restoration measures are applied or not applied. When no measures are taken it is a realistic estimation that wave heights will increase at least 15cm in the year 2050 when the sea level rise will continue as expected.

References

Websites

- acs.org, *pubs.acs.org/subscribe/journals/esthag-w/2005/nov/tech/jp_katrina.html*, visited 3-11-2008
- ambiente.venezia.it, *ambiente.venezia.it/partecipazione/lagunavenezia/Web/Flora/Zostera%20noltii.htm*,visited 6-25-2008
- americaswetlandresources.com, *americaswetlandresources.com/background_facts/detailedstory/index.html*, visited 4-9-2008
- aquat.edu, *caquat1.ifas.ufl.edu/panhemn2.jpg*, visited 4-9-2008
- coast2050.gov, *coast2050.gov*, visited 10-4-2008
- cofairhope.com, *cofairhope.com/images/Bulltongue.jpg*, visited 4-9-2008
- dhh.louisiana.gov, dhh.*louisiana.gov/offices/page.asp?ID=192&Detail=5248*, visited 10-15-2008
- fema.gov I, *fema.gov/txt/fhm/frm_p1wave.txt*, visited 4-9-2008
- fs.fed.us, fs.*fed.us/database/feis/plants/graminoid/spapat/all.html#botanical%20and%20ecological%20characteristics*, visited 9-10-2008
- gewiekste.nl, *gewiekste.nl/Windsnelh_ber.xls*, visited 10-20-2008
- habitas.org.uk, *habitas.org.uk/flora/photo.asp?item=2125d*, visited 6-25-2008
- jeethang.com, *jeethang.com/asia05/0423/pages/19.water.lilies.html*, visited 4-9-2008
- lacoast.gov, *lacoast.gov/watermarks/1999c-summer/5coast2050/*, visited 3-11-2008
- map24.nl, *map24.nl*, visited 4-9-2008
- marlin.ac.uk, marlin.*ac.uk/species/taxon_Laminariahyperborea.htm#OIm*, visited 6-25-2008
- netcoast.nl, *netcoast.nl/tools/rikz/SWAN.htm*, visited 4-9-2008
- nwf.org, *nwf.org/conservation.cfm*, visited 3-11-2008
- plants.usda.gov, *plants.usda.gov*, visited 9-10-2008
- saveourlake.org, *saveourlake.org/LOD_projects.htm*, visited 9-10-2008
- sfgate.com, *sfgate.com/cgi-bin/article.cgi?f=/c/a/2005/09/05/mng69eihuk1.dtl*, visited 3-11-2008
- swan.nl, *swan.tudelft.nl/modifications/modifications.htm*, visited 11-10-2008
- tudelft.nl, *vlm089.citg.tudelft.nl/swan/index.htm*, visited 4-9-2008
- usace.mil I, *chl.erdc.usace.army.mil/chl.aspx?p=s&a=SOFTWARE;9*, visited 4-9-2008
- usace.mil II, *chl.erdc.usace.army.mil/chl.aspx?p=s&a=ARTICLES;274*, visited 4-9-2008
- usatoday.com, *usatoday.com/money/economy/2005-09-09-katrina-damage_x.htm*, visited 8-15-2008
- vulkaner.no, *vulkaner.no/n/surtsey*, visited 6-25-2008
- weerwetenswaardigheden.nl, *weerwetenswaardigheden.web-log.nl/mijn_weblog_weer_wetenswa/2007/11/index.html,* visited 8-15-2008
- wikipedia.org, *wikipedia.org*, visited 10-20-2008
- wldelft.nl, *wldelft.nl/soft/swan/,* visited 3-11-2008

Literature

- C. Bender, J.M. Smith, 2007, *Methodology and results for nearshore wave simulation in a coupled hydrodynamic and wave model system to evaluate storm surge in coastal Louisiana*, unknown
- N. Booij et al., 2004, *SWAN user manual*
- T. J. Bouma, M.B. De Vries, E. Low, G. Peralta, I.C. Tanczos, J. Van De Koppel, P.M.J. Herman, 2005, *Trade-offs related to ecosystem engineering: a case study on stiffness of emerging macrophytes,* Ecology, no. 86, p. 2187–2199
- B. Burger, 2005, *Wave attenuation in mangrove forests, numerical modelling of wave attenuation by implementation of a physical description of vegetation in SWAN,* Thesis, Delft University of Technology

- Chadwick, D.Reeve, C.Fleming, 2004, *Coastal engineering: processes, theory and design practice,* Spon Press, New York, USA
- A.M. Cooley, A. Reich, P. Rundel, 2004, *Leaf support biomechanics of neotropical understory herbs*, American Journal of Botany, no.91 p.573-581
- M.H.S. Elwany, W.C. O'Reilly, ASCE, R.T. Guza, 1995, *Effects of southern California kelp beds on waves*, Journal of waterway, port, ad coastal engineering, no.2, p.143-150
- X.Fang, 2002, *Reproductive biology of smooth Cordgrass (Spartina Alterniflora)*, Thesis, Louisiana State University
- N. Kobayashi, A.W. Raichle, T. Asano, 1993, *Wave attenuation by vegetation,* Journal of Waterway, Port, Coastal, and Ocean Engineering, no. 119, p. 30-48
- LDNR/CRD, 1998, *Ecosystem Response to a freshwater diversion: the Caernarvon experience*
- S.M.Lovas, A.Torum, 2000, *Effect of the kelp Laminara hyperborea upon sand dune erosion and water particle velocities,* Coastal Engineering, no.44, p.37-63
- Y. Mazda, D. Kobashi, S. Okada, 2005, *Tidal-scale hydrodynamics within mangrove swamps, Wetlands Ecology and Management*, no. 13, p. 647–655
- M.C. Meijer, 2005, *Wave attenuation over salt marsh vegetation, a numerical implementation of vegetation in SWAN,* Thesis project, Delft University of Technology, The Netherlands
- F.J. Mendez, I.J. Losada, M.A. Losada, 1999, *Hydrodynamics induced by wind waves in a vegetation field,* Journal of Geophysical Research, no. 104, p. 383-396
- F.J. Mendez, I.J. Losada, 2004, *An empirical model to estimate the propagation of random breaking and nonbreaking waves over vegetation fields,* Coastal Engineering, no. 51, p. 103-118
- Moller, T. Spencer, J. R. French, D. J. Leggett, M. Dixon, 1999, *Wave transformation over salt Marshes: a field and numerical modeling study from north Norfolk, England*, Estuarine, Coastal and Shelf Science, no. 49, p. 411–426
- J.M. Smith, 2007, *Modelling nearshore waves for hurricane Katrina*, Engineer Research and Development Center Coastal and Hydraulics Laboratory, Vicksburg
- W. Stone, A. Sheremet, X. Zang, Q. He, B. Liu, B. Strong, 2003, *Landfall of two tropical systems seven days apart along southcentral Louisiana*, Proceedings of Coastal Sediments ’03, Clearwater Beach, USA
- W. Stone, X. Zang, A. Sheremet, 2005, *The role of barrier islands, muddy shelf and reefs in mitigating the wave field along coastal Louisiana*, Journal of Coastal Research, no. 44, p. 40-55
- P.A. Tschirky, 2000, *Waves and wetlands, an investigation of wave attenuation by emergent, freshwaterwetland vegetation,* Thesis project, Queen's University, Canada
- USACE, 2004, *Louisiana coastal area, Louisiana ecosystem restoration study*
- L.C. Van Rijn, 1990, *Principles of fluid flow and surface waves in rivers, estuaries, seas and oceans*
- T.Wamsley, J.Smith, 2008, *Evaluation of restoration alternatives through numerical surge and wave modeling*
- J. Westerink, J. Smith, V. Cardone, A. Cox, R. Jensen, T. Wamsley, C. Dawson, D. Resio, B. Ebersole, A. Kennedy, 2007, *Hurricane wind, wave, and surge computations deficiencies and research needs*, presentation 10th IWWHF-CHS

Appendices, Final report

Wave attenuation over marshlands

Determination of marshland influences on New Orleans' flood protection

M. Vosse
November 17th 2008

Thesis committee:
Prof.dr. S.J.M.H. Hulscher
Dr. ir. C.M. Dohmen - Janssen
Dr.ir. M. van Ledden
Ir. A.J. Lansen

ROYAL HASKONING

University of Twente
Enschede - The Netherlands

Appendix numbers are coupled with the chapters in the main report.

Table of contents

Appendix 1.3A: Early wave-vegetation methods

The methods are presented in chronological order because theories are often related. The described theories are mentioned a lot in literature, but it is not a complete list of theories developed. It is nevertheless a good way to create understanding of the development of this study area.

Morrison
(Burger 2005 from Morrison 1950) Morrison is one of the first who developed a formulation for force on a pile in surface waves. This is the basis for many energy dissipation formulations based on vertical cylinders.

Camfield
(Tschirsky 2000 from Camfield 1977) Camfield also developed a method to describe vegetation influence on waves. The vegetation resistance is treated as an additional bottom friction in which effects as motion of vegetation are neglected. Camfield encountered the problem that too less data was available to create friction factors for marsh vegetation.

Dean
(Tschirsky 2000 from Dean 1978) Dean created the following formulation between incident wave height and transmitted wave height over marsh grass (Equation 3A.1). The formulations are based on vertical cylinders, placed in a squared position in flume measurements.

$$\frac{H_2}{H_1} = \frac{1}{1 + AH_1}$$

$$A = \frac{C_D Dl}{6\pi s^2 h}$$

Eq. 3A.1: C_D= drag coefficient (estimated as 1), D= grass stem diameter, s= averaged spacing stems, h= depth, H_1= incident wave height, H_2= transmitted wave height, A= damping coefficient, l= length of the grass

Knutson
(Tschirsky 2000 from Knutson 1982) Knutson performed a field study to evaluate the mode1 proposed by Dean. Field data are used from measurements in a smooth Cordgrass marsh. The distribution of the plants was of course more complex than the assumed squares, and the bathymetry was also not taken into account in detail. The C_D of 1, proposed by Dean for smooth vertical cylinders, differed significantly.
A part of the problem was assumed to be related to the fact vegetation was emerged above the water. The explanation was that when emerged vegetation bends, more volume of vegetation comes in the water column to affect the waves. Knutson added a coefficient to compensate for this and other vegetation characteristics (plant drag coefficient, C_p Equation 3A.2). In this case a C_p was agreed on of 5, resulting in a root mean square error in transmitted wave heights of 0.022m. (The observed transmitted wave heights ranged from 0.02 - 0.17 m). The model was assessed as valid for emerged vegetation, but it was estimated that the coefficients should be calibrated per vegetation type and probably also per marsh with the same vegetation type. In cases where the depth exceeded the plant height, Knutson suggested the use of Camfield's model.

$$A = \frac{C_p C_D Dl}{3\pi s^2 h}$$

Eq. 3A.2: The same damping coefficient formula as in Eq. 3A.1 with an additional plant drag coefficient C_p,

Dalrymple
(Tschirsky 2000 from Dalrymple 1984) Dalrymple developed a method based on the previous theories. In this theory, vegetation is represented as rigid vertical cylinders. Energy dissipation occurs based on wave characteristics in relation to vegetation characteristics as diameter, length and density. One of the recognized problems was the ignorance of vegetation motion, one of the reasons the drag value should still be calibrated. The resulting equation is still similar to Dean's formulation, but with a more complex damping coefficient (Equation 3A.2).

$$A = \frac{2C_D}{3\pi}\left(\frac{D}{b}\right)\left(\frac{a_0}{b}\right)\left(\sinh^3(ks) + 3\sinh(ks)\right)\left(\frac{4k}{3\sinh(kh) * \sinh(2kh + 2kh)}\right)$$

Eq. 3A.2: The same damping coefficient as applied by Dean, but more physical properties of vegetation are described in it. Still an unknown C_D. D=diameter, b=spacing between cylinders, a_0= initial wave amplitude, k=wave number, h=depth, s=vegetation height

Asano and Kobayashi

(Kobayashi 1993) Asano and Kobayashi presented an analytical model to describe wave damping due to submerged vegetation. With continuity and momentum equations, the drag of vegetation was modelled. The effect of the vegetation was assumed equal to the drag force acting on the vegetation. Vegetation motion was not taken into account. The wave attenuation was assumed exponential. With a fitted drag coefficient, the model remained within 10% of the Osana data. They claimed more field data would be required to better predict the drag coefficient for other types of vegetation.

$$H = H_0 e^{-k_i x}$$

Eq. 3A.3: Exponential decay model of Asano and Kobayashi. H=transmitted wave height, H_0=incident wave height k_i=damping rate (imaginary wave number), x=distance of wave propagation through vegetation.

Dubi and Torum

(Tschirsky 2000 from Dubi and Torum 1994) Dubi and Torum used the model approach of Asano and Kobayashi to study wave attenuation over kelp vegetation. With a fitted drag coefficient, the model deviated up to 30%.

Appendix 2.1A: Details of testcases

Dubi Case

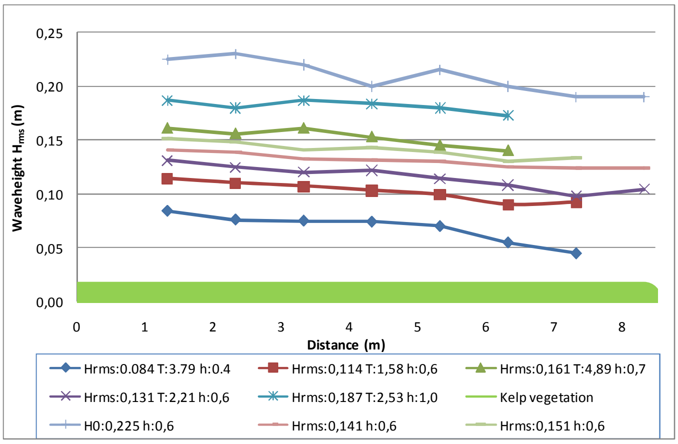

Figure 2.1A.1: Data from a flume experiment performed by Dubi. It is scaled 1:10. (Mendez 1999, Mendez 2004)

Figure 2.1A.2: Laminaria Hyperborea, the vegetation represented in the Dubi and Lovas case. About 2m high at 10m depth, so it is scaled 1:10 for the experiment. The plant consists of a stipe with multiple leaves. (vulkaner.no) It is a brown seaweed or kelp. (marlin.ac.uk)

Osana Case

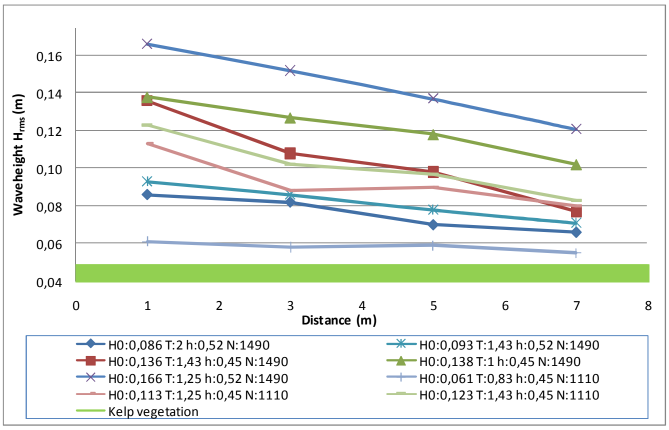

Figure 2.1A.3: Measurements of Osana (Mendez 1999)

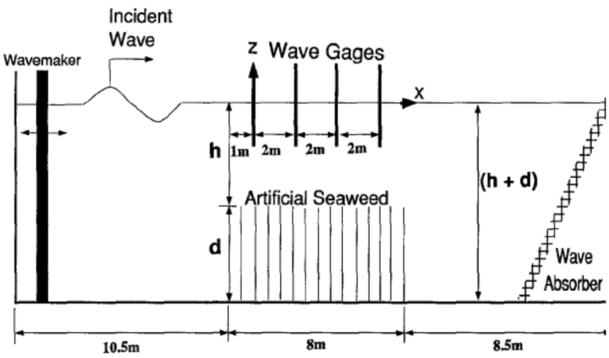

Figure 2.1A.4: Experimental set-up of Osana (Kobayashi 1993)

Lovas Case

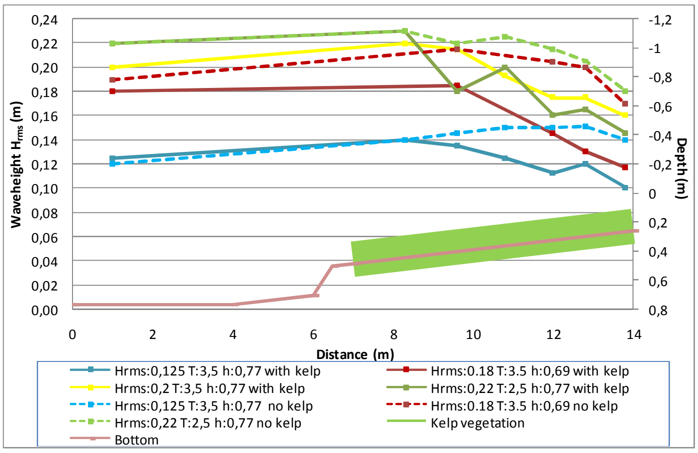

Figure 2.1A.5: Results of Lovas' experiments. The sloping bottom is presented at the secundary y-axis, relative to the maximum water level. (Mendez 2004)

Bouma Case

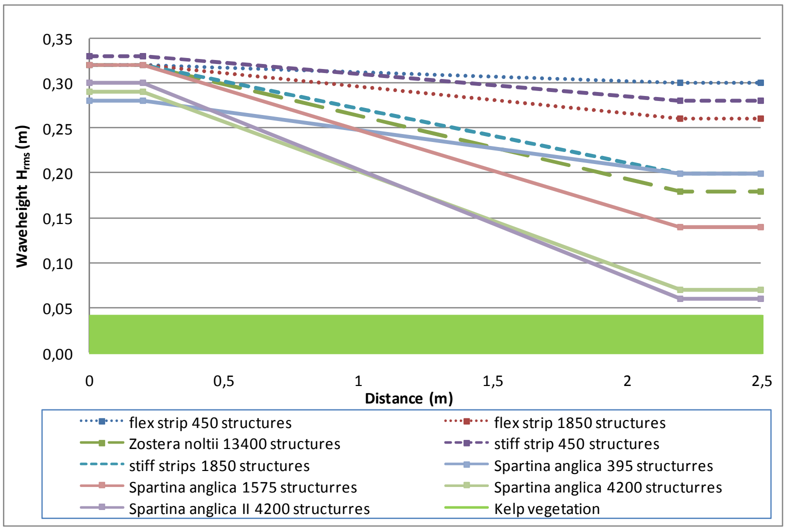

Figure 2.1A.6: Measurements for different vegetation types (Bouma 2005)

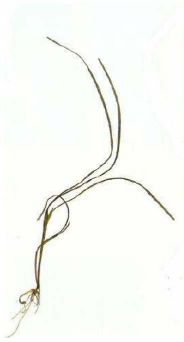
Figure 2.1A.7: Zostera Noltii, used in the Bouma case. A grass specie with a height between 10-30cm and a thickness of 2-3mm. (ambiente.venezia.it)

For the Bouma case the vegetation is different for each measurement. The following characteristics apply (Table 2.1A.1):

Vegetation type	Width (b_v)	Density
(Flexible)	*(m)*	*(structures/m^2)*
Flexible strips (strips of plastic folder)	0.005	450
Flexible strips (strips of plastic folder)	0.005	1850
Zostera noltii (from the field, 0.1m height)	0.005	13400
(Stiff)		
Stiff strips (tie wraps)	0.003	450
Stiff strips (tie wraps)	0.003	1850
Spartina Anglica (grown in greenhouse until average height of 0.1m)	0.003	395
Spartina Anglica (grown in greenhouse until average height of 0.1m)	0.003	1575
Spartina Anglica (from the field, cut to 0.1m)	0.003	4200
Spartina Anglica (from the field, cut to 0.1m)	0.003	4200

Table 2.1A.1: Vegetation specifics for the different experiments in the Bouma case (Bouma 2005)

NL Case

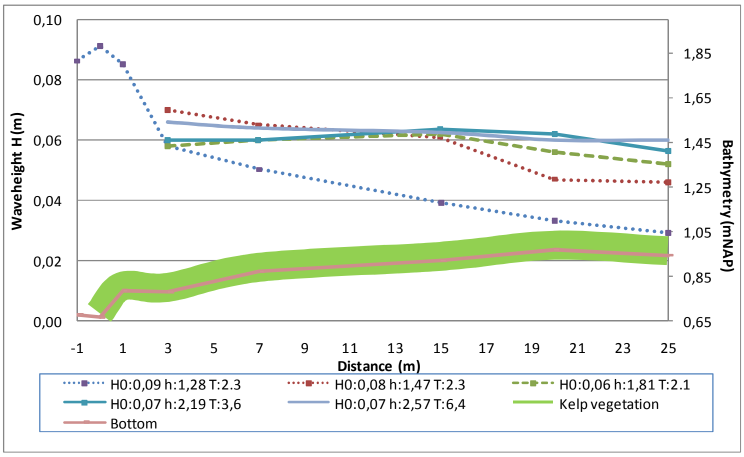

Figure 2.1A.8: Measurements at the Paulinapolder, Netherlands. Measurements near the edge are just available for one measurement. (Meijer 2005 from WL|Delft Hydraulics 2003)


Figure 2.1A.9: Spartina Anglica or Cord grass. The dominant vegetation in the Dutch case and also used in the Bouma experiment. (Meijer 2005)

Sensor	Plant height (d_v) (m)	Stem diameter (b_v) (mm)	Density (N) (stems/m^2)
1	0.42	2.3	872
2	0.30	3.5	796
3	0.38	3.9	620
4	0.34	2.9	1476
5	0.36	3.9	1308
6	0.31	3.8	1704

Table 2.1A.2: vegetation characteristics of the experimental area. Sensor 6 is on the left edge of the marsh in Figure 2.1A.8. (Meijer 2005 from WL|Delft Hydraulics 2003)

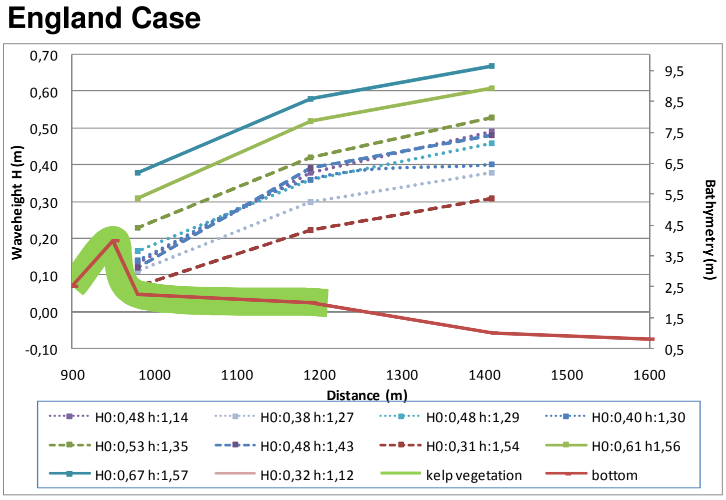

Figure 2.1A.10: Measurements of Moller (1999)

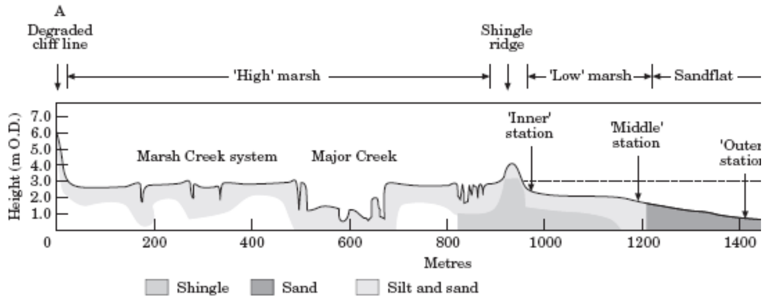

Figure 2.1A.11: Experimental set-up of Moller (1999)

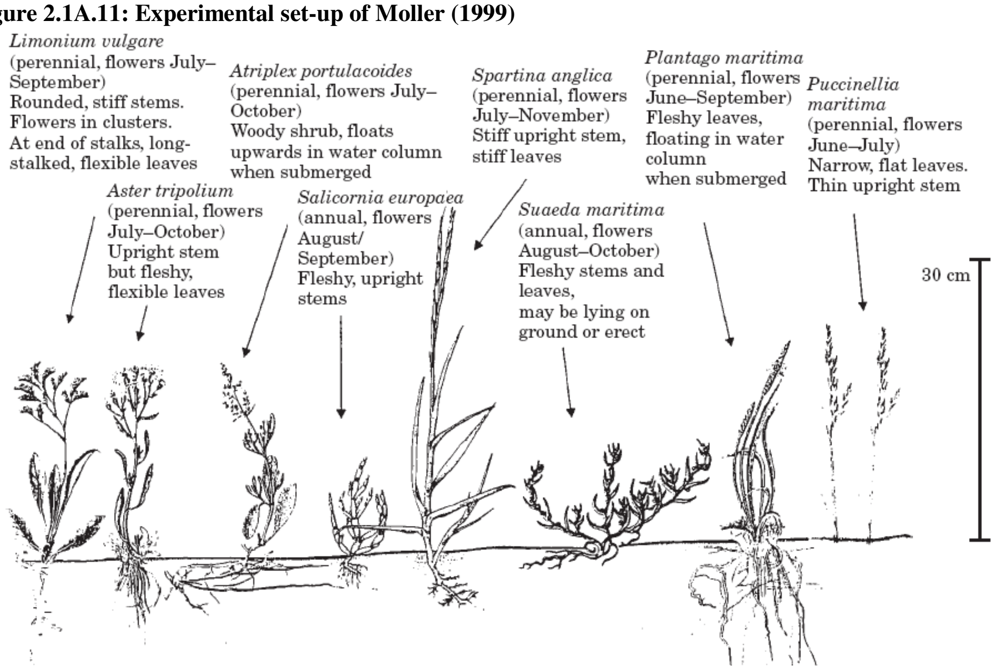

Figure 2.1A.12: A large variety of vegetation in the England case. Detailed characteristics and the distribution over the salt marsh are unclear. (Moller 1999)

Appendix 2.2A: SWAN file of the Osana case

```
$***********MODEL INPUT**************************************
CGRID 0. 0. 0. 20000. 6. 25 100 SECTOR 80. 130. 100 0.05 2 40
INPGRID BOTTOM 0. 0. 0. 1 1 20000. 6.
READINP BOTTOM 1. 'bot\Osana.bot'  1 0 FREE
$
BOU SHAPE BIN PEAK DSPR POWER
BOUN SIDE S CCW CON PAR 0.093 1.43 90. 500.
$
OFF QUAD
OFF WCAP
FRICTION COLLINS 2.5
$
$************ ACCYRACY and NUMBER OF ITERATIONS OF SWAN************
NUM ACCUR 0.01 0.01 0.01 99. STAT MXITST=5
$
$************ OUTPUT REQUESTS *************************
POINTS 'loc' FILE   'Osana.loc'
SPEC   'loc' SPEC1D 'Osana.spc'
TABLE  'loc' NOHEAD 'tbl\Osana.tbl' DIST DEP HS RTP TM01 TM02 FSPR
$
TEST 1,0
COMPUTE
STOP
$
```

Appendix 2.2B: Modeling of wave spectra

In Chapter 2, regular wave spectra are applied. For the Dubi and Lovas case this was a JONSWAP spectrum in reality. When a JONSWAP spectrum is used, it is also better to use the significant wave height (H_s) in SWAN. To test the differences between implementation methods, the non-vegetated measurements of Lovas are reproduced (just like in Chapter 2). The non-vegetated situations should be described well in SWAN with the standard friction coefficients.
When this is done, it results in the following Figures (2.2B.1-2.2B.3). It becomes clear from the figures that the differences between the regular and the JONSWAP spectrum are very small when the root mean square wave height (H_{rms}) is applied. They both reproduce the data very well. When the significant wave height (H_s=1.48H_{rms} (Chadwick 2004)) is applied, the results are far worse.
So the assumption of regular waves probably does not introduce a significant uncertainty to the predictions of this study.

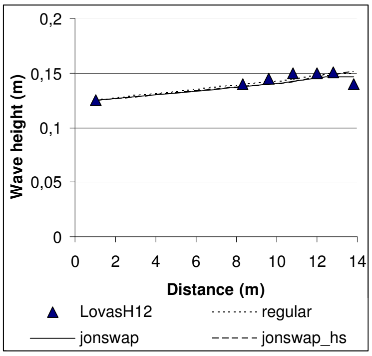

Figure 2.2B.1: Lovas data without kelp compared to SWAN output. Average/max deviation: regular 2/6%, JONSWAP and H_{rms} 3/5%, JONSWAP and H_s 3/8%.

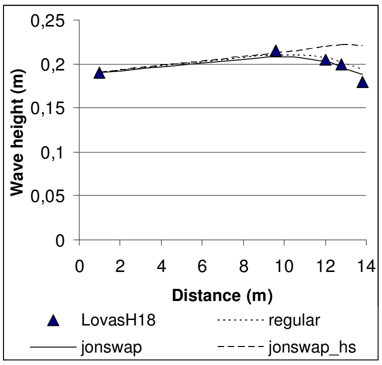

Figure 2.2B.2: Lovas data without kelp compared to SWAN output. Average/max deviation: regular 2/7%, JONSWAP and H_{rms} 2/4%, JONSWAP and H_s 8/22%.

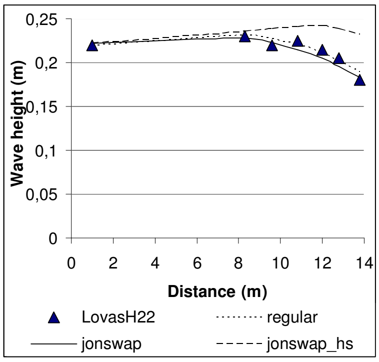

Figure 2.2B.3: Lovas data without kelp compared to SWAN output. Average/max deviation: regular 2/5%, JONSWAP and H_{rms} 3/4%, JONSWAP and H_s 14/29%

In the Dutch, England and Vietnam case the wave spectrum is unclear. When a JONSWAP spectrum is assumed in stead of a regular spectrum, the best-fit Collins coefficients would be higher. When H_s is rewritten to H_{rms} and applied in a regular spectrum, the best-fit Collins coefficients would be lower. Both methods would change the actual values of the 'stiffness factor' a certain amount, but the basic patterns would probably be the same. As mentioned, it is unclear what does comply better with reality because the actual spectra are unclear.

Appendix 2.3A: Best-fit Collins coefficient

The following figures show that different experiments within a case need different friction coefficients when they are reproduced in SWAN. Figure 2.3A.1 shows the reproduction of the Dubi case. The left measurement has an average deviation of 1% and a maximum of 2%, with a Collins coefficient of 1. For a Collins coefficient of 2 the deviations are 7 and 16%. The right measurement with the same vegetation needs a Collins coefficient of 2 to reach the average/maximum deviations of 1%/6% and has deviations of 6%/14% with a Collins coefficient of 1. This shows that in the Dubi case the optimum coefficients vary, and are that far separated that the desired maximum deviations (10%) are exceeded when applied to other measurements of the case.

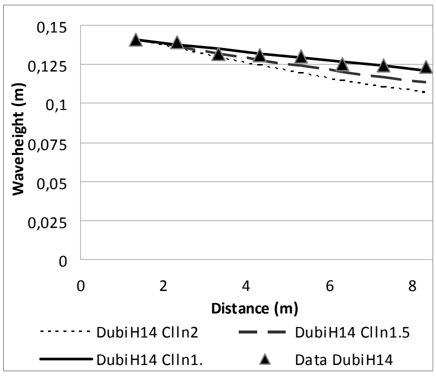

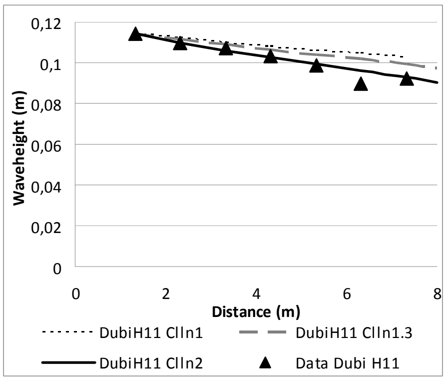

Figure 2.3A.1: The Dubi case.

The Osana case is presented in Figure 2.3A.2. In the middle figure (enlargement of the left figure) it is visible that the optimum is a Collins value of about 15, the absolute differences are very small (left). In the right figure, another optimum value (3 to 4) is applicable for the same vegetation.

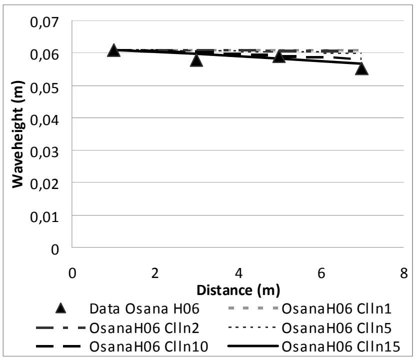

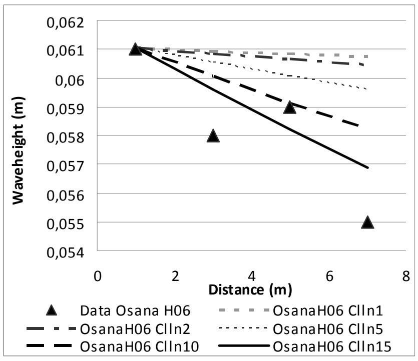

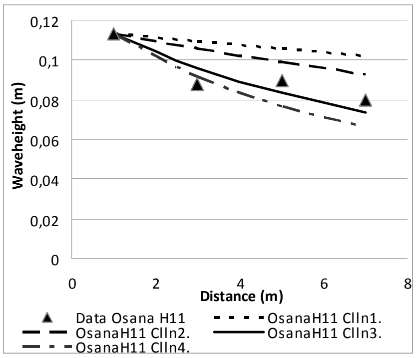

Figure 2.3A.2: Osana case.

As expected, the different vegetation species in the Bouma case are represented by different friction coefficients, Figure 2.3A.3. In the left figure the optimum is between 0.1 and 0.2, in the right figure about 10.

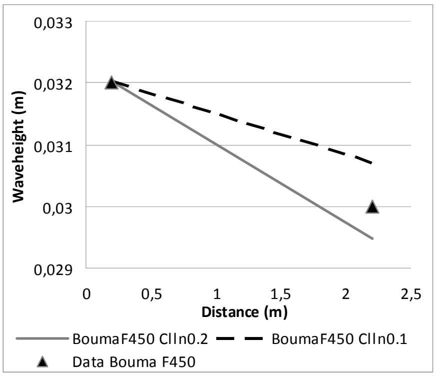

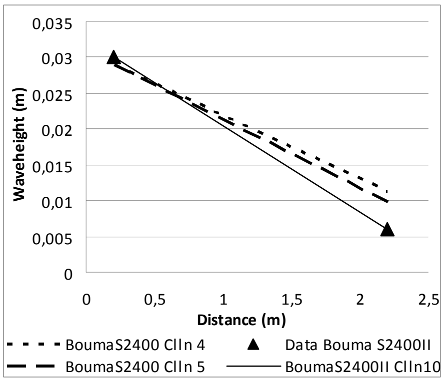

Figure 2.3A.3: Bouma case.

Appendix 2.4A: Friction coefficient averaged over all cases

The mean value of all the best fitting Collins coefficients is about 2.2 (for sand 0.015). All of the measurements are calculated with this value to check the ability of just one fixed coefficient for all of the vegetation species. The R^2 of the total dataset (without the England case and the edge of the Dutch case) is very well with a value of 0.87. This is as expected, because the coefficient is the average of all the best-fit coefficients. So this results are biased. For the Osana case it results in a reasonably good fit, but other cases deviate far more than 10%. Table 2.4A.1 shows the percentage of measurements that has a certain maximum deviation.

	Percentage of measurements within a case that have a certain maximum deviation			
Case	<10%	10-19%	20-30%	30<
Osana	75%	25%	-	-
Dubi	25%	25%	38%	12%
Lovas	-	-	-	100%
Bouma	11%	11%	22%	55%
NL	40%	20%	20%	20%
Eng	-	-	-	100%

Table 2.4A.1: Results when all cases are run with a Collins coefficient of 2.2.

Appendix 2.6A: Trends in the best-fit Collins coefficient

Vegetation influence determination using the best-fit Collins coefficients

The best-fit Collins coefficient is used to find relations between the friction coefficient and the different parameters. Hereto the best-fit friction coefficients are plotted against all of the different parameters known of the cases. These parameters are the wave height, wave period, vegetation height, depth, relative depth and density.

Wave height in relation to Collins coefficient

The Bouma case is not used in this analysis because wave heights are almost steady and a large variation in vegetation is applied.
Per case, so per vegetation composition, it results in the following trendlines: Nl case: y = -197x + 18, Eng case: y = -1x + 0, Dubi case: y = -3x + 2, Osana case: y = -74x + 12, Lovas case: y = 0x + 1. So in total, and when every case is investigated separately, the trend is that the Collins coefficient decreases with wave height. As clear from the low R^2 values, the relation between wave height and the Collins coefficient is not conclusive.

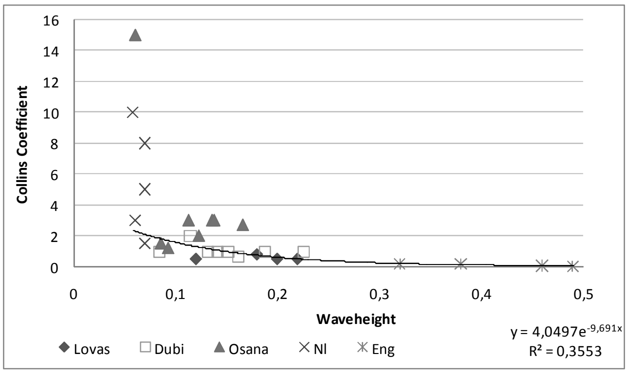

Figure 2.6A.1: Fitted Collins coefficients in comparison to wave heights

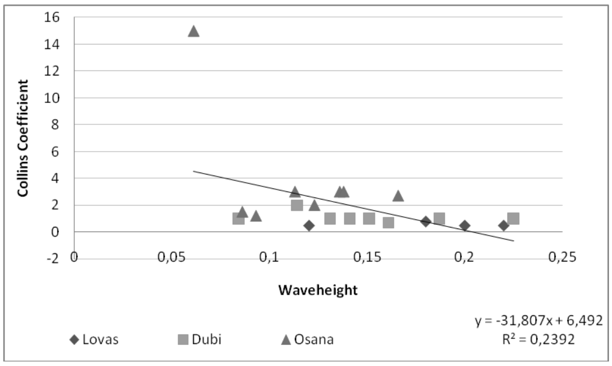

Figure 2.6A.2 Fitted Collins coefficients in comparison to wave heights without field measurements

Peak period in relation to Collins coefficient

When the peak period is compared to the Collins coefficient the following results are obtained (Figure 2.6A.3-4). The Bouma case is not taken into account because of a steady period combined with a large variation in vegetation. The England case is not taken into account because of the bad 'best-fit'.

Per case, so per vegetation composition, it results in the following trendlines (rounded to integers): NL case: y = -1x + 7, Dubi case: y = 0x + 2, Osana case: y = -8x + 15, Lovas case: y = 0x + 0. So in total, and when every case is investigated separately, the relation between the Collins coefficient and the period is kind of visible. In general, a lower period results in a Collins coefficient that is a little bit higher..

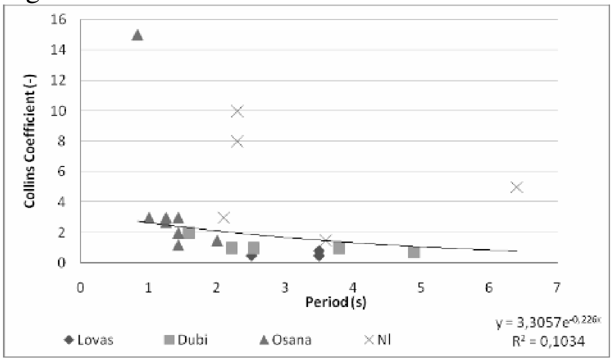

Figure 2.6A.3: Fitted Collins coefficients in comparison to wave period.

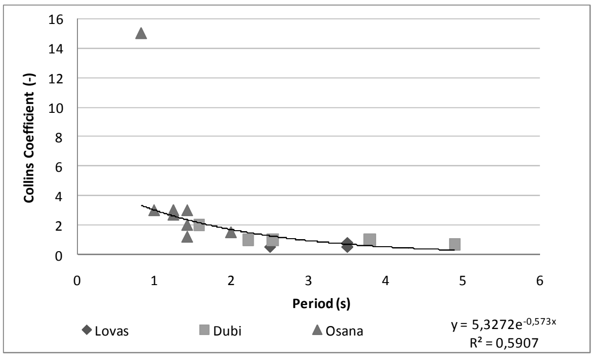

Figure 2.6A.4: Fitted Collins coefficients in comparison to wave period. Just the uniform vegetated flume cases.

Vegetation height in relation to Collins coefficient

The trend between vegetation height and the Collins coefficient is that higher vegetation results in a higher Collins coefficient, what sounds reasonable. The different vegetation types tested in the Bouma case (for instance very stiff ones) indicate that the type of vegetation is also very important. (Figure 2.6A.5.)

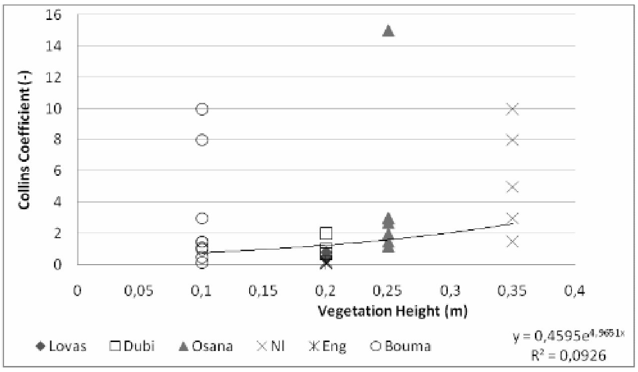

Figure 2.6A .5: Fitted Collins coefficients in comparison to vegetation height.

Depth in relation to Collins coefficient

Because of the fixed water levels in the Bouma and Lovas case, these measurements are left outside the graphs of depth related to the Collins coefficient (Figure 2.6A.7/8). With a correlation coefficient of just 0.01 this is a weak relation. No real trends are visible. When the field measurements are excluded a more comparable vegetation type remains. This results in a clearer relation.

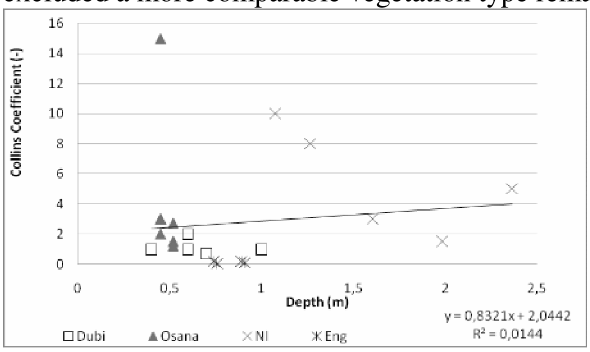

Figure 2.6A.6: Fitted Collins coefficients in comparison to water depth. The Dutch case is disturbing the trend of the other cases.

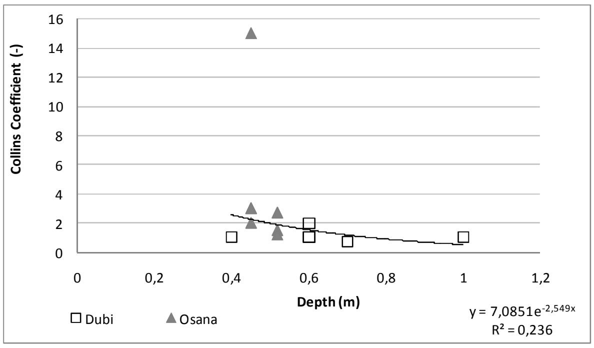

Figure 2.6A.7: More uniform vegetation type results in a more clear relation between depth and the Collins coefficient.

Relative depth in relation to Collins coefficient

The depth is divided by the vegetation height. Again the trend is very weak for the whole data set and clearer for the vegetation that is more alike.

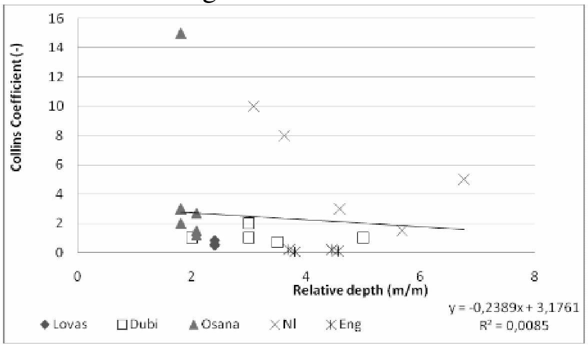

Figure 2.6A.8: Fitted Collins coefficients in comparison to the relative water depth (depth divided by vegetation height)

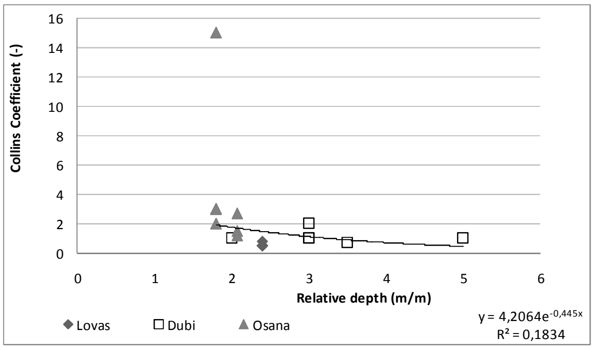

Figure 2.6A.9: Fitted Collins coefficients in comparison to the relative water depth for the Lovas Dubi and Osana case.

Vegetation density in relation to Collins coefficient

The density is expressed in units/m^2. Because in The Netherlands the measurements are expressed in stems/m2 it is multiplied by the value of units/stems obtained from Bouma (2005) (1.75 times the stems). This results in an average of 1976 structures/m2. The vegetation density of the England case is expressed in g/m^2 and is changing over time. Because of the difficult translation towards units/m^2 this case is not presented here.

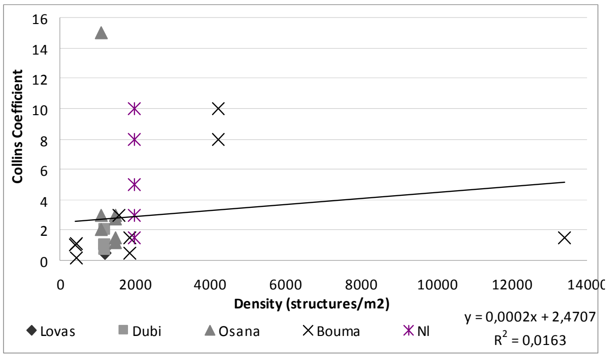

Figure 2.6A.10: Density versus the Collins coefficient does not provide a clear relation.

Conclusion

The conclusions drawn from this analysis are limited. Some trends can be spotted, but the data has a lot of variety on multiple parameters, resulting in a lot of scatter. The predictable trends are as expected. For instance, a higher vegetation density results in a higher friction coefficient. Because many measurements have about the same density, the relation is very weak. Also as expected, a higher friction coefficient occurs when vegetation height increases. The friction coefficient seems to decrease with increasing period, also decreases with increasing wave height, decreases with increasing depth and decreases with increasing relative depth (depth divided by vegetation height). All of the trendlines through the points have a R^2 below 0.6. This indicates that no real correlation between a separated parameter and the Collins coefficient is found.

Appendix 2.6B: Hydraulic aspects in one parameter

The data set is too small to change one parameter and keep the rest fixed to a certain value (Appendix 2.6A). To compensate for the variety in period, wave height and water depth, a coefficient is created that includes all of these factors. It is done with the amplitude of the near bottom horizontal velocity. Because this velocity factor takes most hydraulic aspects into account, the different vegetation properties can be compared in a more fair way. The method is expected to result in a better fitting trendline which improves by adding vegetation characteristics.
The maximum amplitude of the horizontal velocity is presented in Equation 2.6B.1.

$$\hat{U}(z) = \omega a * \frac{\cosh(k*(h+z))}{\sinh(kh)}$$

$$\hat{U}(bottom) = \frac{\omega a}{\sinh(kh)} = \frac{\frac{2\pi}{T}\frac{H}{2}}{\sinh\left(\frac{2\pi}{L}h\right)} = \frac{\frac{2\pi}{T}\frac{H}{2}}{\sinh\left(\frac{2\pi}{T\sqrt{gh}}h\right)} = \frac{\frac{\pi}{T}H}{\sinh\left(\frac{2\pi}{T\sqrt{gh}}h\right)}$$

Eq. 2.6B.1: Wave height, period and depth combined in the maximum amplitude of the horizontal velocity near the bottom. (Van Rijn 1990)

Figures 2.6B.1/3 show the results when all of the used parameters are included in one parameter on the x-axis. The resulting trendlines are reasonable, but the improvements due to the addition of vegetation characteristics do not occur. This is presented in Table 2.6B.1. The correlation (R^2) of 0.69 between horizontal velocity and the friction coefficient suggests a relation between the two aspects. The attribution of vegetation characteristics to the x-axis does not create a clearer relation with the Collins coefficient, the correlation remains the same. Therefore it is hard to draw conclusions from this analysis about the relation between vegetation characteristics and the friction coefficient.

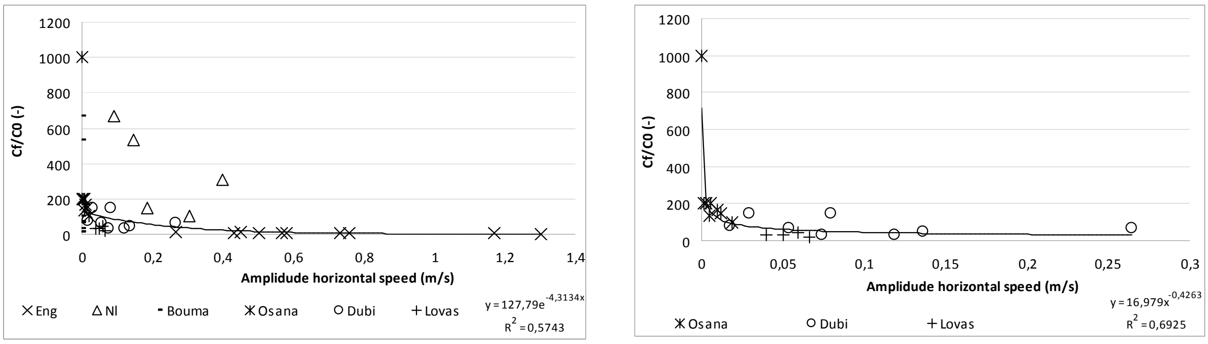

Figure 2.6B.1: Fitted Collins divided by the standard Collins of 0.015 on the y-axis, the horizontal amplitude of the orbital motion on the x-axis. R^2 = 0,574 for all of the cases and 0.693 for the uniformly vegetated cases (Dubi/Lovas/Osana)

When a large part of the deviation is caused by vegetation height or density, it could be an improvement when these factors are also taken into account in the parameter on the x-axis.

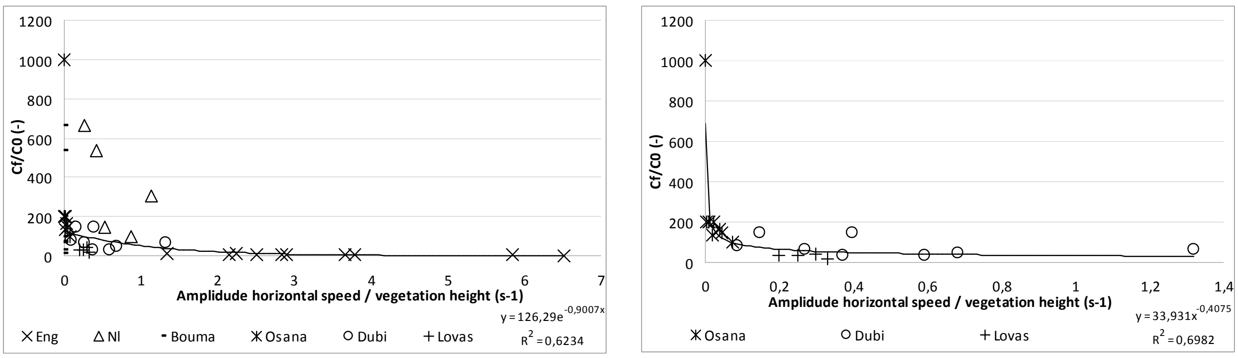

Figure 2.6B.2: The horizontal amplitude of the orbital motion divided by vegetation height on the x-axis. R^2 = 0,623 for all of the cases and 0.698 for the uniform vegetated cases (Dubi/Lovas/Osana)

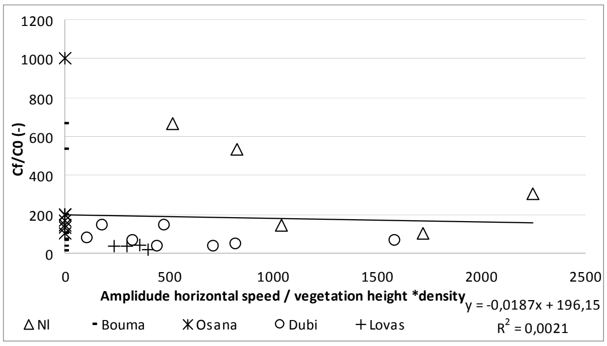

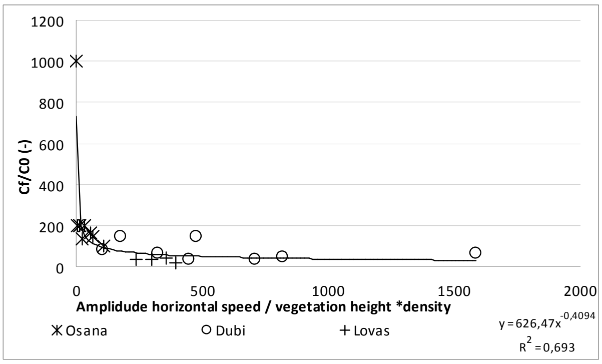

Figure 2.6B.3: On the x-axis, the horizontal amplitude of the orbital motion is divided by vegetation height and multiplied by the density. R^2 = 0,002 for all of the cases and 0.693 for the uniform vegetated cases (Dubi/Lovas/Osana)

Table 2.6B.1: Relation between the Collins coefficient and vegetation properties, when all of the hydrologic characteristics are captured in the maximum orbital velocity

Fitted Collins coefficient divided by the Collins coefficient of sand, in relation to :	
amplitude of the horizontal speed	R^2=0.692
amplitude of the horizontal speed divided by the vegetation height	R^2=0.698
amplitude of the horizontal speed divided by the vegetation height times density	R^2=0.693

(Only the Osana / Dubi / Lovas case because the NL / Bouma / England case just caused scattering

Appendix 2.6C: Subsets

The average of the fitted Collins coefficients is about 2.2. When all cases are run with this value, it could be possible to create subsets that fit better or worse. For instance, a certain vegetation height can perform significantly better than other vegetation heights. When this occurs, it can be concluded that vegetation height is an important factor for the deviations from a constant Collins coefficient. England cannot be represented very well, so it is not taken into account for this analysis.

The subsets are created with about the same amount of data points. The sets are based on vegetation density, vegetation height, wave period, wave height or relative depth. With these subsets, no clear results are obtained on which aspect is most important for the deviations. Despite that wave height and vegetation height seem to cause the most differences for the selected subsets. Table/Figure 2.6C.1 presents the results. For the significant differences between the subgroups it seems that most of the high correlation groups just have a lot of data from the good fitting Osana case. Furthermore no specific trendlines occur for the selected subsets. Therefore no real conclusions can be drawn from this analysis, differences between the separate cases are probably too large to treat it as one set.

Table 2.6C.1: Resulting correlation coefficients per subset.

Density	1000-1200 units/m^2	1201-1500 units/m^2	1501-2000 units/m^2
	R^2= 0.75	R^2= 0.92	R^2= 0.75
Period	<2 s	2-3 s	3< s
	R^2= 0.7	R^2= 0.87	R^2= 0.79
Wave height	<0.10 m	0.10-0.15 m	0.15< m
	R^2= 0.90	R^2= 0.27	R^2= 0.50
Vegetation height	0.1 m	0.20-0.25 m	0.35 m
	R^2= 0.3	R^2= 0.78	R^2= 0.5
Relative depth (vegetation height/ depth)	<0.33	0.33-0.45	0.45<
	R^2= 0.97	R^2=0.67	R^2= 0.97

Figure 2.6C.1: The composition and results of the subsets.

Density (rest Bouma too extreme) 1000-1200 units/m2 Dubi (all)/Lovas (all)/Osana (3/8) R2=0.75	1201-1500 units/m2 Osana (5/8) R2=0.97	1501-2000 units/m2 NL (all)/Bouma (3/9) R2=0.75

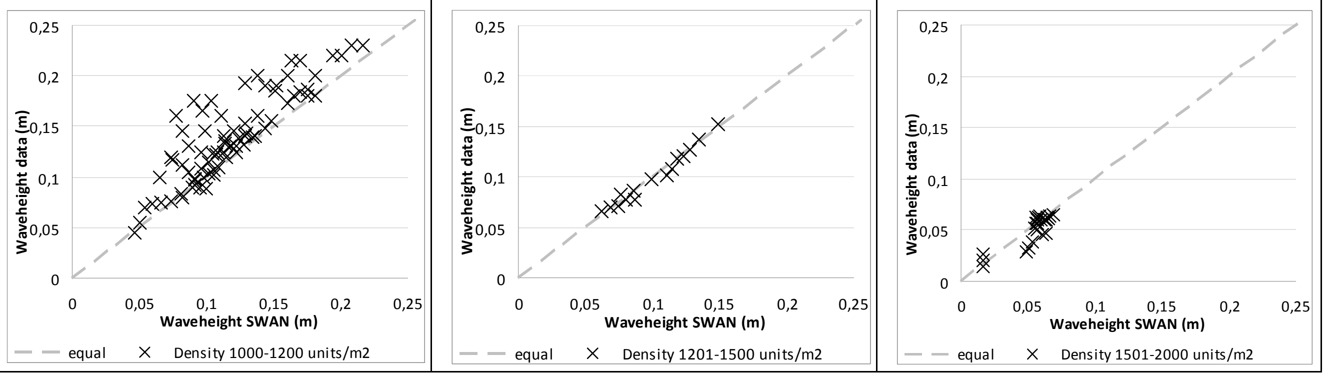

Period (Bouma constant, left out)
<2 s
Dubi (4/8)/Osana (7/8)
R2=0.74

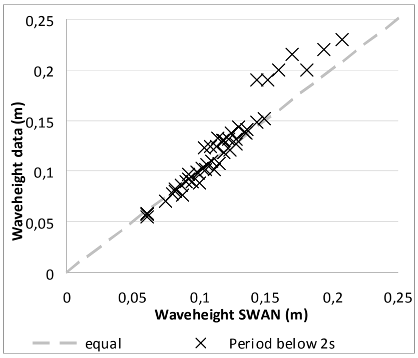

2-3 s
Lovas (1/4)/Dubi (2/8)/Osana (1/8) /NL (3/5)
R2=0.87

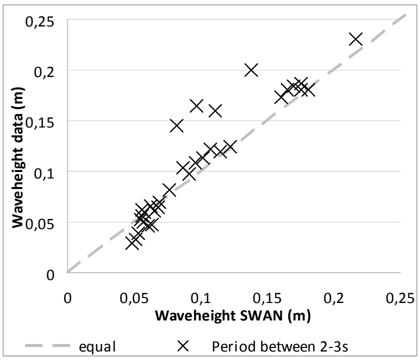

3< s
Lovas (3/4)/Dubi (2/8)/NL (2/5)
R2=0.79

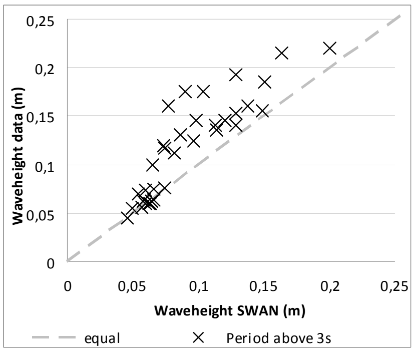

Wave height <0.10 m
R2=0.90

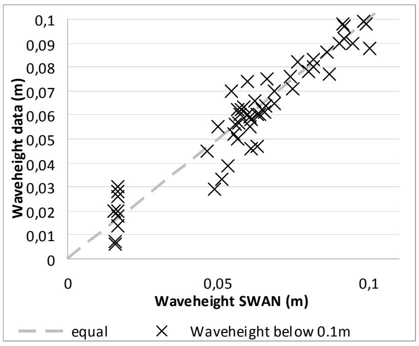

0.1-0.15 m
R2=0.27

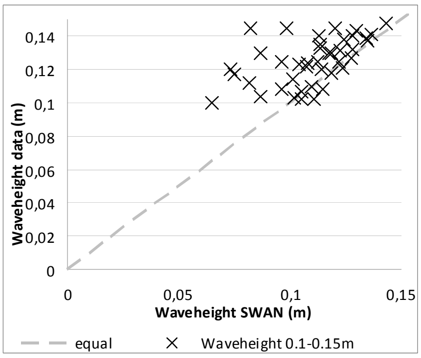

0.15< m
R2=0.50

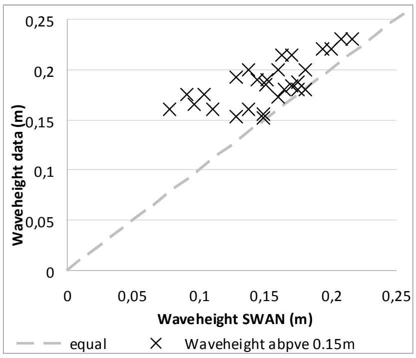

Vegetation height 0.1 m
Bouma
R2=0.30

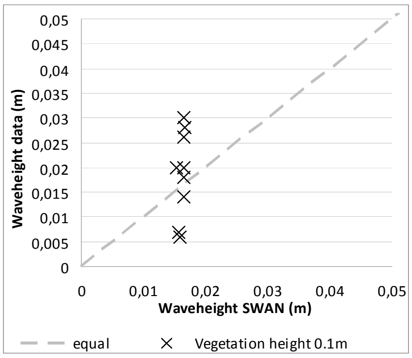

0.2-0.25 m
Osana Lovas Dubi
R2=0.78

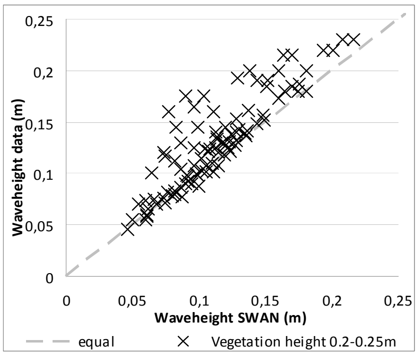

0.35 m
NL
R2=0.50

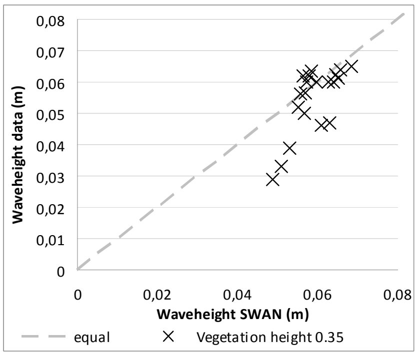

Relative depth (dv/h) <2.2
Osana/Bouma/Dubi (1/8)
R2 0.97

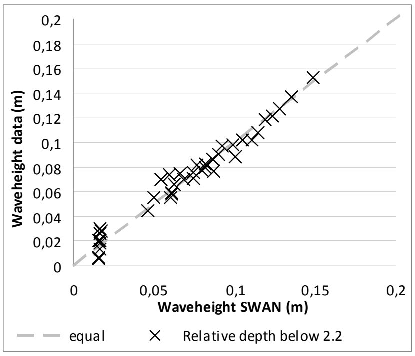

2.2-3
Lovas/Dubi (5/8)
R2 0.67

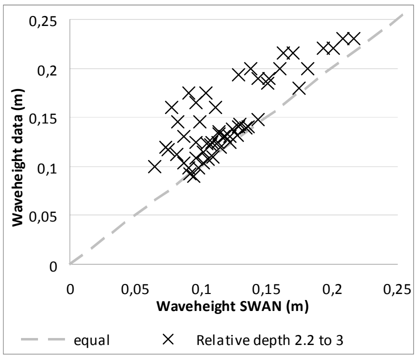

3<
Dubi (2/8) / NL
R2=0.97

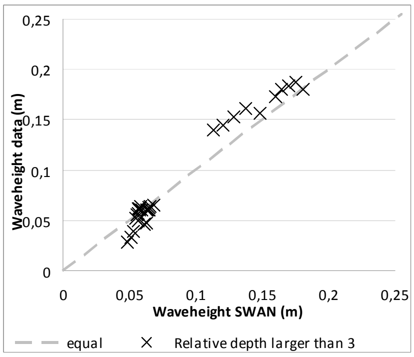

Appendix 3.1A: Details of the Vietnam cases

To check the model for mangrove vegetation, it is possible to use two field measurements from Vietnam. The first is near Thuy Hai, the second is near Vinh Quang (Burger 2005 from Mazda 1997).

For the Vinh Quang (VQ) case, the wave heights, water depth and wave reduction are extracted from Figure 3.1A.2. This is not the best data set, but it is the only data set found for woody vegetation. Furthermore it is known that the average wave period is 6.5 seconds. The bathymetry is assumed linearly and rises 0.05m in 100m. The vegetation is described in detail and characteristics are presented in Figure 3.1A.3. The measurements that are used are presented in Table 3.1A.1.

Table 3.1A.1: Measurements used from Vinh Quang, Vietnam (Burger 2005 from Mazda 1997). R is the wave reduction rate in % per meter.

	VQH05	VQH08	VQH10	VQH12	VQH14	VQH16
h (m):	0.15	0.45	0.3	0.8	0.8	0.8
H0 (m):	0.05	0.08	0.10	0.12	0.14	0.16
R (%/m):	0.5	0.22	0.2	0.13	0.25	0.4

(Burger 2005) For Thuy Hai (TH) there is no information on wave conditions, just on the wave height reduction at certain depths (Figure 3.1A.2). For this reason, the wave conditions at sea are assumed equal for both cases. So with the known water depth at open sea in Thuy Hai, wave heights are extracted for that depth from Vinh Quang. This is an arbitrary method, but no better data is available. The advantage of this case is that there are three areas with each a homogeneous vegetation distribution. This is the case because mangroves (Candelia Candel) are planted in the area in different years. Zone A is 0.5 years old, zone B 2-3 years old and zone C 5-6 years old.
For area C, the densities (N=units/m^2) are used from Burger (2005). This is based on the fact there is one tree per m^2. The different densities for the third layer of area A and B are estimated based on the smaller treetops (Table 3.1A.2). The rest of the vegetation dimensions are presented in Figure 3.1A.4. The bathymetry is assumed linearly and rises 0.15m in 800m for area A, 0.07m in 300m for area B and 0.05m in 300m for area C. The measurements that are used are presented in Table 3.1A.3.

Table 3.1A.2: Densities (units/m^2) of the different layers of the different areas in TH

Area	N1	N2	N3
Area A	1	1	25
Area B	1	1	50
Area C	1	1	100

Table 3.1A.3: Measurements used from Thuy Hai, Vietnam (Burger 2005 from Mazda 1997). R is the wave reduction rate in % per 100 meter.

	Ah05	Ah07	Ah09	Ah105	Bh05	Bh07	Bh09	Bh105	Ch05	Ch07	Ch09	Ch105
h (m)	0.5	0.7	0.9	1.05	0.45	0.55	0.75	0.9	0.40	0.50	0.70	0.85
H0 (m)	0.15	0.2	0.24	0.28	0.06	0.12	0.16	0.19	0.04	0.08	0.11	0.14
R (%/100m)	10	6	5	5	14	13	12	10	18	18	18	18
Hend (m)	0.06	0.12	0.16	0.19	0.04	0.08	0.11	0.14	0.02	0.04	0.06	0.07

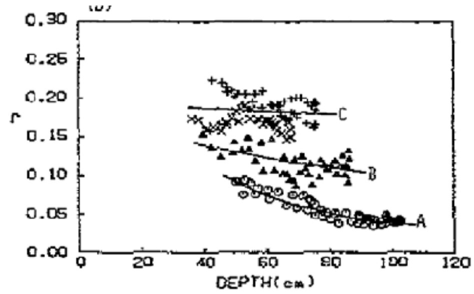

Figure 3.1A.1: Thuy Hai, Vietnam. Rate of wave reduction in relation to depth. (Burger 2005 from Mazda 1997)

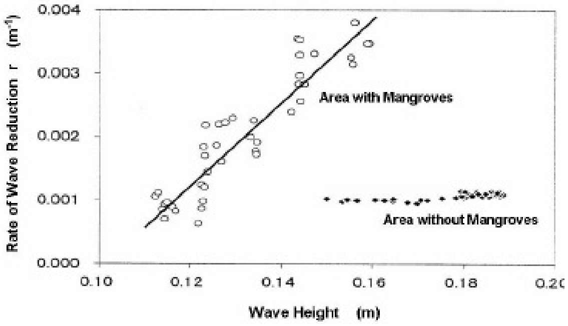

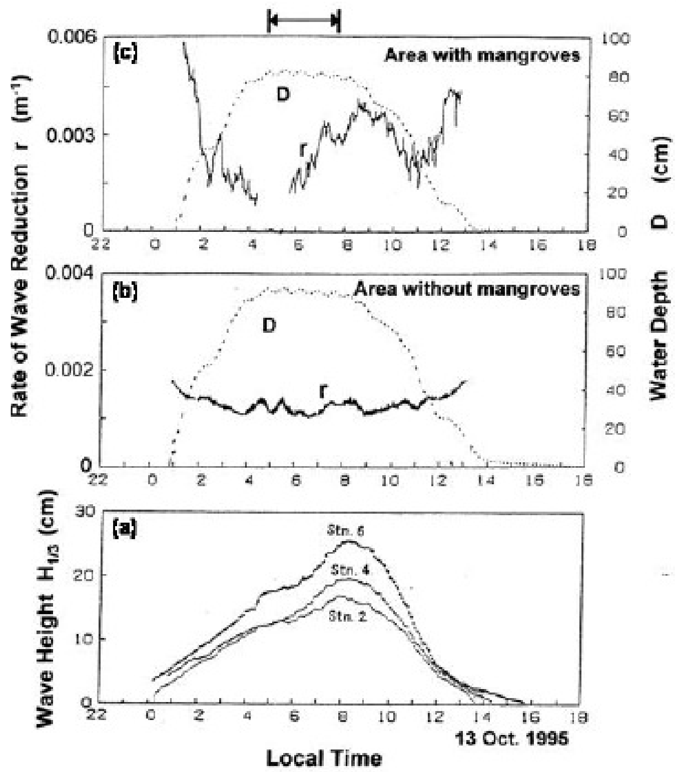

Figure 3.1A.2; Right/above. Vinh Quang, Vietnam. Water depth, wave reduction and wave height. Marked (arrow)is the period with a constant water level. Wave periods occurred with an average of 6.5 seconds. (Burger 2005 from Mazda 1997)

Dimensions (m)	
Density (-/12,5 m^2)	1.0
Wt	0.117
Hf	0.82
Density roots (-/m^2)	131
Wr	0.073
Hr	13.8

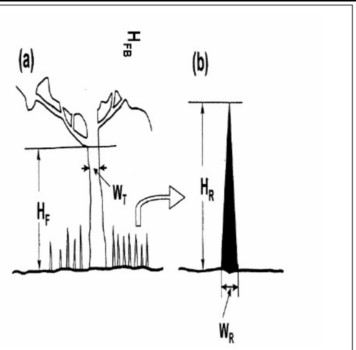

Figure 3.1A.3: Vegetation dimensions VQ (Sonnertia Sp.). The water never reaches the treetop, so this density is irrelevant. (Burger 2005 from Mazda 1997)

Dim (m)	Area A	Area B	Area C
A	0.03	0.10	0.15
B	0.0	0.10	0.13
C	0.02	0.05	0.08
D	0.03	0.05	0.06
E	0.40	0.30	0.30
F	0.30	0.50	0.75
G	0.10	0.45	0.75
H	1.0	1.0	1.0

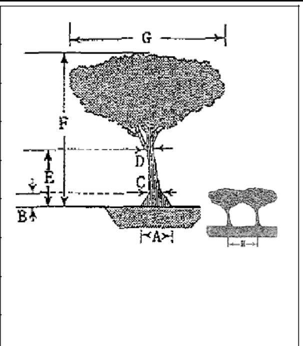

Figure 3.1A.4: Vegetation dimensions TH. (Burger 2005 from Mazda 1997)

When the data is reproduced in SWAN it results in the following best-fit Colins friction coefficients (Table 3.1A.4).

Table 3.1A.4: Resulting friction coefficients

Case	Range in Collins coefficients
VQ	0.016-0.151
THA	0.014-0.019
THB	0.026-0.044
THC	0.037-0.112

Appendix 3.2A: Parameter test of Mendez friction formula

In this appendix, the influence of different parameters is shown within the friction formula based on vegetation. All of the figures show a standard case with just one variable that changes. The standard case is set to vegetation height 30cm, depth 1m, wave height 20cm, density 1500 units/m^2, period 2.5s and vegetation width 0.03m. Without adaptation, the Collins of the standard case is 0.53.

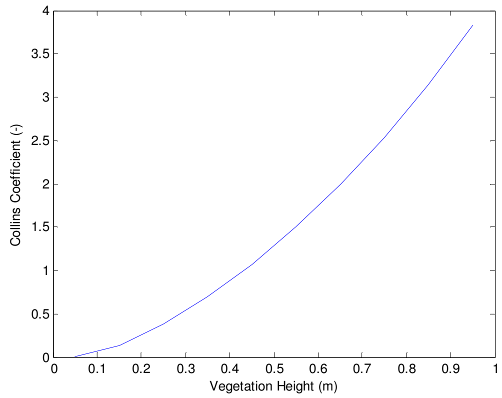

Deviating vegetation height: 5-95cm
Deviating Collins: ~0-3.8

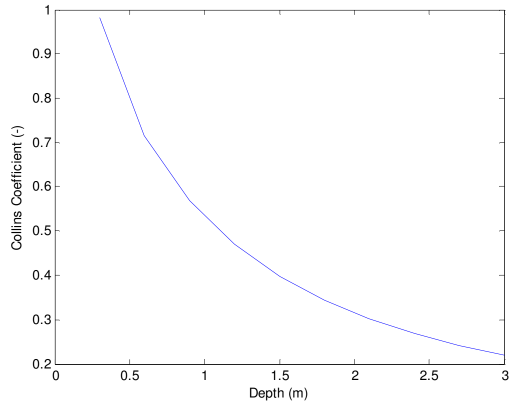

Deviating depth: 0.3-3m
Deviating Collins: ~0.2-1

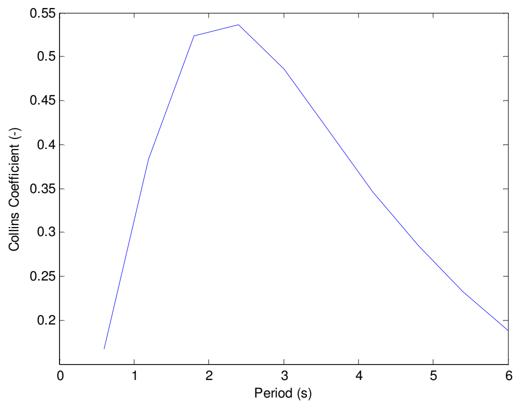

Deviating period: 0.6-6s
Deviating Collins: ~0.1-0.54

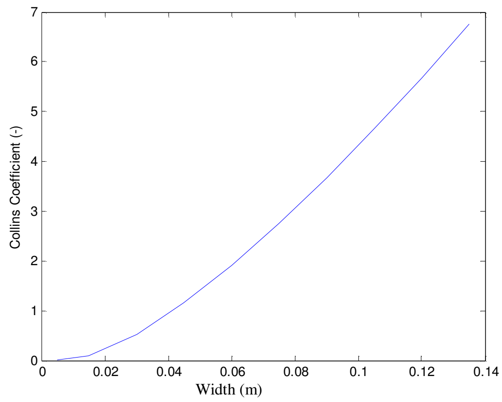

Deviating vegetation width: 0.005-0.135m
Deviating Collins: ~0-6.5

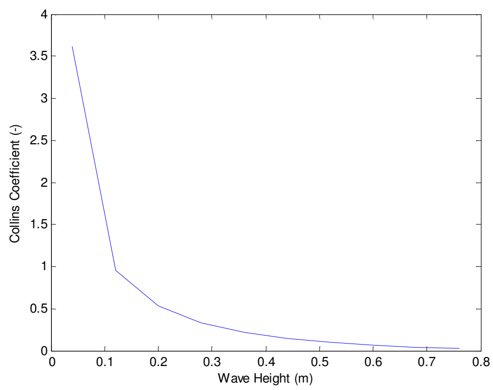

Deviating wave height: 0.04-0.76m
Deviating Collins: ~0.0-3.5

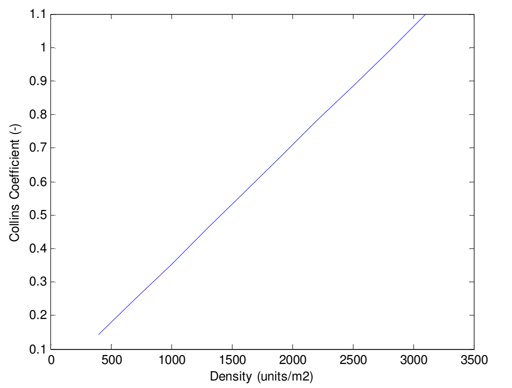

Deviating density: 400-3100 units/m^2
Deviating Collins: ~0.15-1.1

Appendix 3.3A: Stiffness per case

The Young's Modulus of each vegetation species is:

- Dubi / Lovas: E = 32 MN/m^2 (Mendez 1999)
- Osana: E = 9.8 MN/m^2 (Mendez 1999)
- Vietnam: E = 800 MN/m^2 this is the average value for wood, perpendicular to the grain. (wikipedia.org) For the treetops a value of 200 MN/m^2 is used because it consists of leaves and small braches. Therefore a value between the Dutch and the Bouma case is used.
- Bouma flex: E = 100 MN/m^2 this is estimated based on the values of 14 different species presented in Cooley (2004).
- NL / Bouma E = 300 MN/m^2 this is estimated based on the values of 14 different species presented in Cooley (2004).

Appendix 3.3B: Parameter test of stiffness factor

In this appendix, the influence of different parameters is shown within the developed formula for stiffness. The figures show a standard case with just one changing variable. The standard case has the following properties: relative depth (vegetation height / depth) = 0.33, vegetation width = 0.01m, stiffness 300MN/m^2. Without adaptations, the stiffness factor is 95.6 for this case.

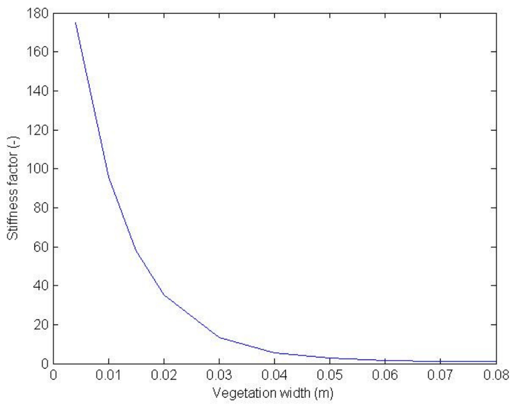

Deviating vegetation width: 0.004-0.08m
Deviating stiffness factor: ~0.0-170

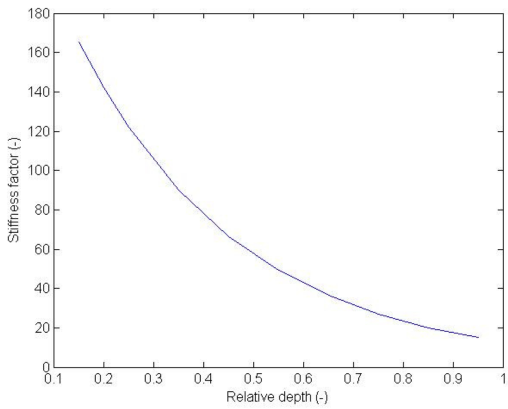

Deviating relative depth: 0.15-0.95
Deviating stiffness factor: ~20-160

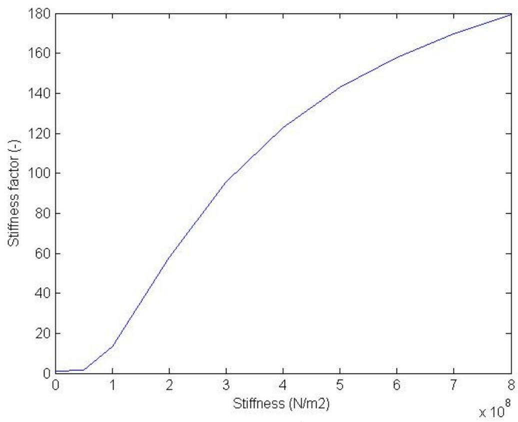

Deviating stiffness: 0-800MN/m^2
Deviating stiffness factor: ~0-180

Appendix 3.4A: Matlab script

The developed Matlab script is presented below:

```
%____________starting values___________________
%--------------------------------------------------------------
run vegetation_characteristics %obtaines vegetation characteristics
Cf=ones(249,229)*1;% Collins for a first run or
load 'previous_output.mat' % to continue a previous run
max_dev_percentage =999; %starting value of the maximim percentage of deviation in Collins coefficients
max_dev_percentage(2) =999;
max_dev_Collins=999; %starting value of the max absolute deviation in Collins
max_dev_Collins(2)=999;
nr_cells_exceeding_10percent_deviation=999; %starting value of the number of cells that exceed the 10% deviation
nr_cells_exceeding_10percent_deviation(2)=999;

%____________iterations________________________
%---------------------------------------------------------------
Max_iterations=40
for p=3:(Max_iterations+2)
  Iteration=p-2
  Of_the= Max_iterations
  if max_dev_percentage (p-1)<10 %
    'Results obtained, deviation in collins below 10%'
     max_dev_percentage (p) =0;
     max_dev_Collins (p)=0;
     nr_cells_exceeding_10percent_deviation (p)=0;
  elseif nr_cells_exceeding_10percent_deviation(p-1)> nr_cells_exceeding_10percent_deviation(p-2) &
          .                     max_dev_percentage(p-1)> max_dev_percentage(p-2) &
                                   max_dev_Collins(p-1)> max_dev_Collins(p-2)
    'Not converging, take average of the last two collins coefficients of the non converging cells'
   Cf(pnts_above_10prct)=0.5*Cf(pnts_above_10prct)+0.5*CollinsMatlab(pnts_above_10prct)
   max_dev_percentage (p) =999;%not converged yet
   max_dev_Collins (p)=999;
   nr_cells_exceeding_10percent_deviation (p-1)=999;
   nr_cells_exceeding_10percent_deviation (p)=998;  %starts the next run
  else
   'Deviation Collins exceeds 10%, but converges'
   CollinsMatlab=Cf;
   save SWAN\friction\CollinsMatlab.txt CollinsMatlab -ascii %to run SWAN with
   'Collins values saved to run in SWAN, run status:'
   [status]=dos('runSWAN.bat' , '-echo');
   'SWAN is runned'

   %__________________input for the calculations_______
   %--------------------------------------------------------------
   load SWAN\results.mat %loads the output of the SWAN run
   [m,n] = size(Cf);
     for i=1:n
        for j=1:m
        Hs(j,i)=Hsig(j,i); %significant wave height
        if   Hs(j,i)>0.001;  else  Hs(j,i)=0.001; %prevents calculations with 0
        end
        Tp(j,i)=RTpeak(j,i); %Peak period
        if   Tp(j,i)>0.1;    else  Tp(j,i)=0.1; %prevents calculations with 0
        end
        h1(j,i)=Depth(j,i);
        if   h1(j,i)>0.0001;  else  h1(j,i)=0.0001; % prevents calculations with 0
        end
        h2(j,i)=h1(j,i); %stems of trees also through layer one
        if   h2(j,i)>0.0001;  else  h2(j,i)=0.0001; %  prevents calculations with 0
        end
        h3(j,i)=h2(j,i)-dv1(j,i)-dv2(j,i);
        if   h3(j,i)>0.0001;  else  h3(j,i)=0.0001; % prevents calculations with 0
        end
        end
     end
```

```
    [q,w]=size(Hs);
    Hs_middle= ones(q,w); % in between measuring points
    for r=1:(q-1)
        for b=1:(w-1)
        Hs_middle(r,b)=(Hs(r,b)+Hs(r+1,b)+Hs(r,b+1)+Hs(r+1,b+1))/4;
        end
    end

  %_________________general calculations____________________
  %------------------------------------------------------------------------------
    [m,n] = size(Cf);
         for i=1:n
            for j=1:m
            rho=1000;%water density (kg/m3)
            g=10;  %acceleration of gravity (m/s2)
            sigma(j,i)=(2*pi)/Tp(j,i);  %wave frequency (rad/s)
            L(j,i)=(g*h1(j,i))^0.5*Tp(j,i); %wavelength with shallow water assumption
            alpha1(j,i)=dv1(j,i)/h1(j,i); %relative vegetaion height (m/m)
              if    alpha1(j,i)<1;  else  alpha1(j,i)=1;%relative height has a maximum value of 1
              end
            alpha2(j,i)=dv2(j,i)/h2(j,i);
            if    alpha2(j,i)<1;  else  alpha2(j,i)=1;
            end
            alpha3(j,i)=dv3(j,i)/h3(j,i);
            if    alpha3(j,i)<1;  else  alpha3(j,i)=1;
            end
            a(j,i)=0.5*Hs_middle(j,i); %wave amplitude in the middle of the vegetation field (m)
            z1(j,i)=-h1(j,i)+0.5*dv1(i);%depth for orbital velocity calculation, half vegetation height
            z2(j,i)=-h2(j,i)+0.5*dv2(i);%
            z3(j,i)=-h3(j,i)+0.5*dv3(i);%
            omega(j,i)=(2*pi)/Tp(j,i); % angular frequency
            k(j,i)=(2*pi)/L(j,i);  %wave number

  %_________energy dissipation with vegetation characteristics__________
  %-------------------------------------------------------------------------------------
            %orbital velocities
            uc1(j,i)=cosh(k(j,i)*(h1(j,i)+z1(j,i)))/(sinh(k(j,i)*h1(j,i)))*omega(j,i)*a(j,i);
            uc2(j,i)=cosh(k(j,i)*(h1(j,i)+z2(j,i)))/(sinh(k(j,i)*h1(j,i)))*omega(j,i)*a(j,i);
            uc3(j,i)=cosh(k(j,i)*(h1(j,i)+z3(j,i)))/(sinh(k(j,i)*h1(j,i)))*omega(j,i)*a(j,i);
            K1(j,i)=uc1(j,i)*Tp(j,i)/bv1(j,i);%Keulegan–Carpenter number
            K2(j,i)=uc2(j,i)*Tp(j,i)/bv2(j,i);
            K3(j,i)=uc3(j,i)*Tp(j,i)/bv3(j,i);
            Q1(j,i)=K1(j,i)/(alpha1(j,i)^0.76);
            Q2(j,i)=K2(j,i)/(alpha2(j,i)^0.76);
            Q3(j,i)=K3(j,i)/(alpha3(j,i)^0.76);
            alpha_total(j,i)=(dv1(j,i)+dv2(j,i)+dv3(j,i))/(h1(j,i));
               if alpha_total (j,i)>1
                  alpha_total (j,i)=1;
               end
           St_Factor1(j,i)=260.83*exp(-9.2221*bv1(j,i)*10^6*rho/E1(j,i)*g*alpha_total l(j,i))+1;% Stiffness factor
           St_Factor 2(j,i)=260.83*exp(-9.2221*bv2(j,i)*10^6*rho/E2(j,i)*g*alpha_total (j,i))+1;
           St_Factor 3(j,i)=260.83*exp(-9.2221*bv3(j,i)*10^6*rho/E3(j,i)*g*alpha_total (j,i))+1;
           Cd1(j,i)=St_Factor1(j,i)*exp(-0.0138*Q1(j,i))/Q1(j,i)^0.3;
           Cd2(j,i)=St_Factor2(j,i)*exp(-0.0138*Q2(j,i))/Q2(j,i)^0.3;
           Cd3(j,i)=St_Factor3(j,i)*exp(-0.0138*Q3(j,i))/Q3(j,i)^0.3;

            %energy dissipation mendez (N/m/s)
            Edm1(j,i)=0.28*rho*Cd1(j,i)*bv1(j,i)*N1(j,i)*(k(j,i)*g/(2*sigma(j,i)))^3*(sinh(k(j,i)*alpha1(j,i)*h1(j,i))^3+
            3*sinh(k(j,i)*alpha1(j,i)*h1(j,i)))/(3*k(j,i)*cosh(k(j,i)*h1(j,i))^3)*Hs(j,i)^3;
            Edm2(j,i)=0.28*rho*Cd2(j,i)*bv2(j,i)*N2(j,i)*(k(j,i)*g/(2*sigma(j,i)))^3*(sinh(k(j,i)*alpha2(j,i)*h2(j,i))^3+
            3*sinh(k(j,i)*alpha2(j,i)*h2(j,i)))/(3*k(j,i)*cosh(k(j,i)*h2(j,i))^3)*Hs(j,i)^3;
            Edm3(j,i)=0.28*rho*Cd3(j,i)*bv3(j,i)*N3(j,i)*(k(j,i)*g/(2*sigma(j,i)))^3*(sinh(k(j,i)*alpha3(j,i)*h3(j,i))^3+
            3*sinh(k(j,i)*alpha3(j,i)*h3(j,i)))/(3*k(j,i)*cosh(k(j,i)*h3(j,i))^3)*Hs(j,i)^3;

%___________energy dissipation SWAN________________________
%------------------------------------------------------------------------------------
            Egolf(j,i)=1/8*rho*g*Hs(j,i)^2; %wave energy in shallow water
```

```
            Urms(j,i)=omega(j,i)*a(j,i)/(sinh(k(j,i)*h1(j,i)));% near bottom orbital velocity
            Cb_divided_by_Cf(j,i)=g*Urms(j,i);  %bottom friction with Collins coefficient Cf
            Eds(j,i)= Cb_divided_by_Cf(j,i)*sigma(j,i)^2/(g^2*(sinh(k(j,i)*h1(j,i)))^2)*Egolf(j,i);%is dissipation/Collins

 %__________calculate collins coefficient________________________
 %-------------------------------------------------------------------------
            Cf(j,i)=(Edm1(j,i)+Edm2(j,i)+Edm3(j,i))/Eds(j,i); %
            if 10000000>Cf(j,i) &Cf(j,i)>0.006; %no problem
            else  Cf(j,i)=0.006; %minimum bottom roughness sand and prevention NaN
            end
%___________rest calculations________________________________
%------------------------------------------------------------------------------------
            dev_Collins (j,i)=abs(Cf(j,i)-CollinsMatlab(j,i));
         end
      end
    [m,n] = size(Cf);
    for i=1:n
       for j=1:m
       perc(j,i)=100*((abs(dev_Collins (j,i)))/CollinsMatlab(j,i));%percentage deviation Collins from prev iteration
       end
    end
    max_dev_percentage (p)=max(max(perc))
    pnts_above_10prct=find (perc>10 );
    nr_cells_exceeding_10percent_deviation (p)=length(pnts_above_10prct)
    max_ dev_Collins(p)=max(max(dev_Collins))

   %monitor points in serie of iterations
   Hs_development(:,p)=[Hs(1,1) Hs(50,50)];
   end
end
```

Appendix 4.1A: New Orleans grid

The bathymetry (Figure 4.1A.1) and two earlier applied friction files on the grid (Figure 4.1A.2/3).

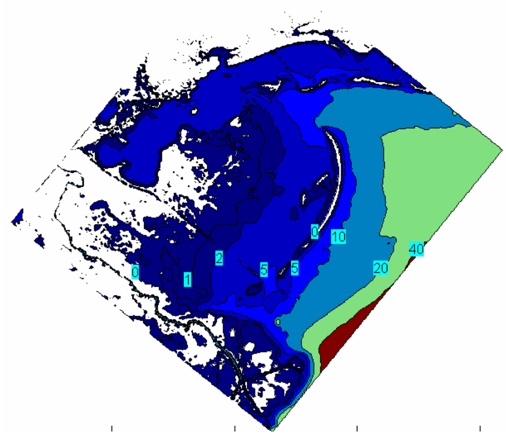

Figure 4.1A.1: The bathymetry of the area. The white areas are above sea level, the other values indicate the meters below sea level.

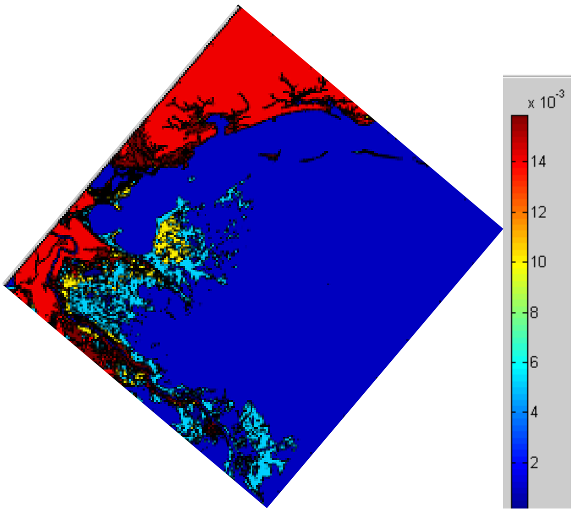

Figure 4.1A.2: Collins friction coefficient as used for the storm surge barrier design.

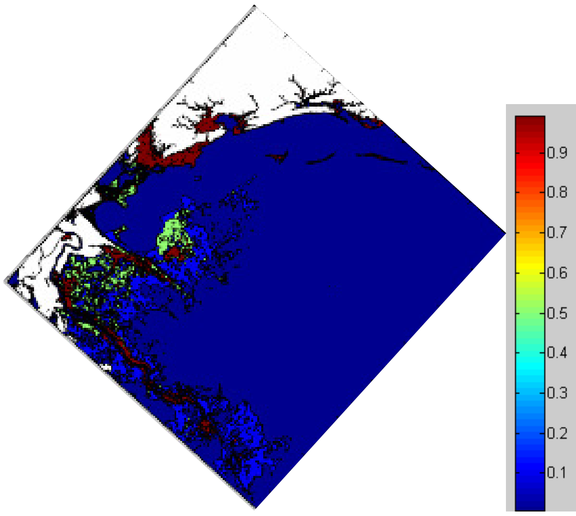

Figure 4.1A.3: Roughness height (m) representing vegetation, used in the LACPR project.

The SWAN grid is supported by Figure 4.1A.4 because both the figure as the grid are dominated by brackish marsh in that area.

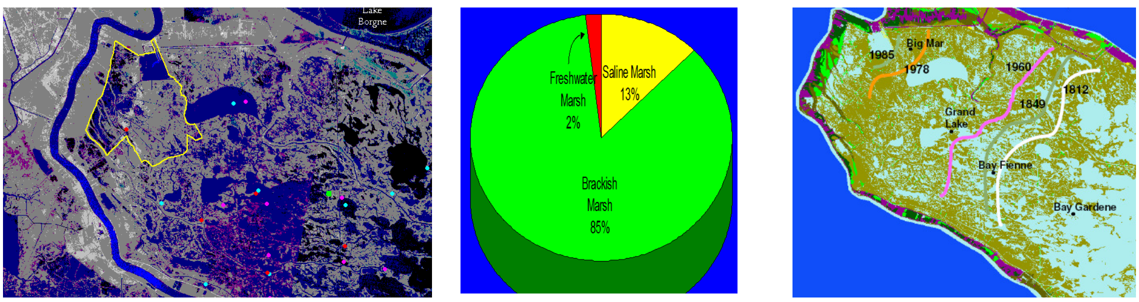

Figure 4.1A.4: The observed area near the existing diversion Caernarvon. The area mainly consists of brackish marsh in 1995. The right picture shows the movement of the intermediate/brackish marsh border that quickly moves towards the levees. (LDNR/CRD, 1998)

Appendix 4.2A: Vegetation per land type

In this appendix it is explained what the different characteristics per land type are based on.

Salt marsh

Salt marshes in the USA consist for 60-100% of Oyster Grass, also named Spartina Alterniflora (americaswetlandresources.com). From measurements in Louisiana it resulted that the average height is 1.72m, and the width is about 0.01m (Fang 2002 / plants.usda.gov). The stiffness and the density are assumed equal to the Spartina Anglica in the Dutch case. So ~2000 units/m^2 and 300MN/m^2. Figure 4.2A.1 shows a typical homogeneous salt marsh.

Figure 4.2A.1: Salt marsh, dominated by Oyster Grass (americaswetlanresources.com)

Brackish marsh

The brackish marsh is dominated (for more than 50%) by Wire Grass or Spartina Patens (americaswetlandresources.com). On average, its length is 0.85m, the average width is 0.004m (fs.fed.us / plants.usda.gov). The stiffness and the density are assumed equal to the Spartina Anglica in the Dutch case. So ~2000 units/m^2 and 300MN/m^2. Figure 4.2A.2 shows Wire Grass.

Figure 4.2A.2: Brackish marsh, dominated by Wire Grass (plants.usda.gov)

Intermediate marsh / Fresh marsh

Intermediate marsh is mainly populated by Cattail, Segde and Wire Grass (americaswetlandresources.com). Heights of these species are between 0.85m (Wire Grass) and 1.60m (Segde). The width is between 0.004m (Wire Grass) and about 0.01m (Cattail/Segde). Therefore the average height is set to 1.40m and the width to 0.01m. The stiffness and the density are assumed equal to the Spartina Anglica in the Dutch case. So ~2000 units/m^2 and 300MN/m^2. Figure 4.2A.3 shows an intermediate marsh.

Figure 4.2A.3: Intermediate marsh with Cattail, Segde and Wire Grass.

Fresh marshes are very diverse. In the fresh marshes in the USA, about 92 vegetation species are counted. The ones that are also present in the intermediate marsh, but also Water lilies, Bull tongue and Maidencaine are often present. For simplicity, the same values are used as in the intermediate marsh. Because there is hardly any fresh marsh in the study area, this will have little influence. Figure 4.2A.3 shows some specific fresh marsh species.

Another special type of marsh that occurs in fresh and intermediate marshes is the flotant marsh. This is a floating marsh on water. It can possibly be modelled as a special layer that is always in the top of the water column (see Figure 3.2.2 in Chapter 3 of the main report). Because intermediate and fresh marshes just occur in a few small areas, and it is unclear where the flotant marshes are, this type of marsh is not taken into account (americaswetlandresources.com).


Water lilies (jeethang.com)


Bull tongue (cofairhope.com)


Maidencaine (aquat.edu)

Figure 4.2A.4: Specific fresh marsh species.

Forested area

The forested sections of the study area are mainly located along canals because some higher lands are present there. It is assumed that in the forested areas there are some bushes near the bottom, then a stem and then a treetop. Figure 4.2A.5 shows a few of the forested strips. Although there is a lot of variety, the modelling is done for all of the forested areas in the same way. Because these areas are very small, this is not seen as a big problem.

Layer 1: the bushes are assumed to be 1.20m high with (on average) 0.005m thick stems and a density of 300 units/m^2. The combination of small twigs in combination with leaves is assumed to have a stiffness that is a little higher than Spartina marshes. Therefore the value of 400MN/m^2 is chosen.
Layer 2: is the wooden stem. It is assumed to be 3m high, 0.08m thick, a density of 0.02 units/m^2 (1 per 7m^2) and a stiffness of 800 MN/m^2.
Layer 3 is assumed to be equal to layer 1.

Figure 4.2A.5: Small strips of forested areas that quickly transform into very large grass lands.

Appendix 4.2B: Output 0-scenario

The Collins coefficient exceeds the bottom friction of sand in the area near the south of St. Bernard and a little in the Biloxi marsh at the right of the figure, Figure 4.2B.1. The low depth, orbital velocity and wave period are causing this effect (Figure 4.2B.2/4).

Figure 4.2B.1: Resulting Collins coefficients for the 0-scenario. Contour lines: 0.0061 1 5 10

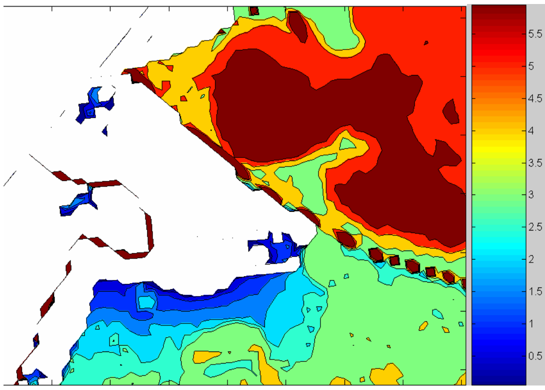
Figure 4.2B.2: Depth in the area. Only the blue areas are below 3m deep. Orange 4-4.5m.

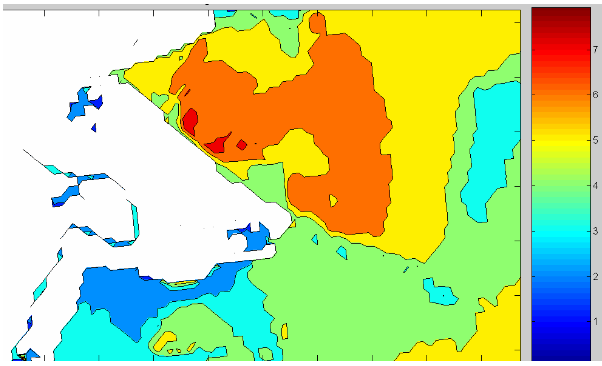
Figure 4.2B.3: Wave period in the area. Only the blue areas have a wave period below 4 seconds. Yellow=5-6s, orange 6-7s.

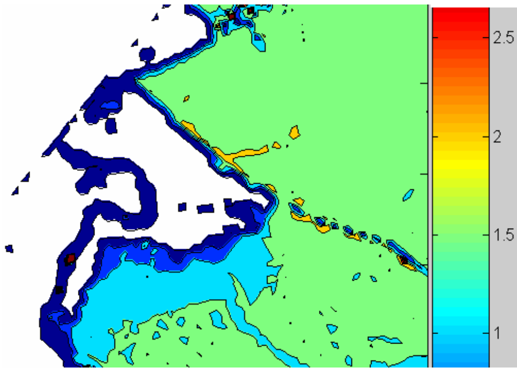

Figure 4.2B.4: Orbital velocity in the area. Only the blue areas have a wave period below 1.5m/s. Green 1.5-2m/s.

Appendix 4.3A: Scenario marsh restoration

The most important restoration measures that are considered by the Army Corps of Engineers (USACE) are presented in Figure 4.3A.1. The expected results for the year 2050 are presented in Figure 4.3A.2.

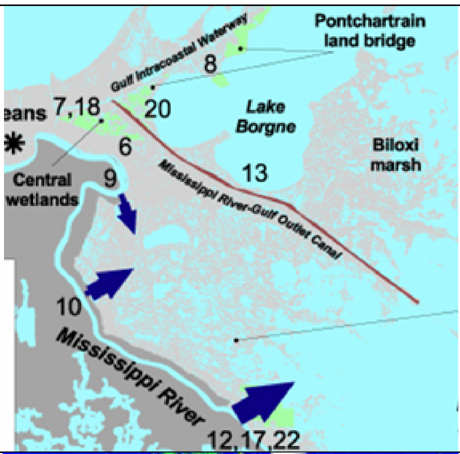

Figure 4.3A.1: Considered restoration measures:

6: rehabilitate the Violet siphon
7: post authorization change for the diversion of water through Inner Harbour Navigation Canal for enhanced influence into Central wetlands
8: marsh nourishment on New Orleans East land bridge
9: modification of (existing) Caernarvon diversion
10: medium diversion at White's Ditch
12,17,22: two medium diversions and sediment delivery via a pipeline
13: environmental restoration features
18: sediment delivery via pipeline to central wetlands
20: sediment delivery via pipeline at Golden Triangle
(USACE 2004)

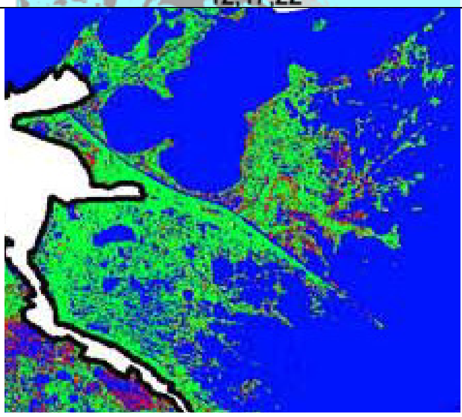

Figure 4.3A.2: Expected results when restoration measures are included for 2050. Almost no land gain (a few yellow dots) and still some erosion (red areas). (USACE 2004)

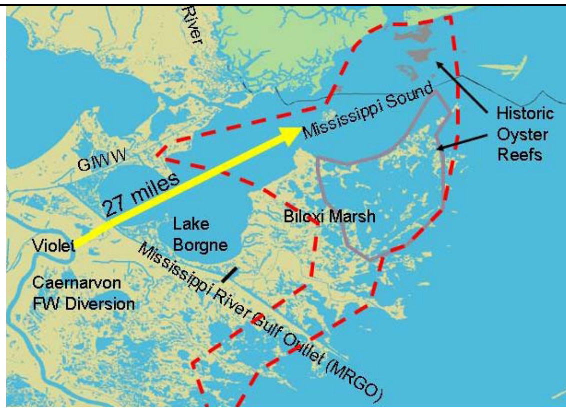

Figure 4.3A.3: The Violet diversion (measure 6) should be able to restore some of the outer parts of the marshes (Lake Ponchartrain Basin Foundation)

In this report the estimations of Wamsley (2008) are used, as presented in the main report. This recovery is based on the measures presented above. So it is assumed a few areas recover a bit. This is also expected by the Lake Ponchartrain Basin Foundation (LPBF) (saveourlake.org). Figure 4.3A.3 explains why Wamsley and LPBF expect some restoration in the outer parts of the marshes in contradiction to the expectations of USACE. This more positive forecast is used because otherwise the differences with the 0-scenario would be minimal.

When the results of the currently active Caernarvon diversion is analyzed, it seems that the surrounding area of a diversion gets denser populated because more open water disappears between the marshes. Between 1990 and 1995, the percentage of the area's surface that is land increased from 55% to 68%. Figure 4.1A.4 shows the area influenced by the dispersion (LDNR/CRD, 1998). Because of this data, the 0-scenario is calculated with an average vegetation density of 50%. Because most of the vegetated area is not restored yet and the area on which the data is available was denser on average because of its higher bottom level. The restored areas in the scenario with marsh restoration are estimated on an average land density of 75% in 2050.

Implementation restoration scenario

The densities and bottom levels are changed (as mentioned in the main report) in the following areas, Figure 4.3A.4.

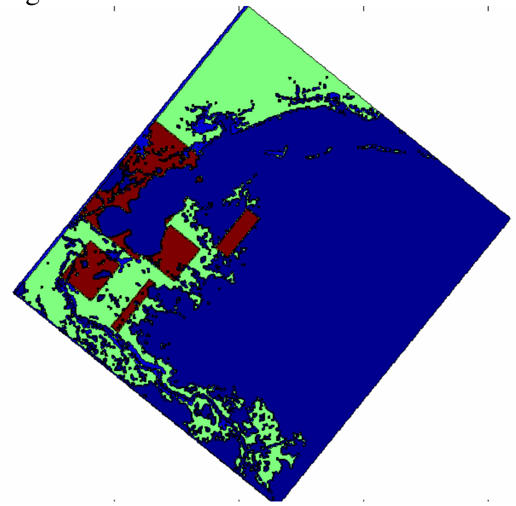

Figure 4.3A.4: Locations (in red) of the adaptations for the restoration scenario.